SEISMIC PERFORMANCE OF SELF-ANCHORED TANKS LOCATED IN HIGH SEISMIC REGIONS IN TURKEY

A Thesis

by

İrsen Nihan KOCRAS

Submitted to the

Graduate School of Sciences and Engineering
In Partial Fulfilment of the Requirements for
the Degree of

Master of Science

in the
Department of Civil Engineering

Özyeğin University
August 2023

SEISMIC PERFORMANCE OF SELF-ANCHORED TANKS LOCATED IN HIGH SEISMIC REGIONS IN TURKEY

Approved By:

Asst. Prof. Bülent Erkmen, Advisor,
Department of Civil Engineering
Özyeğin University

Asst. Prof. Taner Yılmaz,
Department of Civil Engineering
Özyeğin University

Prof. Dr. Ufuk Yazgan,
Department of Earthquake Engineering
Istanbul Technical University

Date Approved: 12 July 2023

This thesis is dedicated to my parents and my husband.
For their endless love, support and encouragement

ABSTRACT

This study examines the seismic performance of three unanchored industrial liquid storage tanks that are located in the Kocaeli industrial area, which has a significant earthquake risk. One of the tanks is an existing tank in an industrial facility located in the region, while the other two were designed to have different anchorage ratios.

The finite element analysis software ABAQUS was used to build 3-D finite element models in order to assess the seismic performance of the tanks. The seismic behaviour of the tanks was studied by performing time-history analyses using the recorded earthquake records that were scaled for the tank location. The spring-mass model, on which the developed tank models are based, models liquid content as two-point masses that were spring-adjusted to the tank wall. This approach was based on American Petroleum Institute (API 650). Tank-liquid interaction, base uplift, tank sliding off its foundation, damage to the tank's wall shell plates as well as bottom base plates, and the tank earthquake performance were all analysed. In addition, the effects of different friction coefficients between tank base and its foundation on tank seismic performance were studied.

The seismic analyses were carried out using data related to eleven earthquakes. This data was scaled to meet the seismic design spectrum for the tank location and chosen in compliance with the Turkish Building Earthquake Code. Tank base sliding, base uplift and material damage were monitored to assess potential tank damages.

The main objective of the study was to investigate the effects of tank anchorage ratio on seismic performance of unanchored tanks located in high seismic regions. This was achieved by performing time history analysis of the tanks using 11 earthquake

records. Also, tank base uplift and sliding over the foundation failure modes were also evaluated on the basis of the effect of anchorage ratio on tanks.

The second objective of the research was to examine the impact of friction between the tank base plate and tank foundation on tanks seismic performance. For this purpose, the tank's seismic performance was evaluated by considering two different friction coefficients.

The findings of this study contribute new and valuable insights into the existing literature on the seismic performance of unanchored tanks and the effects of anchorage ratio on their seismic performance. In addition, the study provided a better understanding of the effects of unanchored tanks base friction on their seismic performance. Consequently, these findings will contribute to procedures used for seismic design of unanchored tanks and enhance the seismic performance of tanks at highly seismic regions.

ÖZETÇE

Bu çalışmada, deprem riskinin yüksek olduğu Kocaeli sanayi bölgesinde bulunan tehlikeli sıvı ihtiva eden üç adet ankrajsız sanayi tankının deprem yükleri altındaki performansı incelenmiştir. Tanklardan biri bölgedeki bir endüstri tesisinde mevcutken diğer ikisi farklı ankraj oranlarına sahip olarak tasarlanmıştır. Tankın deprem performansını belirlemede ABAQUS sonlu elemanlar programı kullanılarak 3D model oluşturulmuştur. Tankların deprem davranışını incelemek için zaman tanım alanında analiz metodu kullanılmıştır. Deprem kayıtları tankların konumuna göre ölçeklenmiştir. Geliştirilen tank modellerinin temel aldığı kütle-yay modeli, sıvı içeriğini iki nokta kütlesi olarak modeller ve bu kütlesel noktalar tank duvarına yaylarla bağlanır. Tank analiz modeli API 650 yönetmeliğine dayanmaktadır. Tank-sıvı etkileşimi, taban yükselmesi, tankın tabanından kayması, tank duvar kabuk plakalarının ve taban plakalarının hasarı ve tankın deprem performansı tümüyle analiz edildi. Ayrıca, tank tabanı ile temel arasındaki farklı sürtünme katsayılarının tank deprem performansı üzerindeki etkileri de incelendi.

Deprem analizleri, on bir farklı deprem verisini kullanılarak gerçekleştirildi. Bu veriler, tankın bulunduğu bölge için deprem tasarım spektrumunu karşılamak üzere ölçeklendirildi ve Türkiye Bina Deprem Yönetmeliğine uygun olarak seçildi. Potansiyel tank hasarlarını değerlendirmek için tank taban kayması, taban yükselmesi ve malzeme hasarı takip edildi.

Çalışmanın temel amacı, yüksek deprem riski taşıyan bölgelerde konumlanan ankrajsız tankların deprem performansına ankraj oranının etkilerini incelemekti. Tankların deprem yükleri altındaki yapısal davranışları zaman tanım alanında dinamik analizlerle belirlenmiştir. Ayrıca, tank taban yükselmesi ve temel kayması gibi

başarısızlık modları da ankraj oranının tanklar üzerindeki etkisi temel alınarak değerlendirildi.

Araştırmanın ikinci amacı, tank taban plakası ile temel arasındaki sürtünmenin tank deprem performansı üzerindeki etkisini incelemekti. Bu amaçla, tankın deprem performansı, iki farklı sürtünme katsayısı dikkate alınarak değerlendirildi.

Bu çalışmanın bulguları, ankrajsız tankların deprem performansı ve ankraj oranının etkileri konusundaki mevcut literatüre yeni ve değerli katkılar sağlamaktadır. Ayrıca, bağlanmamış tankların temel taban sürtünmesinin deprem performansı üzerindeki etkisini daha iyi anlaşılmasını sağlamaktadır. Sonuç olarak, bu bulgular, ankrajsız tankların deprem tasarımında kullanılan prosedürlere katkıda bulunacak ve yüksek deprem riskli bölgelerde tankların deprem performansını artıracaktır.

ACKNOWLEDGMENTS

I would first and foremost like to express my sincere gratitude to my thesis advisor, Asst. Prof. Bülent Erkmen for his invaluable guidance and support throughout my academic life, his patience and tolerance. I could not have done it without him.

I would also like to acknowledge thesis committee members Asst. Prof. Taner Yılmaz and Prof. Dr. Ufuk Yazgan for their valuable feedback and kind comments.

I am incredibly grateful and thankful to Özyeğin University for providing me with financial support and a constructive research environment.

I would like to extend my deepest gratitude to esteemed professors Prof. Dr. Feyza Çinicioğlu, Dr. Derya Deniz, and Dr. Taner Yılmaz for their invaluable contribution to my engineering knowledge. It was truly an honour to have known them and to have gained invaluable knowledge and opportunities to engage in fruitful conversations during my research. Their expertise, guidance, and dedication have played a pivotal role in shaping my educational journey, and I am incredibly thankful for their mentorship and support.

I would also like to express my gratitude to my friends Gülşah Sağbaş, Mahshad Azima, Ozan Eray Aydın, and Ilgın Sandalcı for their invaluable help, support, and motivation. Their presence has made working and spending time with them over the past three years truly enjoyable for me.

I would like to extend my heartfelt gratitude to my mom, dad, little brother, and husband for their encouragement and unwavering spiritual support throughout my studies. Their love and support have played a crucial role in my accomplishments, and I am deeply grateful for their presence in my life.

TABLE OF CONTENTS

LIST OF TABLES

LIST OF FIGURES

This page is intentionally left blank.

CHAPTER I

INTRODUCTION

1.1 Motivation

Liquid storage tanks are important components of modern industrial facilities. They are used for storage of water, nuclear waste, petrochemicals, and various chemical liquids [1]. The behaviour of liquid storage tanks under seismic loads is extremely important since failure of these tanks typically results in large economic losses as well as significant environmental and potentially social effects. The seismic performance of liquid storage tanks is important not only due to structural tank damage but also for the safety of society when they are used as part of critical facilities. This is because these structures often constitute an essential part of a community's lifelines; therefore, need to be in use during after emergencies like earthquakes. Additionally, some facilities may use tanks to store hazardous chemicals concerning human health and the environment facilities such as nuclear plants and petrochemical [2] . Failure of liquid-storage tanks in which petrochemical liquids are stored can cause fires after earthquakes. These fires can be large and may require significant effort to control and may lead to large financial losses [3], [4]. Ensuring a reliable water source for firefighting is crucial for post-earthquake response, and providing safe drinking water immediately after destructive earthquakes is essential to prevent the occurrence of diseases. Also, it is crucial to ensure that tanks storing petrochemicals and liquids like nuclear waste remain functional after earthquakes.

Considering that tanks typically store fluids that are vital for people's well-being and can have a significant impact on the environment and the economy in disaster situations, it is imperative that they demonstrate sufficient performance during such events. Case studies following major earthquakes including the 1994 Northridge earthquake, the 1995 Kobe earthquake [5], and the 2011 Eastern Japan earthquake highlight the importance of tank seismic performance for public health and the country's economy [6]. These events emphasize the need that tanks should withstanding disasters effectively and fulfil their role during and after disaster to ensure safe water supply and mitigate potential damages.

There are two types of liquid storage tanks based on their connection to the foundation: anchored and unanchored, also known as self-anchored per API 650 [7]. Anchored tanks are connected to the foundation using anchor bolts or equivalents to resist overturning moments and lateral loads caused by seismic loads. However, due to cost considerations, tanks in earthquake-prone regions are often not fixed to their foundations if the tank overturning is not critical and the tank sliding over the foundation is negligible or small enough. Unanchored tanks rely on their own weight and friction between the tank base plate and its foundation to resist overturning and tank sliding.

During earthquakes, unanchored tanks experience large overturning moments because the entire tank mass and a significant portion of liquid contents contribute to the moment. When seismic loading changes direction, the previously elevated tank bottom moves downward and the tank elevated portion impacts the foundation, leading to high compressive stresses in the bottom plate, known as elephant foot buckling. Therefore, tank base uplift, which is an important tank seismic performance criterion, should be limited. Additionally, because unanchored tanks are not connected to the foundation, any sliding of the tank base plate or uplift over the foundation should be controlled with design to ensure that connected pipes, valves, or other tank attachments will have relative displacements that are tolerable during earthquakes.

The seismic behaviour of unanchored tanks during earthquakes is highly nonlinear and more complex than what is currently accounted for in design standards. The tank base uplift regulations proposed by codes such as API 650 and Eurocode 8 [8] are based on a mechanical spring-mass model, which may not fully capture the actual behaviour and response of unanchored tanks during seismic events especially if the tank base uplift or sliding occurs.

There are numerous studies, both experimental and theoretical, focusing on the seismic behaviour of anchored liquid storage tanks. Given the significance of these tanks for public health, the environment, and the economy, there is considerable research and a variety of standards available on the seismic performance of liquid storage tanks. However, it is crucial to note that the majority of these studies in the literature are specifically focused on anchored tanks, as they are more commonly used and have been subject to more extensive investigation [9]–[12]. Moreover, there is limited study focusing on seismic performance of unanchored tanks. Most theoretical and computational studies on unanchored tanks do not consider effects of tank base uplift on hydrodynamic loads during seismic events. The uplift of tank base plate under seismic loads is typically estimated by considering various parameters, including tank size, tank aspect ratio, liquid height, tank foundation, local seismicity level, and tank site soil class. However, existing tank codes do not consider the combined effects of all these parameters when calculating the tank uplift value. This lack of comprehensive consideration can result in uncertainties and limitations in the design and seismic performance assessment of unanchored tanks [13]–[15]. Although tank anchorage ratio and tank seismic performance are related there is no study showing the extent of this relationship. Therefore, there is a need for a study showing the relationship between tank anchorage ratios for unanchored tanks and their seismic behaviour.

1.2 Research Objective

In this study, the seismic performance of three unanchored cylindrical steel storage tanks with different anchorage ratios located in a high seismic region was investigated. The tanks were designed without anchorage and assumed to be on rigid foundations. One of the tanks was an existing unanchored tank in a high seismic region, and the other two tanks were designed to have tanks with different anchorage ratios. The anchorage ratio is simply the ratio of the tank's overturning moment to the moment resisting overturning. This study focused on the seismic behaviour of unanchored liquid storage tanks with different anchorage ratio “j” using 3D finite element (FE) models and to determine their seismic performances. The general objective was to determine the relationship between the tank anchorage ratio for unanchored tanks and its effects on tank seismic behaviour including structural damage, tank base uplift, and tank sliding. The study had two particular objectives:

The first objective was to investigate the effects of anchorage ratio j on seismic performance of unanchored tanks. To achieve this, 11 earthquake simulations were conducted for each tank, and the base uplift and sliding results of the tanks were compared under the same seismic events. By analysing the differences in base uplift and sliding behaviour for different anchorage ratios, the study sought to understand the impact of anchorage ratio on tank seismic response for unanchored tanks.

The second objective was to examine the change in base uplift and sliding behaviour of the tanks by considering two different friction coefficients between tank base and its foundation, namely μ = 0.42 and μ = 0.6. To assess the influence of the friction coefficient on tank base uplift and sliding behaviours, 33 nonlinear time history analyses were repeated assuming a friction coefficient of 0.42 and 0.6. By comparing tank seismic performance obtained for different friction coefficients, the study aims to determine the influence of friction coefficient on seismic performance of unanchored tanks.

These study findings will contribute to efforts and design procedures to enhance the seismic behaviour of unanchored steel storage tanks and achieve the following objectives:

1. Determine the seismic performance of unanchored above-ground liquid-storage tanks using 3D advanced finite element technique.
2. Provide insights into effects of anchorage ratio on seismic performance of unanchored tanks.
3. Determine effects of friction coefficients between the foundation and tank base-plate on tank base uplift and base sliding.
4. Identify key tank parameters affecting seismic performance of unanchored steel storage tanks.

1.3 Limitations

This study comprises seven chapters, aligning with its objectives and scope. This study has the followıng limitations:

- The seismic load is applied as ground acceleration history in one directions. In other words, the three components (i.e., two horizontal and one vertical) are not applied.
- The vertical component of ground motion is neglected. The fınıte element modeling approach adopted is not suitable to apply vertıcal seismic load accurately.
- The change of vertical hydrostatic loads due to seismic sloshing on tank base plate ıs not ıncluded sınce vertıcal seısmıc load ıs not applıed
- Tank wall buckling is not considered and it is assumed that tank wall buckling will prevent wıth the design.
- Nonstructural loads and mass are not considered.
- The tank foundatıon is assumed to remain elastic.
- The statıc and dynamic friction coefficients for tank base plate and foundation interactions are assumed to be equal.

1.4 Organization

This study comprises seven chapters, aligning with its objectives and scope.

Chapter 1 includes an introduction to the structures containing liquids, outlining the scope and purpose of the thesis.

Chapter 2 presents a comprehensive literature review on the seismic behaviour of liquid storage tanks, ground connection types of the steel storage tank and their behaviour during historical earthquakes, previous research, tank modelling approach, and seismic design codes.

Chapter 3 focuses on designing prototype tanks based on the API Standard 650 (American Petroleum Institute). These tanks are intended for use in the analytical study discussed in Chapter 4.

Chapter 4 presents the 3D finite element modelling approach employed for unanchored liquid storage tanks using the spring-mass analogy model. It includes parameters used for modelling the prototype tanks and modelling details including tank foundation interaction.

Chapter 5 includes a description of ground motion record selection and scaling procedure to meet tank site design spectrum.

Chapter 6 introduces the time history analysis results including a comprehensive discussion on the behaviour of unanchored storage tanks under seismic load.

Chapter 7 includes a summary of the study including scope and purpose, the findings of the time history analysis, and a discussion of the results regarding effects of tank anchorage ratio as well as selected friction coefficient on seismic behaviour of the unanchored steel storage tank. Also, recommendations for future work are included.

CHAPTER II

LITERATURE REVIEW

2.1 Introduction

This chapter provides a comprehensive literature review on the seismic response of liquid storage tanks. It covers the analysis approach employed in modelling dynamic behaviour of liquid storage tanks. Additionally, the observed performance of liquid storage tanks during earthquakes is summarised including significance and findings of previous studies. The chapter also includes a summary of design guidelines commonly used for the design of liquid storage tanks. The overall objective of this chapter is to offer an overview of the dynamic behaviour of liquid storage tanks under seismic conditions.

2.2 Previous Research

Literature on liquid storage tanks has focused on seismic behaviour of rigidly anchored liquid storage tanks, with notable contributions from various analytical studies. Over the years, numerous theoretical and experimental research have been conducted to examine the dynamic response of liquid-storage tanks. These studies aim to understand and analyse the behaviour of tanks subjected to various dynamic loads, including seismic forces, wind forces, and fluid sloshing. The combination of experimental testing and theoretical modelling provides valuable insights into structural response, stability, and failure modes of liquid-storage tanks under dynamic loading conditions. The findings from these studies contribute to the development of design guidelines and optimization strategies for ensuring the safety and performance of liquid-storage tank structures. Notable contributions were made by Housner [16] Veletsos [17],Veletsos and Yang [18], Malhotra, et al. [19] , Haroun [20] and others. The seismic behavior of anchored liquid-storage tanks is well established by Haroun and Badawi [21].

Veletsos developed an alternative analysis approach for flexible liquid-filled tanks [22]. He proposed a simple procedure to evaluate hydrodynamic forces induced in these tanks under seismic loads. Later, Veletsos and Yang [18] modified Housner's model to estimate the maximum base overturning moment caused by horizontal earthquake motion. They introduced simplified formulas based on the Rayleigh-Ritz energy method to determine the fundamental natural frequencies of liquid-filled tanks.

In 1963, Housner utilised a boundary integral theory to calculate the fluid added mass matrix [23]. This approach, unlike displacement-based fluid finite elements, significantly reduced the number of unknowns in the problem. Haroun [20], [24] also employed the boundary integral theory in 1980 and 1983 to derive the fluid added mass matrix.

These advancements in analysis techniques by Veletsos, Housner, and Haroun contributed to improved understanding and modelling of flexible liquid-filled tanks. Their work offered simplified procedures and reduced computational complexities, enhancing the efficiency and accuracy of analysing the dynamic behaviour of liquid storage tanks.

The seismic behaviour of unanchored liquid storage tanks has received limited attention in terms of understanding and documenting their seismic response. Due to practical and economic considerations, many tanks are constructed directly on compacted soil without anchoring if overturning is not likely and tank sliding is limited and within tolerable limits. However, reliable guidance for predicting tank base uplift, tank behaviour, and water sloshing in unanchored tanks is lacking. The dynamic behaviour of unanchored tanks differs significantly from that of anchored tanks due to the uplift mechanism or potential sliding involved [25]. In a study by Malhotra et al. [26], uplifting behaviour of the base plate of an unanchored tank was investigated. This study aimed to analyse and understand the uplift mechanism for unanchored tanks, providing insights into their seismic response. A simplified nonlinear analysis method was developed as a part of the study. This method aimed to facilitate performance-based seismic design for unanchored tanks, providing a practical approach for considering the dynamic behaviour and response of these tanks during seismic events. Malhotra's study contributed to understanding the behaviour of liquid-storage tanks supported directly on flexible foundations and provided insights for the design of unanchored tanks under seismic loading conditions.

Overall, further research and documentation are needed to enhance the understanding of the seismic behaviour of unanchored liquid storage tanks and to develop reliable predictive methods for their response.

Due to the complex nature of the dynamic uplift phenomenon, accurately predicting and analysing the behaviour of unanchored tanks during seismic events requires comprehensive nonlinear transient analysis methods. These methods aim to capture the interaction between the tank, fluid, and foundation, considering factors such as fluid-structure interaction, soil-structure interaction, and the nonlinear behaviour of the tank structure itself. Understanding and addressing the dynamic uplift of unanchored tanks is crucial for ensuring their structural integrity and safety during seismic events [27]. During earthquakes, unanchored tanks experience significant overturning moments as the entire mass of the tank and its contents contribute to this moment. However, only a small portion of the mass contributes to the overturning resistance, making unanchored steel tanks particularly vulnerable to damage during seismic events. Tank base uplift is often accompanied by large deformations and significant changes in the stress distribution along the tank wall and tank base plate or annular plate. When the seismic loading reverses and the previously uplifted segment moves down, it impacts the ground and introduces high compression stresses into the tank shell. This can lead to buckling of the tank shell in the vicinity of the tank base.

In addition, the behaviour of the contained liquid further complicates the analysis of unanchored tanks during earthquakes. Reliable analysis results require considering the dynamic interaction between the tank, liquid, and foundation. However, modelling such a coupled tank-liquid-foundation system is extremely challenging due to its complex nonlinear behaviour. Consequently, ongoing studies are being conducted in this field to better understand and model the behaviour of unanchored tanks subjected to seismic loading. The complex nature of unanchored tank behaviour during earthquakes underscores the need for comprehensive analysis and design approaches to ensure their structural integrity and mitigate potential damage.

Barton and Parker [10] conducted pioneering research on the seismic response of liquid-filled cylindrical storage tanks using the Finite Element Method (FEM) within the ANSYS structural analysis software. Their study introduced the incorporation of added mass concepts and displacement-based fluid finite elements to accurately consider the influence of the liquid in the tank.

Virella et al. [9] conducted dynamic buckling analyses of anchored steel tanks under horizontal earthquake excitations. They utilised three-dimensional (3D) finite element models and introduced lumped added mass to the shell nodes of these models using massless spring elements. This approach allowed for a comprehensive investigation of the buckling behaviour of the tanks under seismic loads.

Ozdemir et al. [11] studied the application of the nonlinear fluid-structure coupling method to the seismic analysis of anchored and unanchored storage tanks. They specifically focused on capturing the uplift mechanism of the base plate. This was achieved by establishing a relationship between the base uplift and the overturning moment generated by the motion of the liquid within the tank. The research aimed to enhance the understanding of the dynamic behaviour of tanks under seismic loads.

Cylindrical tanks play a crucial role in various civil engineering installations and industrial facilities. They are commonly used for storing liquids such as water, wine, oil, nitrogen, high-pressure gas, petroleum [1],[28]. However, these tanks have been significantly impacted by numerous major earthquakes worldwide. For example, historical records reveal instances of failure and extensive damage to liquid storage tanks, including the notable case during the 1960 earthquake in Chile [29], the 1964 earthquake in Alaska [2], earthquake in Kocaeli [3]. The American Society of Civil Engineers (ASCE) published a document in 2001 called "Seismic Fragility Formulations for Water Systems," which focuses on assessing the vulnerability of water systems to seismic events. Many elevated tanks failed in this earthquake as reported [30],[31]. The 1964 Prince William (Great Alaska), USA earthquake caused significant damage to the oil storage tanks given in [32]. The impact of the aforementioned earthquake drew the focus of earthquake engineering researchers towards the development of seismic design guidelines for liquid storage tanks. Notably, smaller tanks experienced more severe damage compared to larger ones. Instances of elephant foot buckling, damage to connecting pipes, tank shells, and roof failure were observed in some tanks. Furthermore, there were reports of fires occurring in certain tank farms. A significant aspect of this earthquake was the simultaneous occurrence of damage to tank farms caused by the earthquake itself, fires, and sloshing movement. During the 1999 Kocaeli earthquake in Turkey, six cylindrical tanks with floating roofs caught fire due to the ignition of the naphtha contained within them. The fire subsequently spread to the adjacent tanks as shown in Figure 1 and explained by [3],[33].

Figure 1: Tupras refinery fire after 1999 Koaceli Earthquake [34]

Past seismic performance liquid storage tanks indicate that seismic vulnerability of these structures is evident. Several modes of failure have been reported in continuously supported cylindrical tanks during past earthquakes. The most typical types of damage seen in these tanks include buckling of the tank walls caused by high compressive stress, failure of the anchorage system caused by the high overturning moment carried to the base, penetration of the tank wall with anchor bolts caused by the anchorage system's prior failure, and damage caused by sloshing of the free liquid surface on the roof. Wall buckling, roof damage from sloshing, and implosion from a sudden loss of contents are common modes of failure. Large axial compressive stresses can cause elephant-foot buckling of tank walls. Sloshing liquid can damage the roof and the top of the tank wall.

Typically, cylindrical tanks have either anchored or unanchored foundations. An enormous overturning moment occurs in both anchored and unanchored tanks during violent ground motion as a result of the hydrodynamic pressure on the walls [35]. The large overturning moment exerted on the tanks can result in a partial uplift of the tank base. This partial uplift leads to several nonlinear behaviour mechanisms, including variations in the contact between the base plate and the foundation, significant deflections of the base plate, material yielding, and plastic rotation of the base plate. These nonlinear effects play a significant role in the response and behaviour of the tanks under seismic loading conditions [28]. It is crucial for the analysis procedure to be capable of capturing not only the overall seismic responses but also the damage states of various tank components when subjected to seismic loading. This comprehensive analysis approach provides a more holistic understanding of the tank's behaviour and facilitates the assessment of potential damage to different components of the tank structure [36].

The tank base uplifting and tank shell deformation are coupled behaviours which affect the seismic behaviour of the tank mainly by affecting the seismic behaviour of the liquid [37]. Therefore, the initial studies were performed with the assumption that the tank is rigid and fully anchored to a rigid base [12], [16], [37]. Later, some studies considered the flexibility of the tank wall and revealed its considerable influence on the magnitude and characteristics of the resulting response [22],[38],[39]. More recently, Malhotra and Veletsos [40] developed a simplified method of dynamic analysis for unanchored tanks subjected to only one horizontal direction; this simplified method considered the vertical uplifting of the tank base and the flexibility of the tank wall.

However, the implementation of this simplified method in earthquake time-histories is not straightforward [41]–[43]. Similarly, numerical investigations have been conducted using various numerical techniques, primarily the finite element method (FEM), to assess the seismic behaviour of this specific type of tanks. The FEM, among other numerical methods, has been widely employed to simulate and analyse the response of liquid storage tanks under seismic loads. These numerical techniques provide valuable insights into the structural behaviour, dynamic response, and overall seismic performance of these tanks, aiding in their design and safety assessment. In their previous studies, Barton and Parker [10] conducted an analysis of the seismic behavior of cylindrical tanks, considering both anchored and unanchored configurations. They employed a three-dimensional finite element model; however, this model did not incorporate significant deformations or the yielding of the tank base material. Later, Peek and Jennings [44] focused on the examination of unanchored tanks by utilizing a linear finite element model. They introduced nonlinear springs at the bottom of the tank wall to account for the nonlinear effects of the base plate. In a more recent investigation, Virella et al. [24] specifically studied the elastic buckling phenomenon occurring at the top of cylindrical tanks that were fully anchored at the base. Additionally, numerical techniques have been employed in recent studies to forecast the behaviour of three-dimensional large-amplitude liquid sloshing within tanks [28]. The technical literature regarding the seismic performance of unanchored cylindrical tanks is limited. Only a handful of recent experimental studies have delved into the analysis of stress distribution on the tank wall specifically for unanchored tanks [45].

2.3 Design Codes and Standards

Numerous codes and guidelines exist for the design and analysis of liquid storage tanks. Many of these standards are rooted in Housner's seismic response analysis of rigid cylindrical storage tanks conducted in the 1950s. Housner's model incorporates fluid as an impulsive and convective mass component, as depicted in Figure 2. The convective component gives rise to sloshing phenomena in the upper part of the liquid, while the impulsive component behaves as a rigid mass moving with the storage tank.

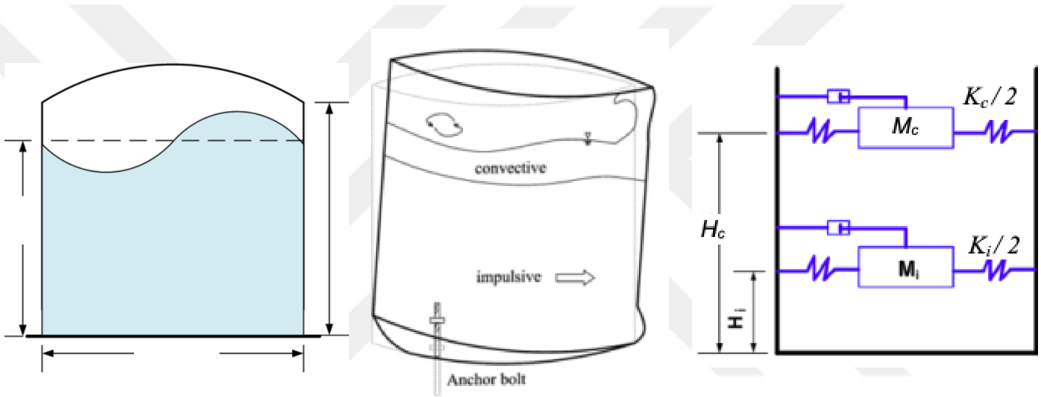

Figure 2: Convective and impulsive liquid components and modelling liquid

A summary of some standards on liquid storage tanks are:

- The American Water Works Association (AWWA) provides codes for the design of steel and concrete storage tanks. AWWA D100 is a widely recognized standard that is specifically used for the design of welded steel tanks for water storage, while AWWA D110 and AWWA D115 are specific to concrete liquid storage tanks

- The New Zealand Code NZSEE [46] on Seismic Design of Storage Tanks includes analysis methods for both rigid and flexible wall storage tanks, based on the study by Veletsos [17].
- Eurocode 8, specifically Part 4: Silos, tanks, and pipelines, is based on the work of Veletsos and Yang [18] and focuses on rigid circular storage tanks. The analysis of flexible circular storage tanks in Eurocode 8 draws from the studies of Haroun & Housner [39], Veletsos [17]and Veletsos & Ventura [47]. Other significant contributions to this code are also mentioned [26]. Eurocode 8 provides a detailed explanation of the impulsive and convective pressure aspects of fluid.
- The American Petroleum Institute (API) offers leading standards for the design of liquid storage tanks, namely API 650 Welded Steel Tanks for Oil Storage[7] and API 620 Design and Construction of Storage Tanks. Housner's research [16] has greatly influenced these codes.

A summary of API 650 procedure for determining seismic loads of anchored tanks is given in this section since this approach is employed in this study for the tanks studied. The important parameters are defined in the following equations.

The effective impulsive weight W_i is defined as a function of total liquid weight W_p as:

When D/H is greater than or equal to 1.333:

$$W_i = \frac{\tanh\left(0.866\frac{D}{H}\right)}{0.866\frac{D}{H}} W_p \tag{2-1}$$

When D/H is less than 1.333:

$$W_i = \left(1 - 0.218\frac{D}{H}\right)W_p \tag{2-2}$$

The effective convective weight:

$$W_c = 0.230\frac{D}{H}\tanh\left(3.76\frac{D}{H}\right)W_p \tag{2-3}$$

Center of action for effective lateral liquid seismic forces:

For impulsive liquid when D/H is greater than or equal to 1.333:

$$H_i = 0.375H \tag{2-4}$$

For impulsive liquid when D/H is less than 1.333:

$$H_i = \left(0.5 - 0.094\frac{D}{H}\right)H \tag{2-5}$$

The effective convective liquid:

$$H_c = \left[1.0 - \frac{\cosh\left(0.866\frac{D}{H}\right) - 1}{\frac{3.67H}{D}\sinh\left(\frac{3.67H}{D}\right)}\right]H \tag{2-6}$$

The impulsive and convective liquid natural periods T_i and T_c are shown Equation (2-7) and Equation (2-8):

For impulsive liquid when D/H is less than 1.333:

$$T_i = \left(\frac{1}{27.8}\right)\left(\frac{C_i H}{\sqrt{t_u/D}}\right)\left(\sqrt{\frac{\rho}{E}}\right) \tag{2-7}$$

Where C_i is a coefficient for determining impulsive period, t_u is equivalent uniform thickness of tank shell, E is elastic modulus of tank material, and ρ is fluid density.

For the effective convective liquid:

$$T_c = 1.8\left[\frac{0.578}{\sqrt{tanh\left(\frac{3.68H}{D}\right)}}\right]\sqrt{\mathrm{D}} \qquad (2\text{-}8)$$

The spring stiffness are simply computed from general relations of mass, period, and stiffness as:

$$T = 2\pi\sqrt{\mathrm{m/k}} \qquad (2\text{-}9)$$

CHAPTER III

PROTOTYPE TANK DESIGN

3.1 Anchorage Ratio, J

API 650 standard, Annex E focuses on the seismic design of storage tanks. The *H*/*D* ratio, which represents the height of the tank divided by its diameter, is an important parameter considered in tank design. This ratio has direct impacts on various aspects, such as the effective weight of the product and calculations related to overturning moments. Additionally, it indirectly affects the design of the support system for the tank. One crucial aspect of tank design is to ensure stability and structural integrity during seismic events or other loading conditions. The tank foundation connection - anchored tank or unanchored (self-anchored) - depends on anchorage ratio criteria as shown in Table 1.

The anchorage ratio is simply the ratio of the tank's overturning moment to the moment resisting overturning. For self-anchor tanks, the API 650 standard specifies that the anchorage ratio (*J*) value should be less than 1.54 for a tank to be unanchored. To establish the relationship between the anchorage ratio and tank seismic performance, tanks with different *J* values are designed, and their seismic behaviour and performance are evaluated in this thesis.

Table 1: Anchorage ratio criteria per API 650

Tank Type	Anchorage Ratio, J
Self-anchored with no uplift	$J \leq 0.785$
Self- anchored with uplift	$0.785 < J \leq 1.54$
Mechanical anchor otherwise unstable	$J > 1.54$

There are three classes of liquid-storage tanks based on the relative magnitude of the overturning moment and the tank's uplift resistance (i.e., anchorage ratio). These are:

- Self-anchored tanks with no uplift: These tanks do not experience tank base uplift and rely on their own weight and friction to remain stable.
- Self-anchored tanks with uplift: These tanks experience tank base uplift during seismic events. They are designed to have a specific anchorage ratio (i.e., $0.785 < J \leq 1.54$). This range ensures that the tanks will have uplift for the selected seismic level while still maintaining stability.
- Mechanically anchored tanks: These tanks require additional mechanical means, such as anchor bolts or other fastening systems, to resist uplift forces and maintain their lateral stability. A higher anchorage ratio indicates that the restraining forces are smaller than the horizontal seismic forces and require larger anchorage forces on the foundation.

In this study, the self-anchored tank design ensures that the prototype tanks will experience uplift for the selected seismic level while still being stable. The tank roof is assumed to be a self-supporting dome, contributing to the overall stability of the tank structure. For the seismic design of liquid-storage tank, the tank site is assumed to have high seismic risk with the following design parameters:

Tanks were classified as seismic use group SUG I. The Seismic Use Group (SUG) for the tank shall be specified by the Purchaser. If this is not specified, the SUG shall be assigned to be SUG I.

The site was classified as seismic site class ZC according to TBDY 2018 [48].

The maximum considered earthquake parameters were taken as S_s = 1.345, S_1 = 0.367, and T_L = 6 sec. Corrosion allowance is assumed to be zero. Seismic force reduction factors R_{wc} and R_{wi}, representing convective and impulsive vibration modes respectively, were taken as 2.0 and 3.5 per API 650.

To facilitate the tank design process, a spreadsheet based on API 650 provisions was developed. The design steps included the design of the tank shell plates, bottom and annular bottom plates, roof plates, determination of seismic parameters, loads, and overturning moment, tank freeboard requirements, anchorage ratio, anchorage type selection, and evaluation of tank sliding and overturning resistances. In total, the seismic performance of three unanchored tanks was studied. Table 2 provides the basic geometric properties of these tanks. Tank-A is an existing in-service tank while Tank-B and Tank-C were designed as a part of this study. The seismic performance of these tanks was evaluated using eleven strong ground motion records selected for the site and scaled to match site design spectrum.

Table 2: Studied tanks of tanks based on their uplift resistance

Tank Type	Diameter (m)	Tank water height (m)	Design liquid height (m)	Anchorage ratio, *J*
Tank-A	10.7	11.4	11.4	1.51
Tank-B	36.6	15.2	15.2	1.10
Tank-C	55.0	21	21.0	0.97

3.2 Seismic Design Forces

Seismic design forces for unanchored tanks are calculated based on various factors, including the tank geometry, material properties, seismic hazard level, and relevant design codes. The design forces consider the dynamic response of the tank and aim to ensure its stability and prevent excessive overturning or sliding during seismic events. The specific calculation methods can vary depending on the design code or standard being used, such as API 650 or Eurocode 8. The seismic design forces typically include horizontal forces (such as base shear and overturning moment) and vertical forces (such as uplift or compression). These forces are determined through complex analyses that consider the tank's mass, flexibility, and interaction with the supporting foundation or soil.

3.3 Model Properties

The tanks were modelled using the general-purpose finite element package ABAQUS software [49]. A sample modelled cylindrical tank view is given in Figure 3. The height of the Tank A to the roof level is approximately 12.4 m and the roof height is 1.0 m. The walls of the tank are formed by welding nine rings of S235 steel plates, approximately 1.4 m high. A 10 mm thick steel plate was used for the lowest ring and 6 mm thick for the top ring. The steel plate used for the roof is 5 mm thick.

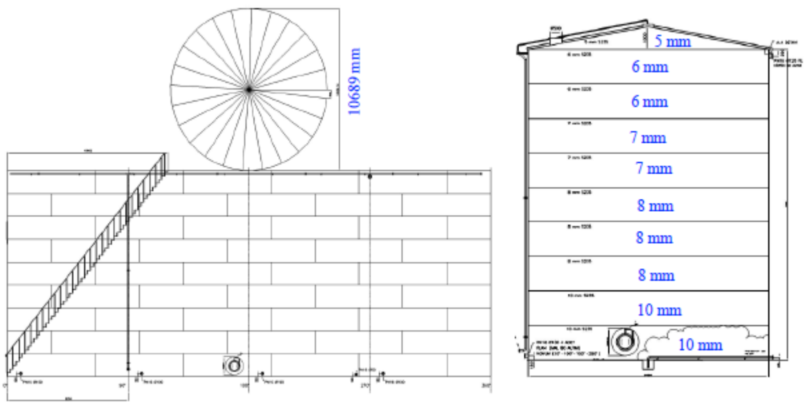

Figure 3: General view and wall thicknesses of Tank A

Tank B has a total height of 14.6 m, including a roof height of 2.4 m. The tank walls consist of six rings of S235 steel plates, each approximately 2.4 m in height. The walls are constructed using 10 mm thick steel plates. The roof, on the other hand, is made of a 13 mm thick steel plate.

Tank C, on the other hand, has a total height of 15.8 m, with a roof height of 0.6 m. The tank walls are formed by welding together seven rings of S235 steel plates, each approximately 2.4 m in height. The thickness of the steel plates used varies, with the lowest ring being 14 mm thick, the top ring being 10 mm thick, and the roof being made of a 5 mm thick steel plate.

The finite elements (FE) meshes have been refined in order to model accurately higher modes of vibration in which more localised displacements may occur. The walls and roof of all the tanks were divided into meshes with an average size of 30 cm.

For the analysis, Tank A, Tank B, Tank C were assumed to be full and the liquid height was taken as 11.4 m, 15.2 m, 21m, respectively.

The liquid pressure corresponding to the specified fill level of the tank was applied statically to the wall and floor plate surfaces of the tank. The empty weight of tanks was applied to the model as a static load. Horizontal earthquake motion was applied to the reinforced concrete foundation of the tank as acceleration. Tank foundation dynamic interaction was modelled using contact interaction, which allowed the tank to slide over the foundation and separate (uplift) from its foundation.

3.4 Seismic Design

The design of tank plates involves determining the appropriate thickness required for the tank's shell plates, bottom plates, and roof plates. The design of tank plate thickness is a critical aspect of tank design to ensure structural integrity and safety. The plate thicknesses are determined for designed tanks using API 650 procedures. In the following sections, a summary of individual plate design is given.

3.4.1 Shell Plate

In the tank design process, determination of tank shell plate thickness is a crucial step. The thickness requirement for the shell plates varies along the height of the tank due to the varying liquid pressures experienced at different points under both static and seismic conditions. To minimize cost and weight, different shell plate thicknesses are often used at different heights.

API 650 provides the 1-Foot Method for calculating tank shell plate thickness. This method involves determining the thickness at specific design points located 0.3 m above the bottom of each shell course. The purpose of selecting these design points is to capture the maximum liquid pressure experienced by the tank at different heights. The required minimum thickness of the shell plate is determined as the maximum value between the design shell thickness (t_d) and the hydrostatic test shell thickness (t_t). The minimum required shell plate thickness at each design point is then determined as the maximum value between (t_d) and (t_t). This fact ensures that the tank shell plates are thick enough to withstand the design pressure and the hydrostatic test pressure at each specific height along the tank. The esign shell thickness (t_d) and the hydrostatic test shell thickness (t_t) formulas are given in Equation (3-1) and (3-2)

$$t_d = \frac{2.6D(H-1)G}{S_d} + CA \tag{3-1}$$

$$t_t = \frac{2.6D(H-1)G}{S_t} \tag{3-2}$$

In some cases, using the theoretically calculated shell plate thickness may not align with the available standard thicknesses of steel plates. To address this, the final shell plate thicknesses for the tanks can be determined based on the available plate thicknesses provided by the steel producer.

Tank A is an existing steel storage tank in the Kocaeli region. The informations on the bottom and wall thickness of the tank walls and the roof design presented in the thesis are based on the actual data obtained from Tank A. These data provide information for subsequent analysis of its seismic performance. Tank A is an existing tank, whereas Tank B and Tank C are tanks that have been designed. This information is given in Table 3. The computed and selected shell plate thicknesses for Tank B and Tank C tanks are provided in, Table 4, and Table 5.

3.4.2 Annular Bottom and Tank Bottom Plates

The annular bottom plate is a crucial component of a liquid-storage tank as it provides support to the tank shell and facilitates load transfer to the foundation while resisting uplift forces. The determination of the annular bottom plate thickness is based on the provisions outlined in API 650. The minimum thickness of the annular bottom plate of the tank is determined as a function of the design shell thickness (t_d) and the hydrostatic test shell thickness (t_t) calculated for the first tank shell plate from the tank bottom. API 650 provides recommended minimum thickness values based on the stress and plate thickness of the first shell course of the tanks. In API 650, there are no detailed requirements for the thickness of the tank bottom plate. This is because the bottom plate is not subjected to significant stresses under static loads as it is supported by the foundation. To simplify the design process and for practical reasons, the thickness of the tank bottom plate is typically selected to match the thickness of the annular bottom plate.

3.4.3 Roof Plate

The roof was assumed to be a self-supporting dome shape. API 650 provides guidelines for the minimum and maximum roof radius values, which are specified as 0.8 times the tank diameter (0.8D) and 1.2 times the tank diameter (1.2D), respectively. For the tanks in this study, a roof radius of 1.0 times the tank diameter (1.0D) was assumed.

The thickness of the tank roof plate was determined according to the provisions outlined in API 650. However, it's important to note that in the 3-dimensional finite element tank models developed for this study, a conservative approach was taken. The tank roof was modelled for the three steel tanks. The modelling of the tank roof allows the interaction between the roof structure, the tank shell and the roof to give a more accurate result in the finite element model. This approach provides an accurate representation of tank behaviour in the analysis, considering the interactions and effects between the tank shell and the roof, while providing accurate results in modelling.

Table 3: Summary of the data for Tank A

TANK-A: DESIGN SUMMARY DATA				
Tank main geometry		**Tank main plates**	**Thickness (mm)**	**Approximate weight (kN)**
Tank diameter (m)	10.7	Annular bottom plate	10	60.7
Design liquid height (m)	12.4	Bottom plate	13	433.3
Roof diameter (m)	21.4	Roof plate	5	175
Tank shell plates				
Shell course	Shell width	Distance (from shell bottom to tank shell top)	Provided shell thickness	Shell weight
	(m)	*H* (m)	(mm)	(kN)
1	1.4	12.4	10	114
2	1.3	11.4	10	91
3	1.3	10.1	8	91
4	1.3	8.8	8	91
5	1.3	7.5	8	91
6	1.3	6.2	7	91
7	1.3	4.9	7	91
8	1.3	3.6	6	91
9	1.3	2.3	6	91
10	1	1	5	70

Tank anchorage ratio (i.e. J) was computed to be 1.51

Table 4: Tank-B Design Summary

TANK-B: DESIGN SUMMARY DATA				
Tank main geometry		**Tank main plates**	**Thickness (mm)**	**Approximate weight (kN)**
Tank diameter (m)	36.6	Annular bottom plate	6	34
Design liquid height (m)	15.2	Bottom plate	6	478
Roof diameter (m)	73.2	Roof plate	25	2047

Tank shell plates						
Shell course	Shell width (m)	Distance (from shell bottom to tank shell top) H (m)	Design shell thickness t_d (mm)	Hydro-test shell thickness t_t (mm)	Provided shell thickness (mm)	Shell weight (kN)
1	2.4	15.2	14	13	14	307.9
2	2.4	12.8	12	11	13	273.7
3	2.4	10.4	9	9	10	205.2
4	2.4	7.9	7	7	10	205.2
5	2.4	5.5	5	4	10	205.2
6	2.4	3.0	3	2	10	205.2
7	0.6	0.6	0	0	10	51.3

Tank anchorage ratio (i.e. J) was computed to be 1.10

Table 5: Tank-C Design Summary

TANK-C: DESIGN SUMMARY DATA

Tank main geometry		**Tank main plates**	**Thickness (mm)**	**Approximate weight (kN)**
Tank diameter (m)	55	Annular bottom plate	10	95
Design liquid height (m)	21	Bottom plate	10	1632
Roof diameter (m)	110	Roof plate	30	5180

Tank shell plates

Shell course	Shell width (m)	Distance(from shell bottom to tank shell top) H (m)	Design shell thickness t_d (mm)	Hydro-test shell thickness t_t (mm)	Provided shell thickness (mm)	Shell weight (kN)
1	2.4	21.4	29	27	32	1026
2	2.4	18.9	26	24	29	924
3	2.4	16.5	23	21	29	924
4	2.4	14.0	19	18	21	667
5	2.4	11.6	16	15	16	513
6	2.4	9.2	12	11	13	410
7	2.4	6.7	9	8	10	308
8	2.4	4.3	6	5	8	257
9	1.8	1.8	2	2	8	192

Tank anchorage ratio (i.e. J) was computed to be 0.97

,

CHAPTER IV

MODELING OF LIQUID STRORAGE TANKS

4.1 Spring- Mass Analogy Model

The finite element method is employed to investigate the interaction between the tank and the liquid, as well as to analyse the actual seismic behavior of tanks containing liquid. Generally, two approaches are followed in modelling of tanks using finite element analysis. The first approach is the finite element method where the liquid inside the tank is directly modelled. Due to the direct modelling of the liquid, this method is quite complex and requires a long time for analysis. Obtaining certain analysis results, such as dynamic changes in liquid pressure, is also more challenging. This method is gaining popularity with the availability of powerful finite element programs and high-performance computers.

In this study, the "mechanical tank model" is preferred due to the large number of analyses and earthquake load cases, the complexity of the contact behaviour between the tanks and the ground (sliding and uplifting of the tank on the ground), which increases the complexity of the seismic analysis, and prolongs the analysis time. This method is relatively simpler and is based on the assumption that it considers the dynamic behaviour of only the impulsive and convective masses. This method is widely used in the literature and relevant industries. Also, the tank regulations, such as API 650 (American Petroleum Institute), used in this thesis are based on this method.

The method employs linear elastic springs to connect the impulsive mass, which moves with the tank, and the liquid masses responsible for sloshing motion at the upper part of the tank to the tank walls. The stiffness (spring constants) of these springs is determined based on the first mode vibration period of the liquid. This approach results in a tank model as depicted in Figure 4. The magnitudes, vibration periods, and placement of these impulsive and convective liquid masses within the tank's height are determined using the formulation provided in API 650 and Section 2.3. This method allows for a simplified yet effective representation of the tank's dynamic behaviour under seismic loads.

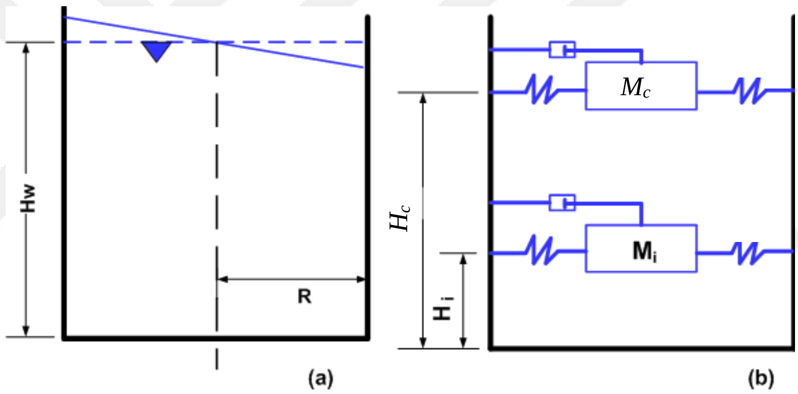

Figure 4: Mechanical Tank Model for Cylindrical Tanks

The mechanical tank model parameters for cylindrical storage tanks are as follows:

- Tank Base: The tank base is assumed to be on a rigid foundation.
- Impulsive Liquid Masses (M_i): Impulsive motion is represented using liquid masses located at the lower levels of the tank. These masses oscillate rigidly in parallel with the tank's motion. The impulsive liquid masses are connected to the lower walls of the tank through linear elastic springs.

- Convective Liquid Masses (M_C): Convective motion is represented using liquid masses located at the upper levels of the tank. These masses exhibit long-duration sloshing motion. The convective liquid masses are connected to the upper walls of the tank through linear elastic springs.

The mechanical tank model adequately represents the general behaviour of cylindrical tanks. Of course, it is possible to further enhance the modelling depending on the specific characteristics and details of the tank. However, this basic approach is a widely used method in the analysis of the seismic behaviour of unanchored cylindrical storage tanks.

4.2 Tank Finite Element Model

The tank 3D finite element model is developed using ABAQUS Software [49]. The developed model is shown in Figure 5 and Figure 6. Tank roof framing is modelled using B31 beam element, which is a 2-node linear beam element, and tank shell and bottom plates are modelled using an S4R shell element, which is a four-node doubly curved general-purpose reduced integration element. The tank-reinforced concrete foundation was modelled as a separate part using S4R shell elements. For tank plates and roof frame elements, nonlinear material definition was used using typical stress-strain curves for S235 steel grade. The foundation was modelled using elastic-perfectly plastic material properties for class C30 concrete. The nominal mesh size for beam and shell elements is 25 cm as shown in Figure 5.

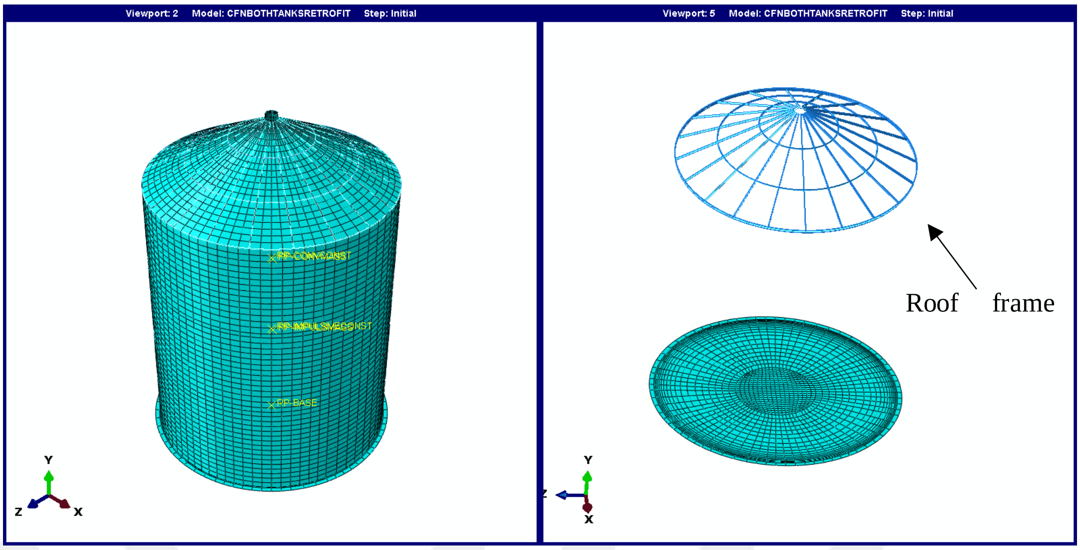

Figure 5: Tank shell, roof framing, and foundation of Tank A

The liquid masses for convective and impulsive components were connected to the tank wall as shown in Figure 6. Two different reference point was specified to assign the liquid masses and another reference point was used to connect this reference point to the tank shells through coupling constraint.

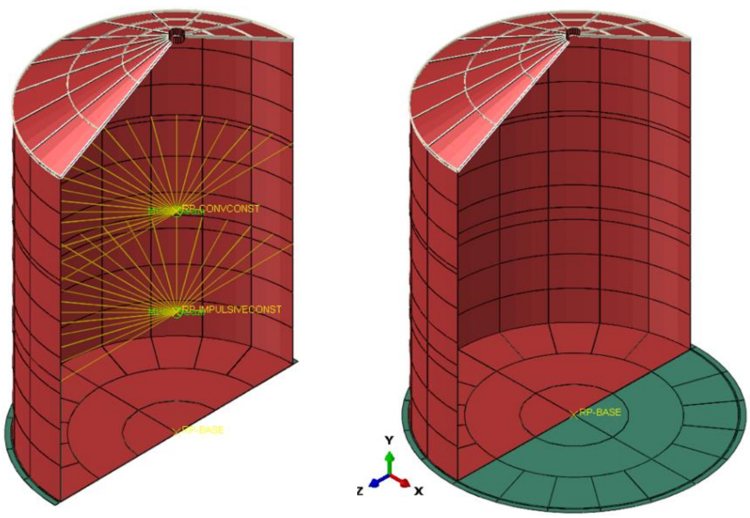

Figure 6: Tank shell, roof framing, and foundation of Tank A

The required parameters to define the tanks spring-mass model are given in Table 6 and computed using API 650 seismic provisions. The impulsive periods of Tank A, Tank B, Tank C are computed as 0.4, 0.74, and 0.89 sec, and convective periods are computed 3.4, 5.3, 6.63 sec, respectively. The tank self-weight and liquid initial hydrostatic pressures were applied as static loads. The ground acceleration was applied to the foundation in the following implicit dynamic analysis step.

Table 6: Summary of spring properties for tanks

Parameter	Unit	TANK-A	TANK-B	TANK-C
M_i	*kg*	740000	3086586	7464282
K_i	*N/m*	151768	2.24E+08	3.73E+08
T_i	*sec*	0.4	0.74	0.89
H_i	*m*	4.7	4.57	5.72
M_c	*kg*	200000	2487999	8043281
K_c	*N/m*	743.386	3.49E+06	7.22E+06
T_c	*sec*	3.4	5.3	6.63
H_c	*m*	8.6	7.38	8.82

4.3 Foundation Structure Interaction

In the analysis of unanchored storage tanks, the consideration of foundation-structure interaction becomes even more crucial. Unanchored tanks are not fixed to the foundation, which allows for sliding and uplifting movements during seismic events. The friction coefficient between the tank base and the foundation significantly affects the tank's sliding behaviour and overall stability.

The friction coefficients were selected as 0.42 and 0.6. As per API 650 standards, the friction coefficient between the tank base and the foundation should not exceed 0.42 to ensure stability. It has been considered to use lower friction coefficients so that the result of the sliding movement can remain in a safer range. However, a value of 0.6 was chosen to assess the probability of the ground beneath the tank being rough. This choice led to higher uplift values, allowing for a comparative examination of the earthquake performances of the tanks under these conditions. The tank base and foundation dynamic interaction was defined using contact interaction with separation allowing tank uplift and re-contact upon load reversal.

CHAPTER V

SEISMIC ANALYSIS

5.1 Ground Motion Selection

5.1.1 Earthquake Ground Motion of the Tank Field

The earthquake ground motion levels to be used in determining the seismic performance of tanks containing liquids and the minimum performance targets for tanks at these ground motion levels have been determined in accordance with the Turkish Building Earthquake Regulation 2018 [48]. Accordingly, the performance evaluation of the tanks must be made at the DD-2 earthquake ground motion level to achieve the seismic performance level. The DD-2 earthquake ground motion is characterised as a rare earthquake ground motion with a 10% probability of exceeding the spectral magnitudes over 50 years. Controlled Damage is the performance objective under the design earthquake of DD-2 It corresponds to a damage level in the structural system elements that are not very severe and mostly repairable.

5.1.2 Seismic Hazard at Tank Sites

The earthquake data for the DD-2 ground motion level was obtained from the Turkey Earthquake Hazard Maps (Figure 7), which were put into effect by the government with the decision number 2018/11275 and the date of 20/01/2018 (https://tdth.afad.gov.tr)[50]. The short-period spectral acceleration coefficient (Ss) for the tank field located at

40.810382° East Latitude and 29.558389° North Longitude was determined as 1.345, and 0.267 was identified as the spectral acceleration coefficient (S1) for a 1.0 second period.

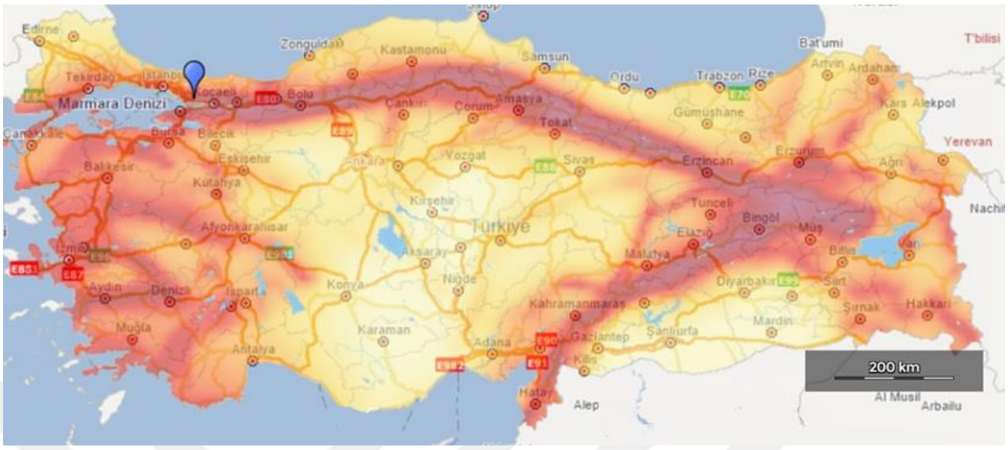

Figure 7: Turkey Earthquake Hazard Map and the location of the tank field

According to TBDY 2018, these coefficients need to be corrected according to the local soil classes. Since there is no data report presenting the results of soil investigations for the tank field or geotechnical report prepared for structural evaluation, the local soil class of the tank field is unknown. At this point, the Kocaeli Metropolitan Municipality Soil Earthquake Investigation Branch Directorate utilised the Kocaeli Province NEHRP Soil Classes map. According to the map, the NEHRP local soil class of the tank field appears to be ZB, but considering the possibility of weaker local soil, it was accepted as ZC to be on the safe side. According to TBDY 2018, the soil type for the ZC local soil class is very dense sand, gravel and hard clay layers or separated, highly fractured rocks. The short period design spectral acceleration coefficient (SDS) and the design spectral acceleration coefficient (SD1) for the 1.0 second period were computed as 1.614 and 0.551, respectively, after the local soil impacts were taken into consideration in accordance with the ZC local soil class.

Yerel Zemin Sınıfı	Zemin Cinsi	Üst 30 metrede ortalama		
		$(V_S)_{30}$ [m/s]	$(N_{60})_{30}$ [darbe /30 cm]	$(c_u)_{30}$ [kPa]
ZA	Sağlam, sert kayalar	> 1500	–	–
ZB	Az ayrışmış, orta sağlam kayalar	760 – 1500	–	–
ZC (1)	Çok sıkı kum, çakıl ve sert kil tabakaları veya ayrışmış, çok çatlaklı zayıf kayalar	360 – 760	> 50	> 250
ZD	Orta sıkı – sıkı kum, çakıl veya çok katı kil tabakaları	180 – 360	15 – 50	70 – 250
ZE	Gevşek kum, çakıl veya yumuşak – katı kil tabakaları veya $PI > 20$ ve $w > \%\ 40$ koşullarını sağlayan toplamda 3 metreden daha kalın yumuşak kil tabakası $(c_u < 25\ \text{kPa})$ içeren profiller	< 180	< 15	< 70
ZF	Sahaya özel araştırma ve değerlendirme gerektiren zeminler: 1) Deprem etkisi altında çökme ve potansiyel göçme riskine sahip zeminler (sıvılaşabilir zeminler, yüksek derecede hassas killer, göçebilir zayıf çimentolu zeminler vb.), 2) Toplam kalınlığı 3 metreden fazla turba ve/veya organik içeriği yüksek killer, 3) Toplam kalınlığı 8 metreden fazla olan yüksek plastisiteli (PI >50) killer, 4) Çok kalın (> 35 m) yumuşak veya orta katı killer.			

(1) according to the NHERP code, ZC refer to the C class: very dense soil and soft rock

Figure 8: The site classification, according to the TBDY 2018 code

Time history analysis was carried out to determine the earthquake performance of the tanks. The selection of earthquake records for time history analysis is detailed in this section. It is important to decide on earthquake recordings that are suitable with the earthquake ground motion level considered in the design while also taking into consideration the earthquake magnitudes, fault distances, source mechanisms, and local ground conditions. In accordance with TBDY 2018, the number of earthquake records to be selected for the calculation should be at least 11. Also, the number of records selected from the same earthquake should not exceed three. Eleven strong ground motion data recorded with stations located on Site Class ZC (i.e., very dense soil and soft rock) were selected for time history analyses. The Pacific Earthquake Engineering Research [PEER] Center NGA-West 2 [51] database was used to obtain the ground motion data. The earthquake records shown in Table 7 were chosen with consideration for the tank farm's features. Present practice for selecting and scaling earthquake ground motions for nonlinear response-history analysis is based on an engineering perspective. The selected earthquakes have a magnitude range of 6.19 to 7.7 and a rupture distance range of 12.5 to 69.2 km. The site class, spectral form during the interest period, free-field recordings, and its magnitude were given preference to determine the ground motion records.

Table 7: Summary of selected ground motion records

ID	Spectral Ordinate	EQ Analysis Name	Earthquake (Year)	Station	Mag.	Distance (km)	Original Scale Factor (ORG)
EQ1	H1	GM1-H1	Imperial Valley-06	Cerro Prieto	6.53	15.19	3.4483
EQ2	H2	GM1-H2	Parkfield (1966)	Cholame-Shandon	6.19	17.64	8.6157
EQ3	H1	GM3-H1	Morgan Hill (1984)	SanJusto Dam (R Abut)	6.19	31.88	8.2367
EQ4	H1	GM4-H1	Chalfant Valley-02	Benton	6.19	21.92	3.4649
EQ5	H1	GM6-H1	Kocaeli_ Turkey (1999)	Fatih	7.51	55.48	3.9683
EQ6	H2	GM6-H2	Sitka_ Alaska (1972)	Sitka Observatory	7.68	34.61	8.2672
EQ7	H1	GM7-H1	Duzce_ Turkey (1999)	Mudurnu	7.14	34.3	6.3549
EQ8	H1	GM8-H1	Sitka_ Alaska (1972)	Sitka Observatory	7.68	34.61	8.8722
EQ9	H1	GM9-H1	Manjil_ Iran (1990)	Abbar	7.37	12.55	1.319
EQ10	H1	GM10-H1	Hector Mine (1999)	Joshua Tree N.M. - Keys View	7.13	50.42	8.7245
EQ11	H1	GM12-H1	Chi-Chi_ Taiwan-04 (1999)	CHY046	6.2	38.14	4.4176

5.2 Ground Motion Scaling Procedure

TBDY 2018 [48] includes two different methods for scaling earthquake records such as simple scaling and spectral matching. In the spectral matching method, wavelets are added to real earthquake records to better match the horizontal elastic design spectrum with the earthquake ground motion spectrum. However, when this method is applied, changes can be observed in the characteristic features of the real earthquake record, and the earthquake record with the added wavelet can become an artificial earthquake record. In order to prevent these unwanted possible situations, the simple scaling method was preferred for evaluating the performance of tanks. According to TBDY 2018, the amplitudes of the spectra of all selected records between 0.2Tp and 1.5Tp periods should not be smaller than the amplitudes of the horizontal elastic design spectrum in the same period range. Here, Tp represents the dominant natural vibration period of the structure. In tanks containing liquid, unlike the buildings covered by TBDY 2018, impulsive and convective behaviour is observed, and it is not possible to talk about a single Tp value. According to the API 650 tank design code, the impulsive period of tanks and the convective period of tanks is calculated. The calculated period values are presented in Table 8.

Table 8: Summary of calculated periods

Parameter	Unit	TANK-A	TANK-B	TANK-C
T_i	*sec*	0.4	0.74	0.89
T_c	*sec*	3.4	5.3	6.63

The ground motions were scaled to match the design spectrum for site class C with S_S =1.345, S_1= 0.367, and T_L=6 sec. These site seismic properties correspond to the design spectrum parameters used for tank design. The scaling of ground motion records to match the design spectrum is considered to be of minimal importance for this study since the objective of this study is not to verify any code or standard recommendations but to develop a simplified approach to predict tank base uplift under seismic loading. However, o ensure that tank base uplift occurs for the tanks under the selected earthquake records, the earthquake records were intentionally scaled to match the design spectrum used in the tank design for this study. The correction factor is 1.01. The resultant scale factors are given in Table 9.

Table 9: Additional correction for ground motions

ID	SELECTED EQ	ORIGINAL SCALE FACTOR (ORG)	1.01*ORG
EQ1	GM1-H1	3.4483	3.482783
EQ2	GM1-H2	8.6157	8.701857
EQ3	GM3-H1	8.2367	8.319067
EQ4	GM4-H1	3.4649	3.499549
EQ5	GM6-H1	3.9683	4.007983
EQ6	GM6-H2	8.2672	8.349872
EQ7	GM7-H1	6.3549	6.418449
EQ8	GM8-H1	8.8722	8.960922
EQ9	GM9-H1	1.319	1.33219
EQ10	GM10-H1	8.7245	8.811745
EQ11	GM12-H1	4.4176	4.461776

Time-acceleration histories of the selected records are given in Figure 9. The selected records have different characteristics in terms of peak acceleration, duration, and distance to the fault. Also, it includes large acceleration pulses such as EQ6, EQ7, and EQ11, which increases their damage potential.

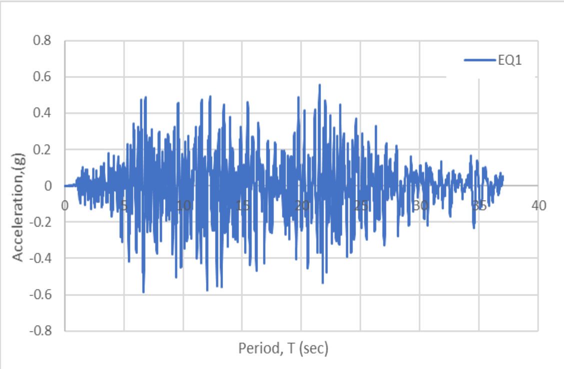
EQ1
Acceleration,(g)
Period, T (sec)
0.8
0.6
0.4
0.2
0
-0.2
-0.4
-0.6
-0.8
0
5
10
15
20
25
30
35
40

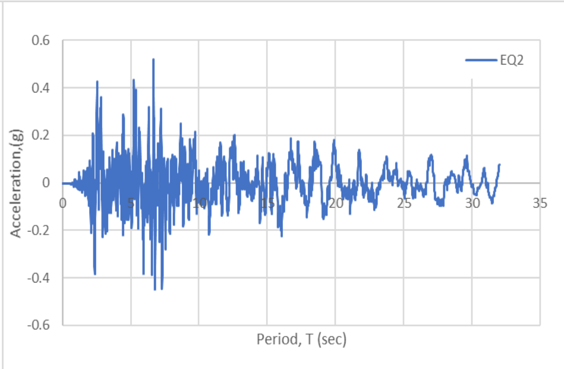
EQ2
Acceleration,(g)
Period, T (sec)
0.6
0.4
0.2
0
-0.2
-0.4
-0.6
0
5
10
15
20
25
30
35

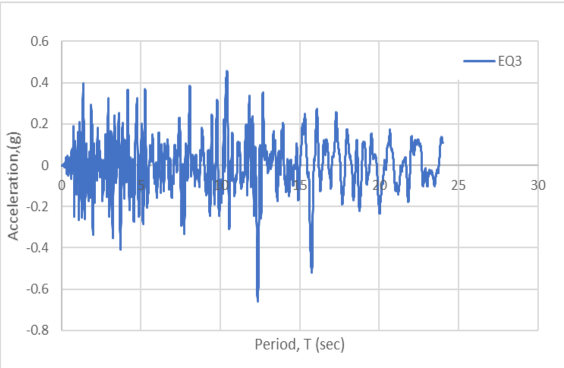
EQ3
Acceleration,(g)
Period, T (sec)
0.6
0.4
0.2
0
-0.2
-0.4
-0.6
-0.8
0
5
10
15
20
25
30

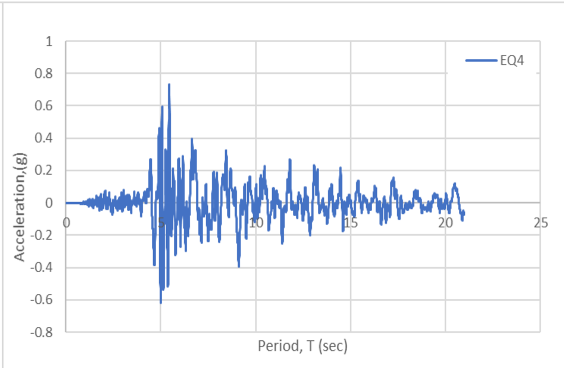
EQ4
Acceleration,(g)
Period, T (sec)
1
0.8
0.6
0.4
0.2
0
-0.2
-0.4
-0.6
-0.8
0
5
10
15
20
25

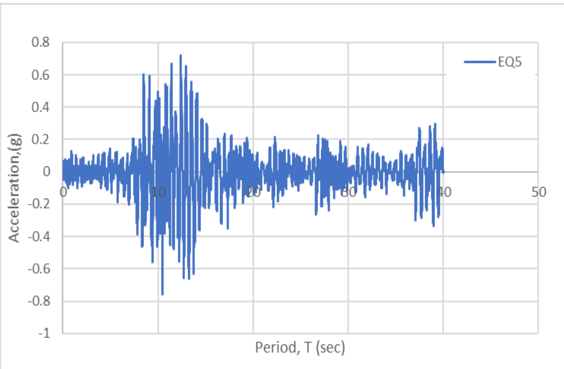
EQ5
Acceleration,(g)
Period, T (sec)
0.8
0.6
0.4
0.2
0
-0.2
-0.4
-0.6
-0.8
-1
0
10
20
30
40
50

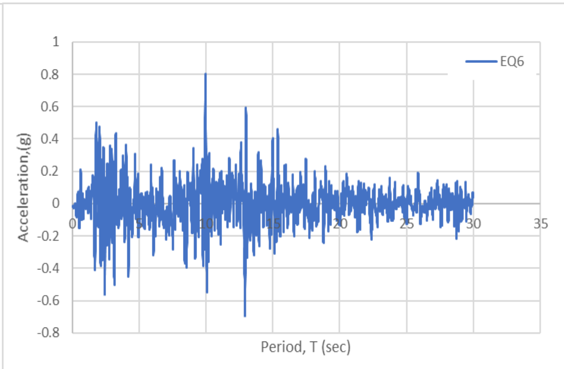
EQ6
Acceleration,(g)
Period, T (sec)
1
0.8
0.6
0.4
0.2
0
-0.2
-0.4
-0.6
-0.8
0
5
10
15
20
25
30
35

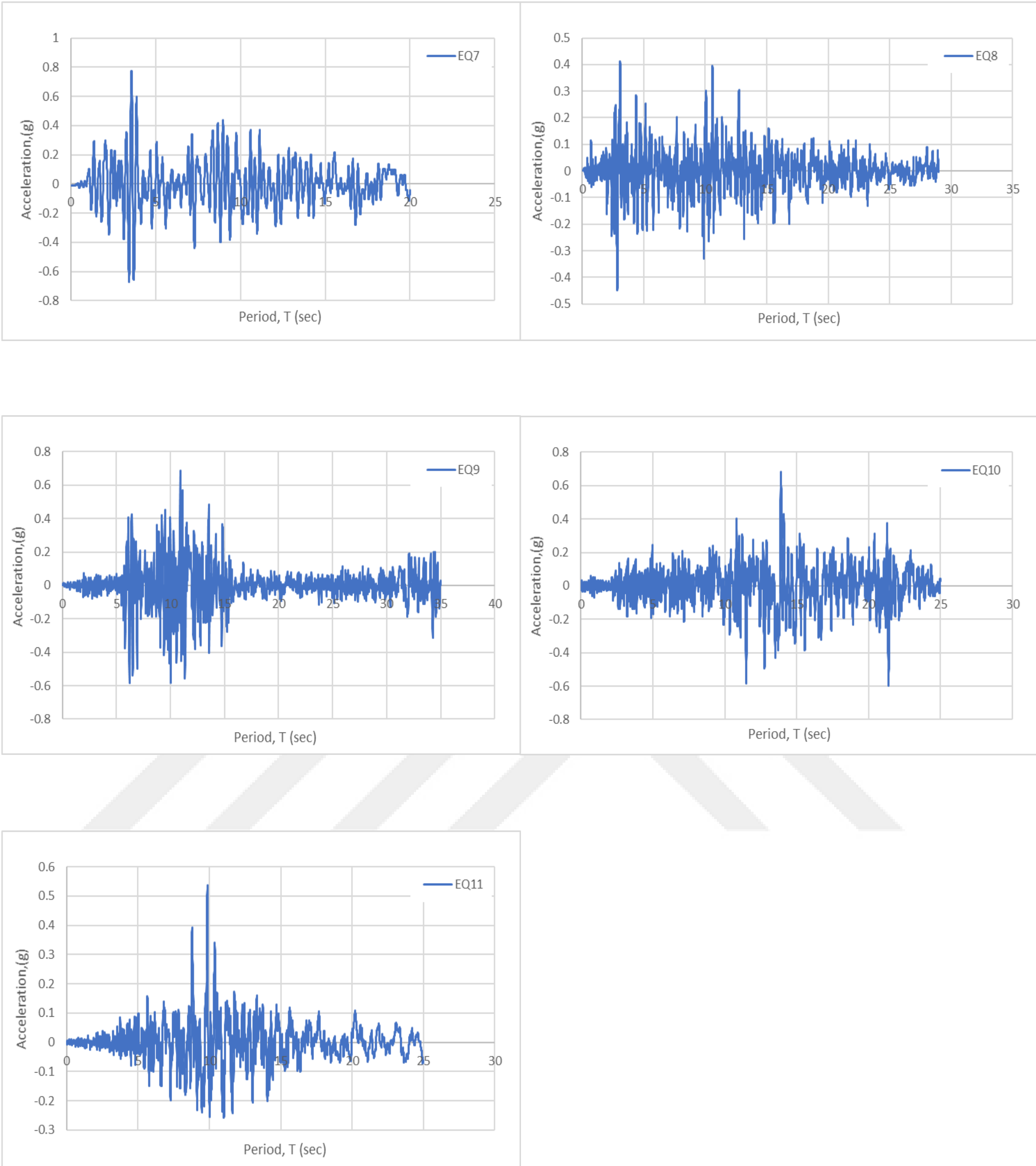

Figure 9: Selected ground acceleration histories

The design response spectrum is a graphical representation of the maximum expected response of a structure to ground shaking at different vibration periods during an earthquake. It is a key tool in seismic design and for understanding the potential structural response to earthquakes. It shows the relationship between the ground motion intensity and the corresponding structural response. The design spectra is developed based on a combination of historical earthquake records, site-specific factors, and structural characteristics. It takes into account factors such as the location of the structure, the seismic hazard level, the design code requirements, and the dynamic properties of the structure.

It is important to note that design response spectra are specific to a particular location, seismic hazard level, and structural configuration. They are typically provided in building codes and guidelines for designing structures that can effectively resist the forces generated by earthquakes.

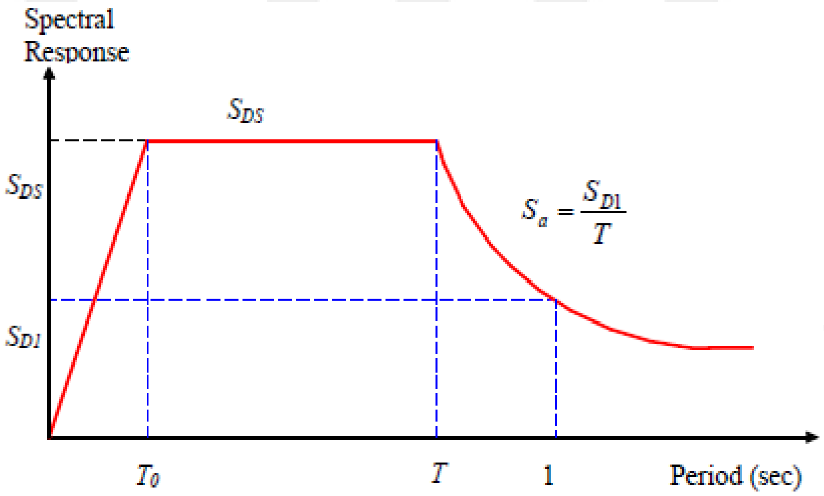

Figure 10: The concept of the design spectrum

The concept of the design spectrum is given in Figure 10 and the related equations (5-1) and (5-2) are calculated for Figure 11. The design spectrum and spectral response acceleration curves for the scaled earthquakes are given in Figure 12.

$$S_{DS} = S_S F_S = 1.345 \times 1.200 = 1.61 \quad (5\text{-}1)$$

$$S_{D1} = S_1 F_1 = 0.367 \times 1.500 = 0.55 \quad (5\text{-}2)$$

- The design spectrum for site class C with S_{DS} =1.345, S_{D1}= 0.367, and T_L=6 sec.

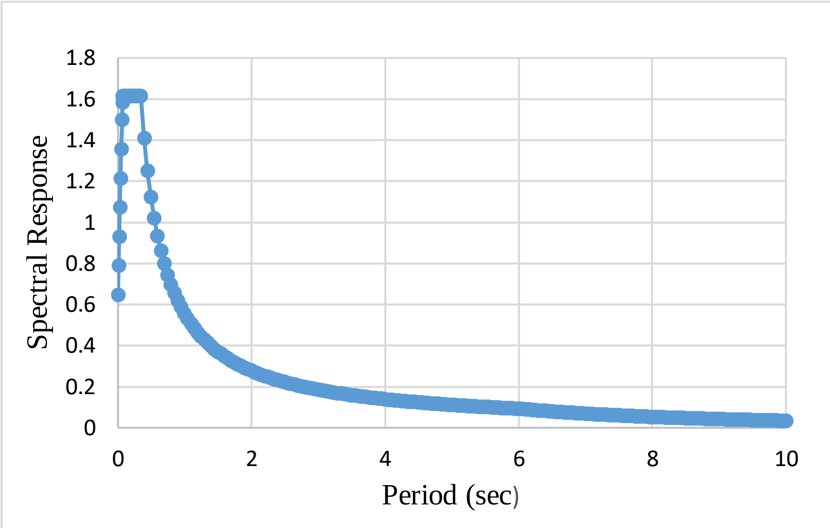

Figure 11: Design Response Spectra

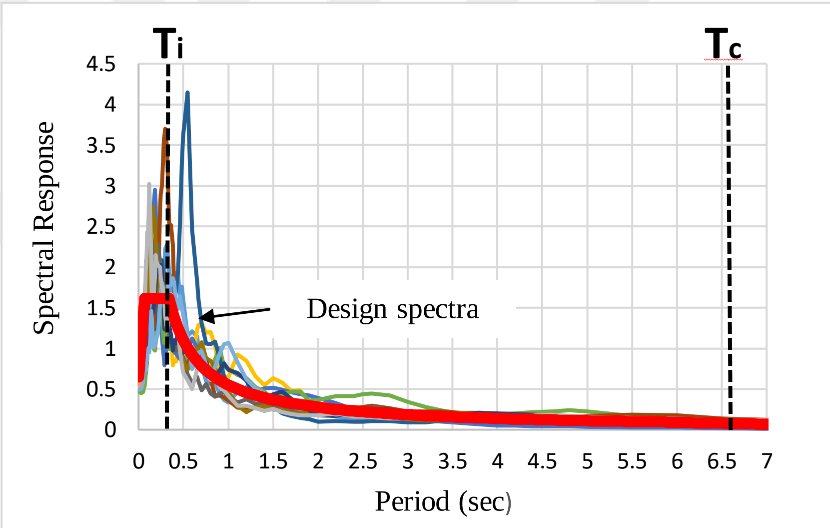

Figure 12: Design and acceleration response spectra belonging to each selected record

CHAPTER VI

RESULTS AND DISCUSSIONS

6.1 Time History Analyses

Time history analyses of unanchored tanks involve studying the dynamic response of tanks subjected to external forces, such as seismic events or wind loads. These analyses aim to evaluate the stability and structural integrity of unanchored tanks under dynamic loading conditions.

Eleven recorded ground acceleration records is selected from the Pacific Earthquake Engineering Research Center (PEER) [51] database for tank time history analyses. The selected ground motions are scaled to match the design spectrum from AFAD [50] for the site. The ground motions are scaled so that their average spectrum will be above the design spectrum for period range between tank impulsive period T_I and liquid convective period T_C [1]. These content details were explained in Chapter 5.

In this section, the results of the analyses conducted to examine the seismic performance of the tanks are presented. The results of the investigated base uplift and base sliding behaviors are summarised in tables. These tables are referred to as Table 10 and Table 11, respectively. The two tables are prepared separately for μ=0.6 and μ=0.42, allowing for the examination of the earthquake performance of unanchored tanks for the specified parameters under both friction coefficients.

Table 10: Maximum sliding and maximum uplift values for μ=0.6

TANK	EQ NAME	UPLIFT(mm)	SLIDING(mm)	AVG UPLIFT (mm)	AVG SLIDING (mm)
TANK-A	GM1-H1	138.41	8.19	135.54	10.34
	GM1-H2	81.60	3.68		
	GM3-H1	241.00	36.18		
	GM4-H1	193.38	6.63		
	GM6-H1	163.83	20.10		
	GM6-H2	58.27	4.72		
	GM7-H1	124.49	9.94		
	GM8-H1	46.43	1.28		
	GM9-H1	190.48	6.59		
	GM10-H1	129.01	13.40		
	GM12-H1	124.07	3.00		
TANK-B	GM1-H1	138.21	6.00	186.56	8.99
	GM1-H2	73.62	1.19		
	GM3-H1	396.94	25.19		
	GM4-H1	169.26	6.02		
	GM6-H1	330.09	10.12		
	GM6-H2	86.21	9.37		
	GM7-H1	217.75	18.84		
	GM8-H1	59.43	1.29		
	GM9-H1	217.32	7.21		
	GM10-H1	213.63	11.51		
	GM12-H1	149.70	2.13		
TANK-C	GM1-H1	11.95	5.61	71.53	8.65
	GM1-H2	60.03	1.44		
	GM3-H1	141.39	6.25		
	GM4-H1	128.22	8.98		
	GM6-H1	161.03	34.00		
	GM6-H2	47.72	8.19		
	GM7-H1	18.16	13.07		
	GM8-H1	0.44	1.14		
	GM9-H1	3.71	3.48		
	GM10-H1	163.74	10.59		
	GM12-H1	50.48	2.34		

Table 11: Maximum sliding and maximum uplift values for μ=0.42

TANK	EQ NAME	UPLIFT(mm)	SLIDING(mm)	AVG UPLIFT(mm)	AVG SLIDING(mm)
TANK-A	GM1-H1	132.25	20.90	116.67	34.14
	GM1-H2	72.43	13.99		
	GM3-H1	190.81	152.45		
	GM4-H1	107.37	28.86		
	GM6-H1	161.08	45.77		
	GM6-H2	47.94	19.92		
	GM7-H1	145.25	12.87		
	GM8-H1	45.41	3.70		
	GM9-H1	142.72	18.97		
	GM10-H1	124.28	45.34		
	GM12-H1	113.80	12.80		
TANK-B	GM1-H1	127.84	34.40	156.06	39.24
	GM1-H2	69.95	4.39		
	GM3-H1	261.76	162.97		
	GM4-H1	147.76	11.67		
	GM6-H1	305.01	67.56		
	GM6-H2	103.26	20.63		
	GM7-H1	184.08	53.85		
	GM8-H1	49.20	2.01		
	GM9-H1	175.92	20.81		
	GM10-H1	159.30	42.63		
	GM12-H1	132.63	10.67		
TANK-C	GM1-H1	3.87	25.09	37.58	40.38
	GM1-H2	34.44	7.04		
	GM3-H1	59.82	47.17		
	GM4-H1	94.83	19.12		
	GM6-H1	69.85	138.33		
	GM6-H2	40.97	34.89		
	GM7-H1	16.81	31.07		
	GM8-H1	0.42	3.14		
	GM9-H1	2.04	12.73		
	GM10-H1	65.08	109.16		
	GM12-H1	25.26	16.46		

6.2 Results of Analyses for μ=0.6

6.2.1 Results of Analyses for Tank A

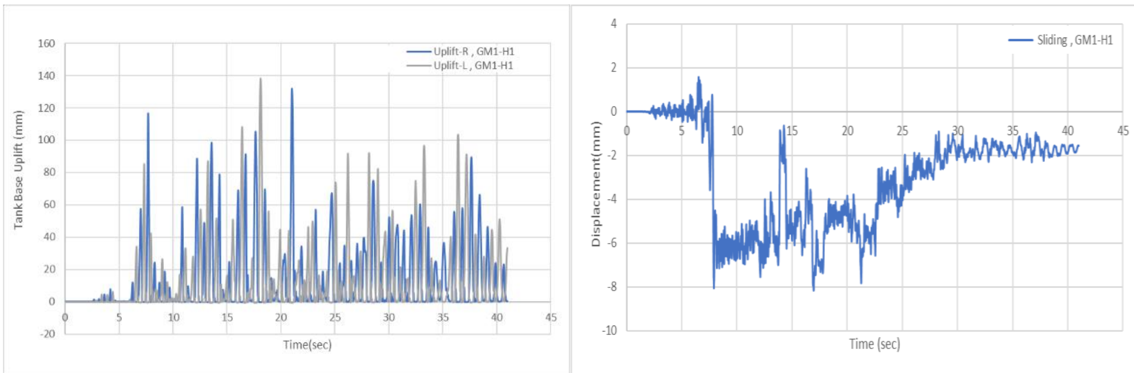

Figure 13: Tank A base uplift history and sliding history under EQ1

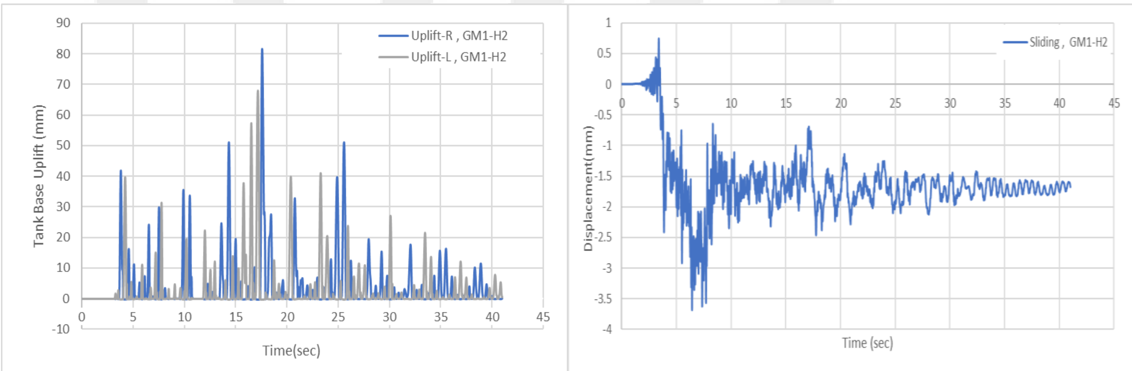

Figure 14: Tank A base uplift history and sliding history under EQ2

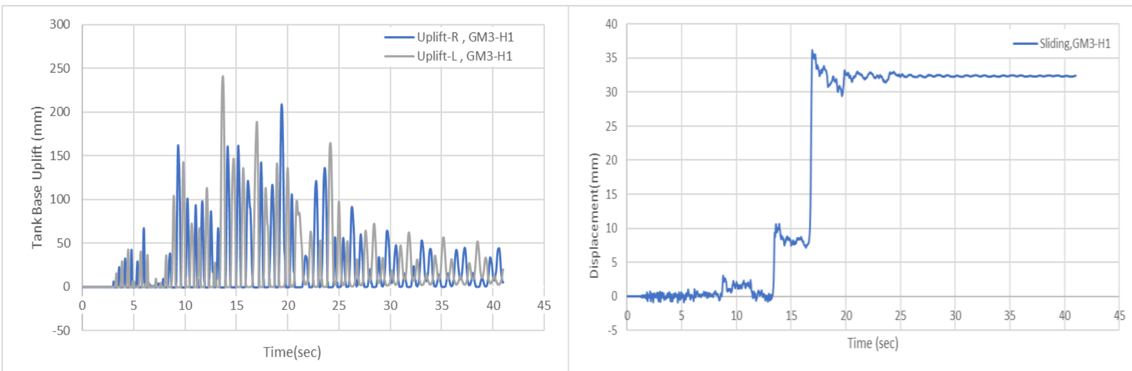

Figure 15: Tank A base uplift history and sliding history under EQ3

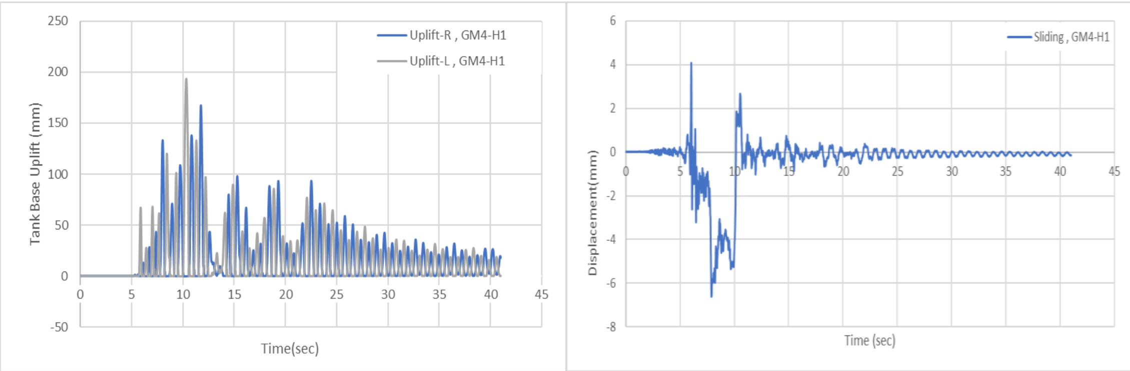

Figure 16: Tank A base uplift history and sliding history under EQ4

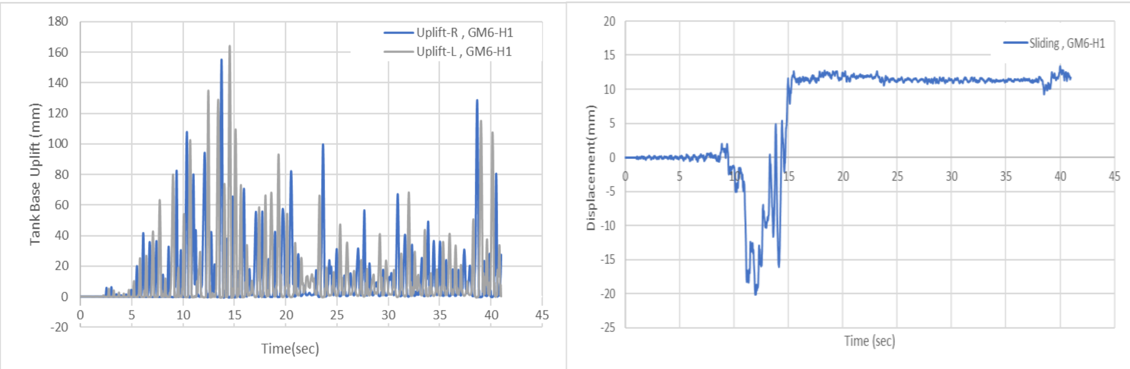

Figure 17: Tank A base uplift history and sliding history under EQ5

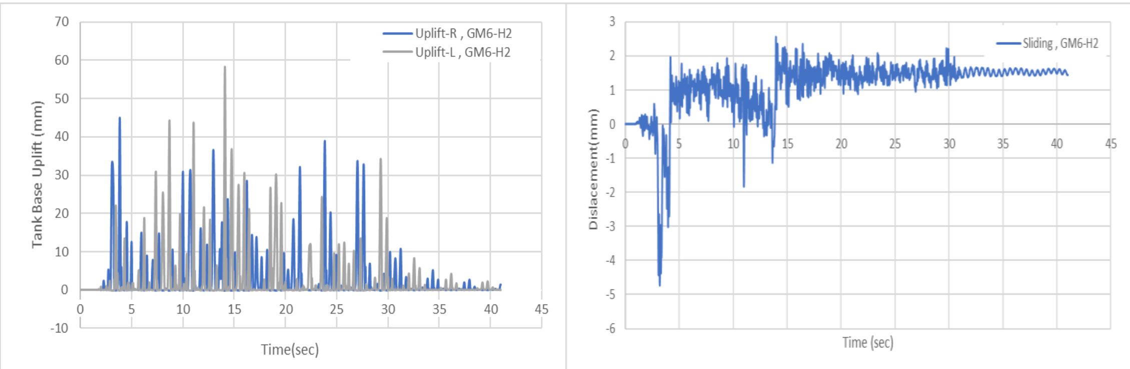

Figure 18: Tank A base uplift history and sliding history under EQ6

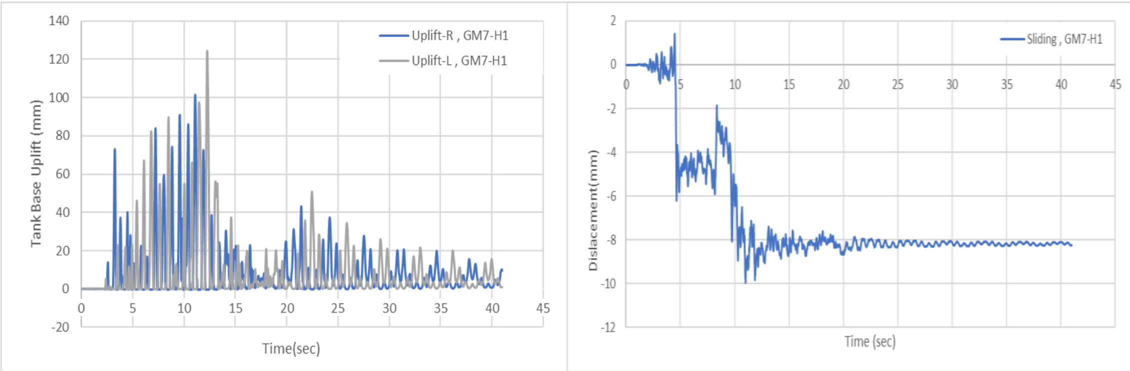

Figure 19: Tank A base uplift history and sliding history under EQ7

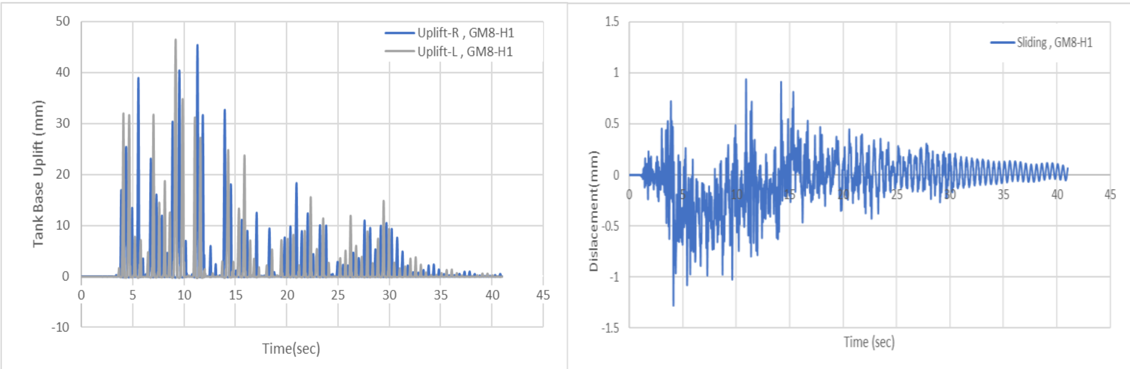

Figure 20: Tank A base uplift history and sliding history under EQ8

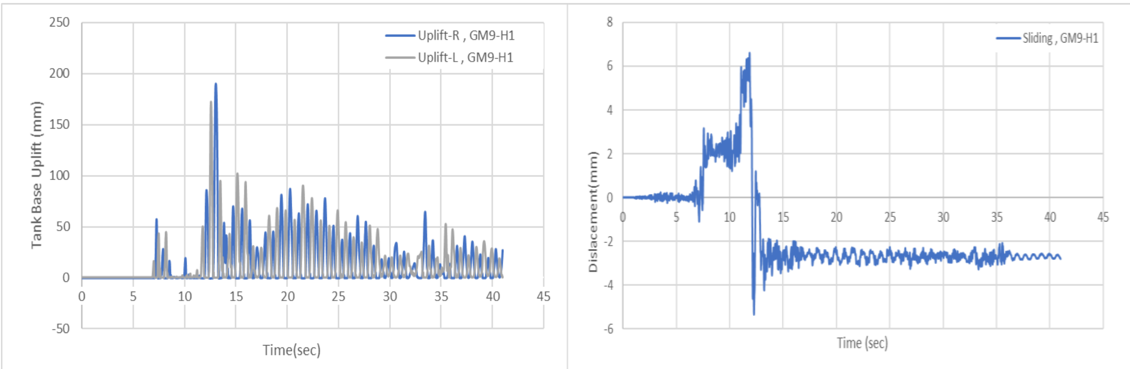

Figure 21: Tank A base uplift history and sliding history under EQ9

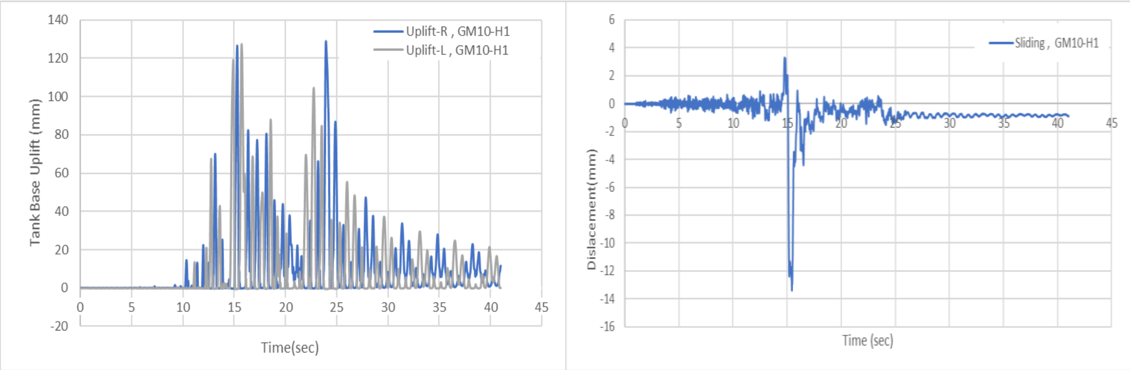

Figure 22: Tank A base uplift history and sliding history under EQ10

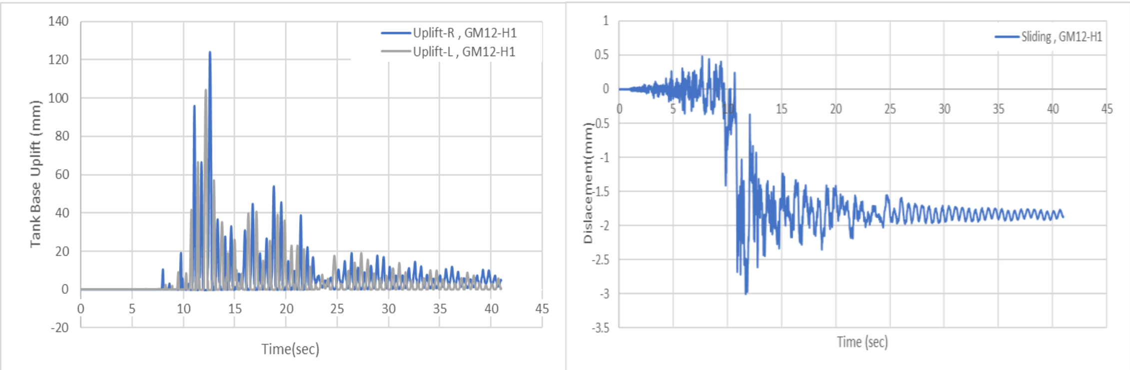

Figure 23: Tank A base uplift history and sliding history under EQ11

6.2.2 Results of Analyses for Tank B

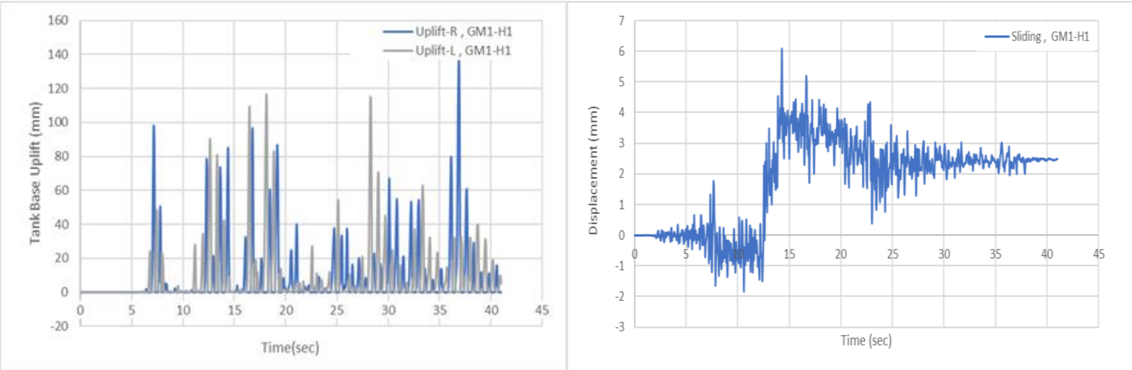

Figure 24: Tank B base uplift history and sliding history under EQ1

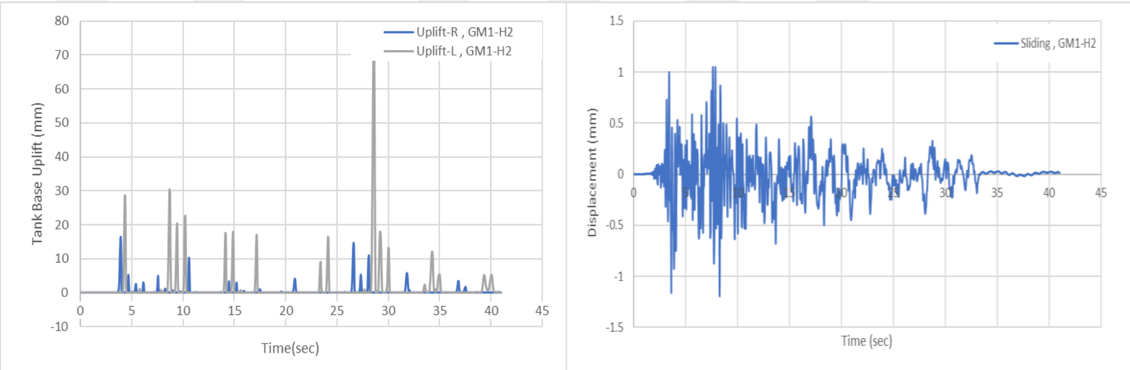

Figure 25: Tank B base uplift history and sliding history under EQ2

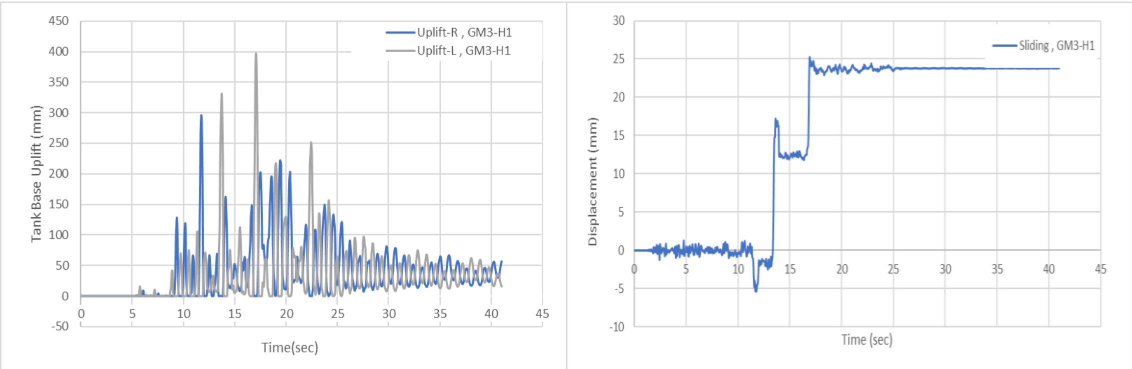

Figure 26: Tank B base uplift history and sliding history under EQ3

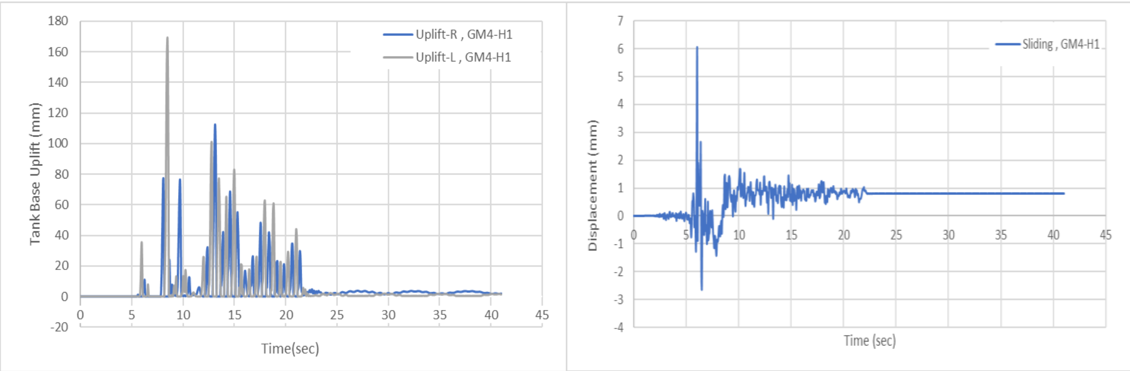

Figure 27: Tank B base uplift history and sliding history under EQ4

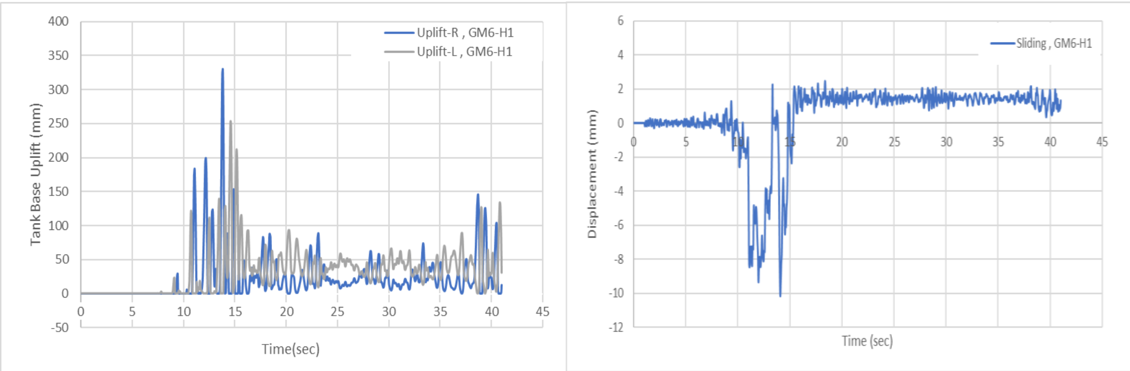

Figure 28: Tank B base uplift history and sliding history under EQ5

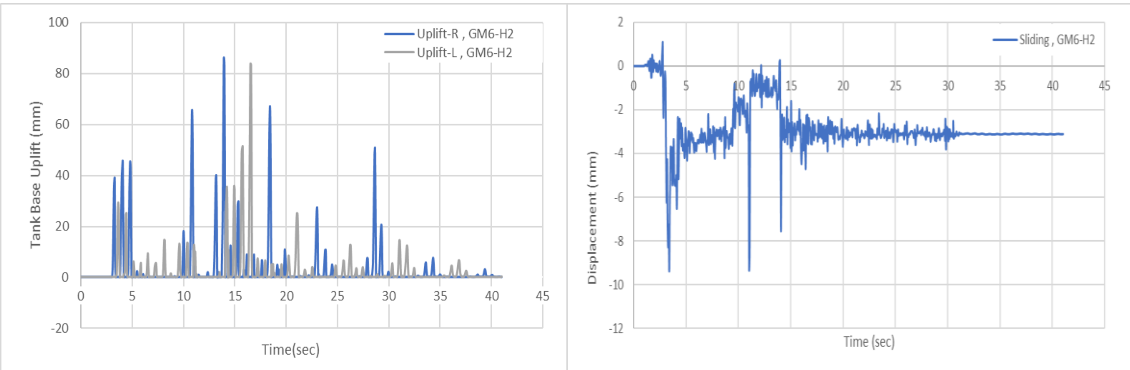

Figure 29: Tank B base uplift history and sliding history under EQ6

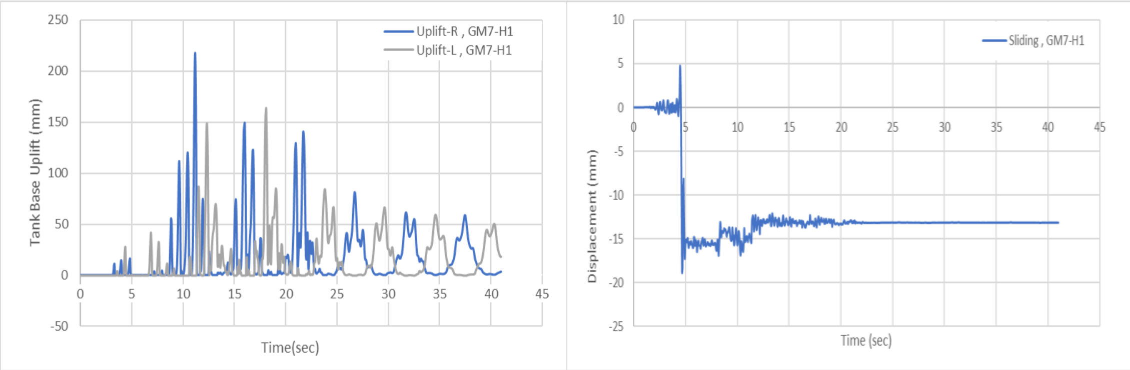

Figure 30: Tank B base uplift history and sliding history under EQ7

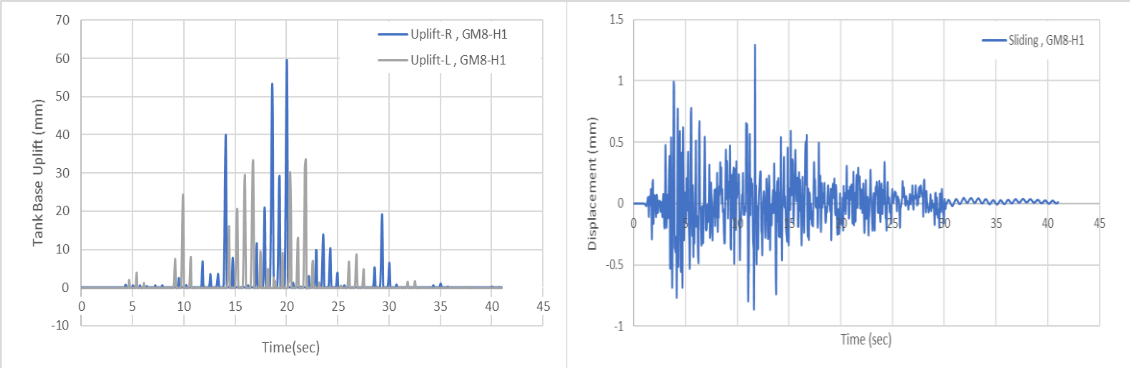

Figure 31: Tank B base uplift history and sliding history under EQ8

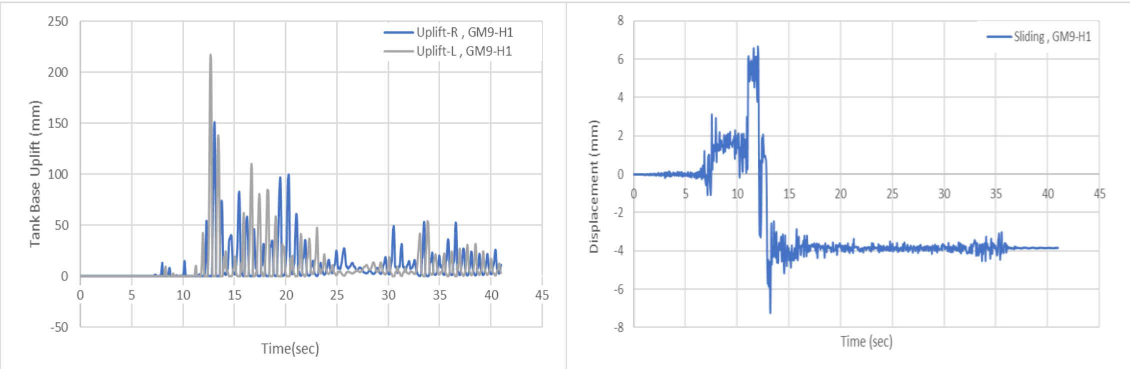

Figure 32: Tank B base uplift history and sliding history under EQ9

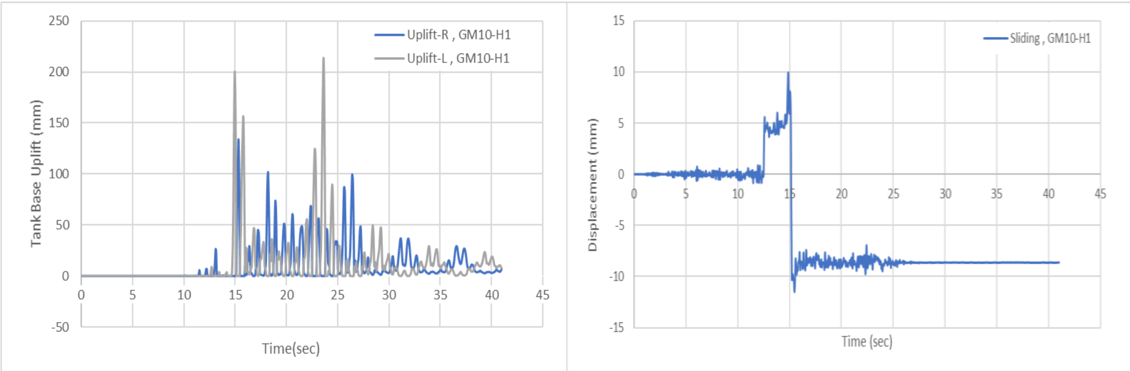

Figure 33: Tank B base uplift history and sliding history under EQ10

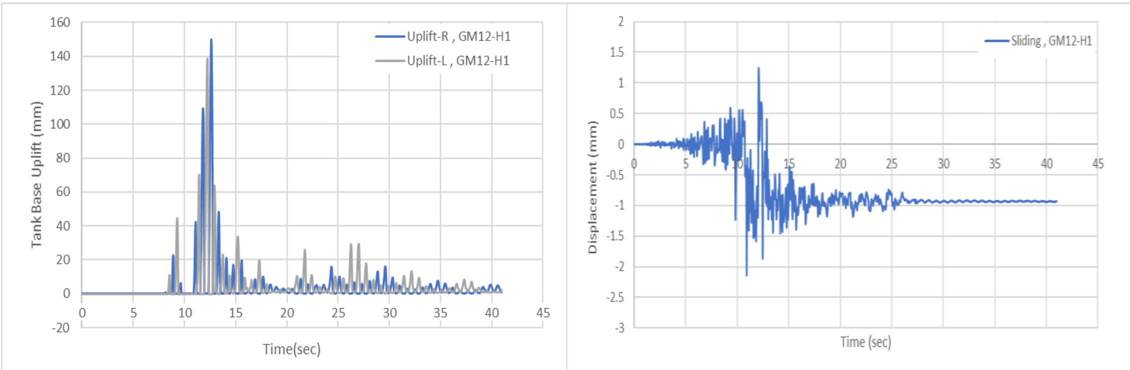

Figure 34: Tank B base uplift history and sliding history under EQ11

6.2.3 Results of Analyses for Tank C

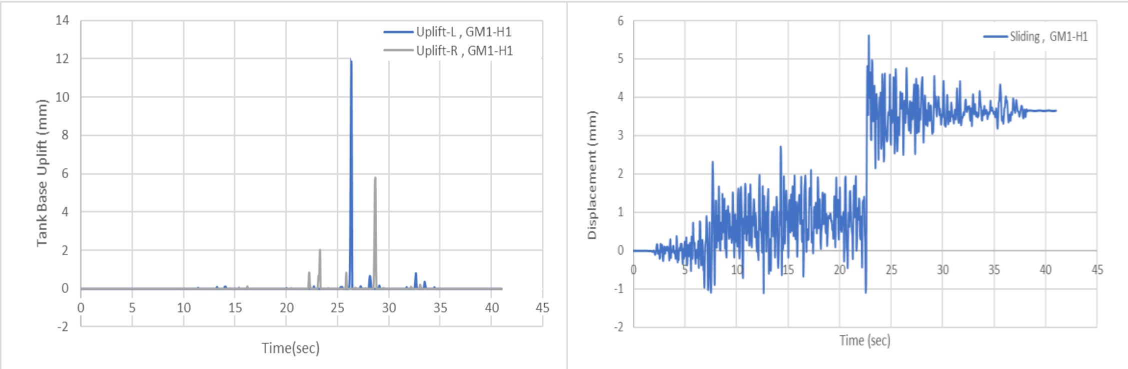

Figure 35: Tank C base uplift history and sliding history under EQ1

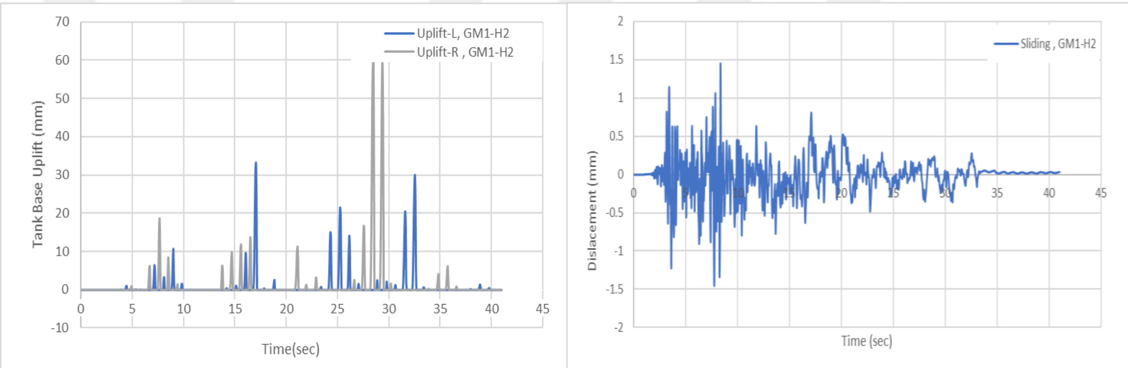

Figure 36: Tank C base uplift history and sliding history under EQ2

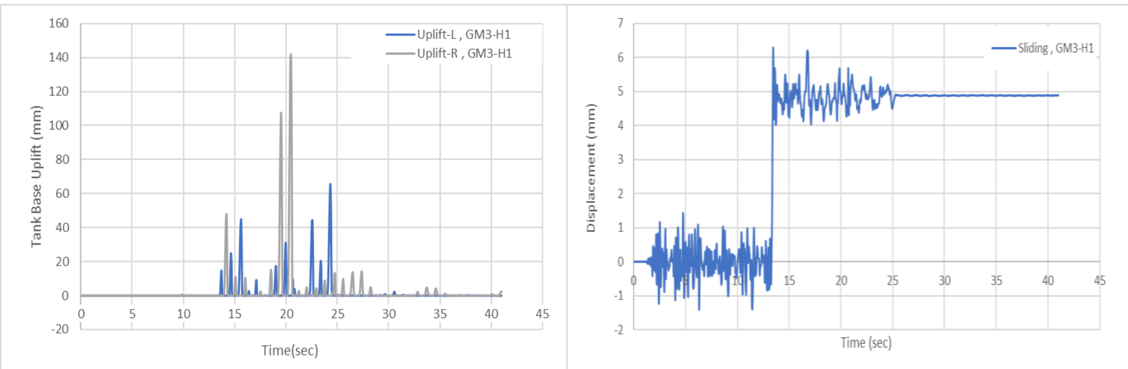

Figure 37: Tank C base uplift history and sliding history under EQ3

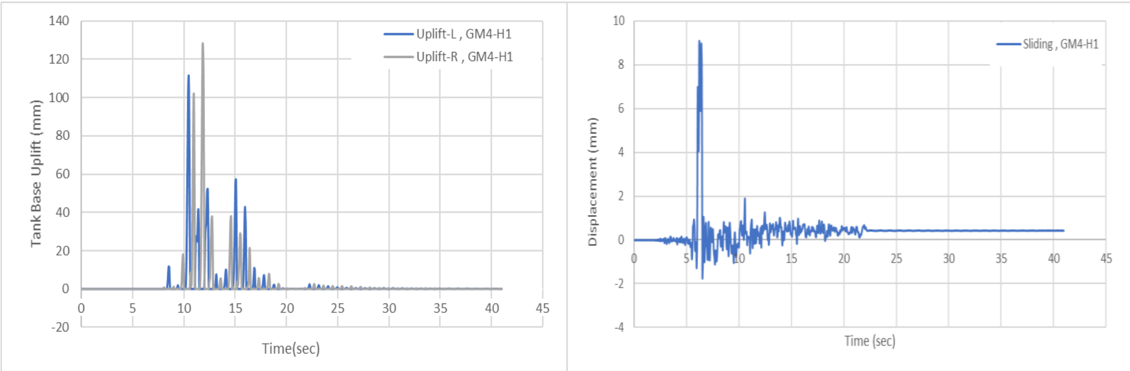

Figure 38: Tank C base uplift history and sliding history under EQ4

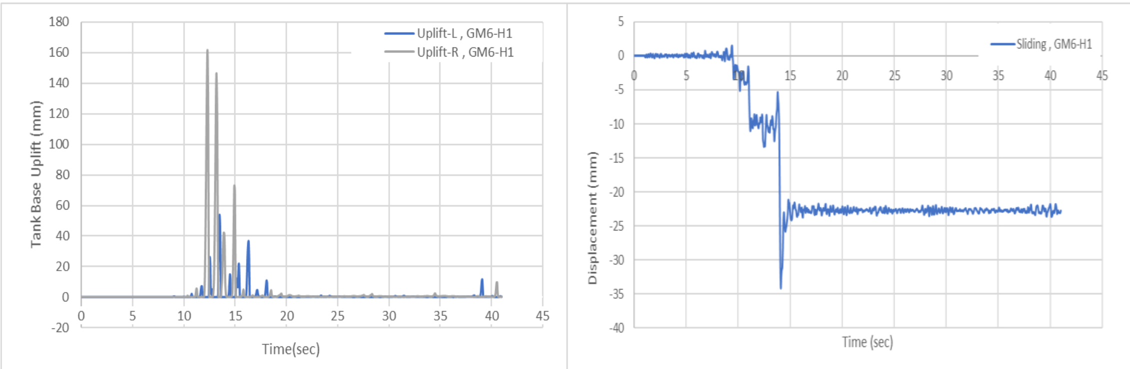

Figure 39: Tank C base uplift history and sliding history under EQ5

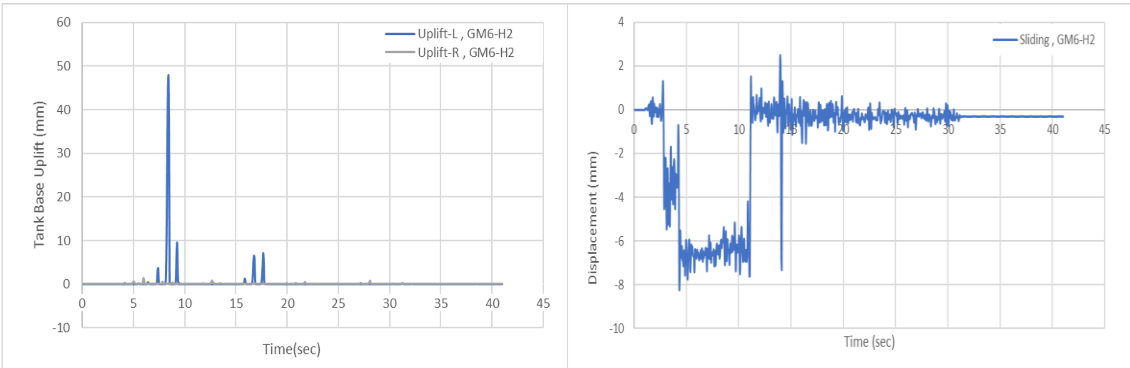

Figure 40: Tank C base uplift history and sliding history under EQ6

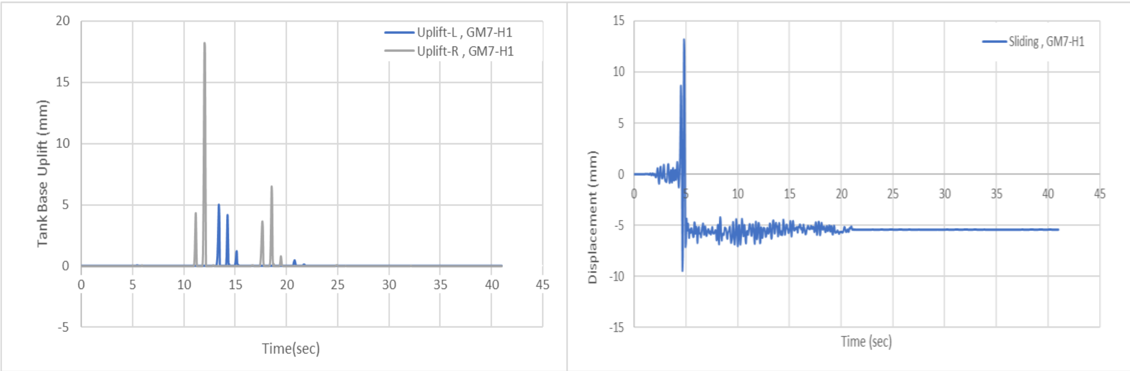

Figure 41: Tank C base uplift history and sliding history under EQ7

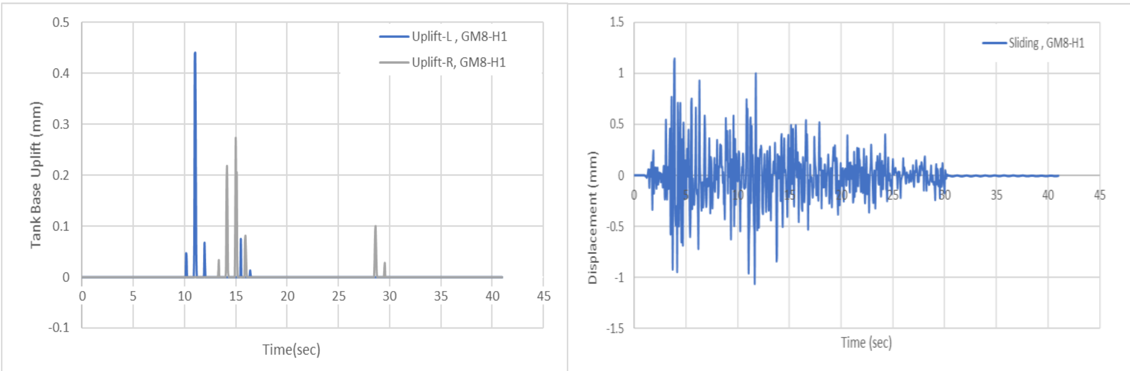

Figure 42: Tank C base uplift history and sliding history under EQ8

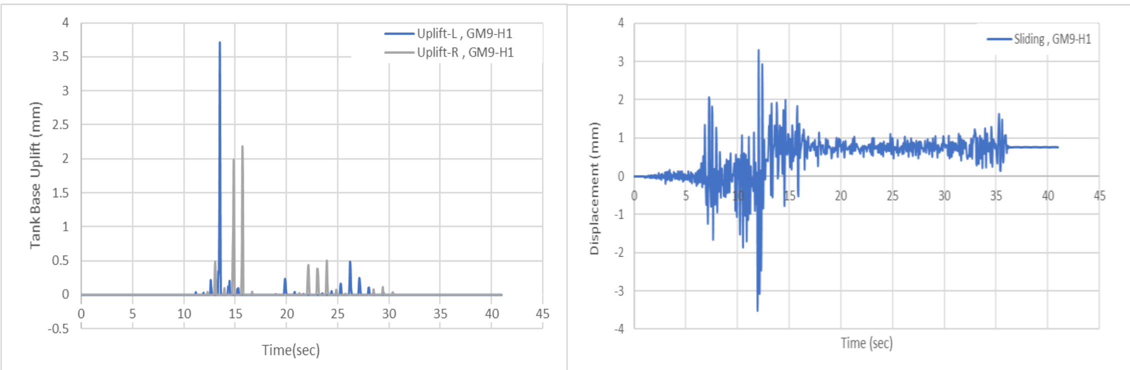

Figure 43: Tank C base uplift history and sliding history under EQ9

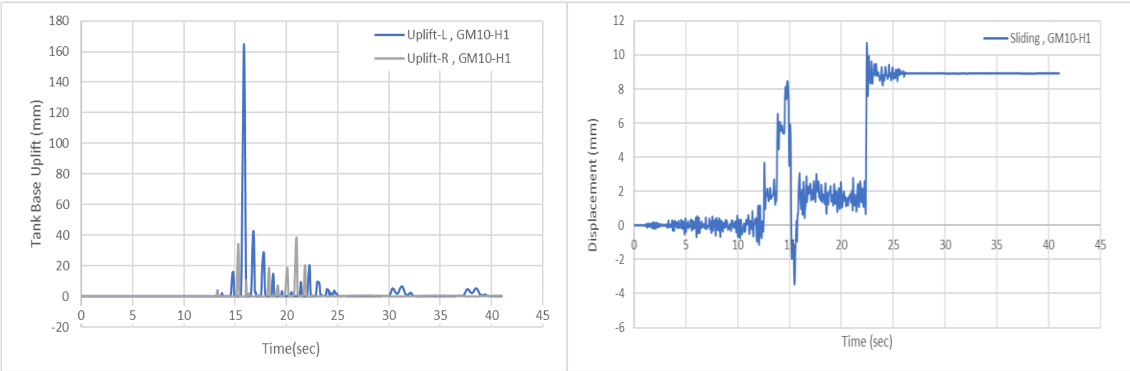

Figure 44: Tank C base uplift history and sliding history under EQ10

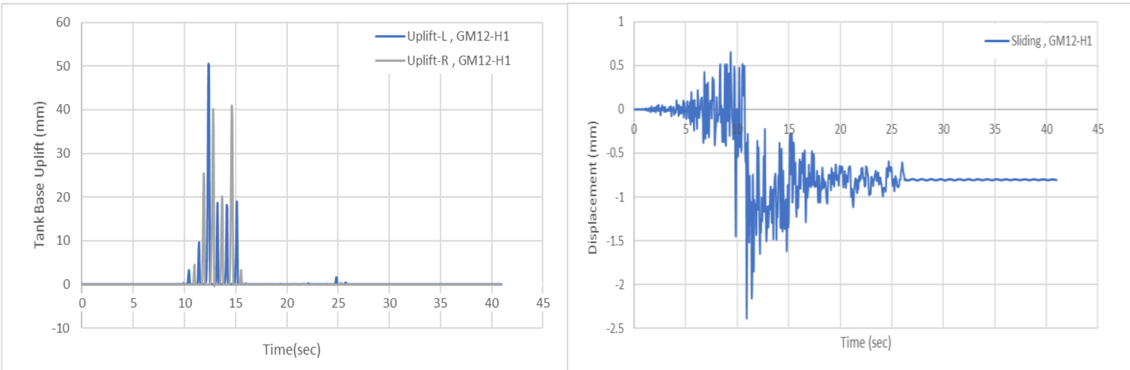

Figure 45: Tank C base uplift history and sliding history under EQ11

6.3 *Results of Analyses for μ=0.42*

6.3.1 Results of Analyses for Tank A

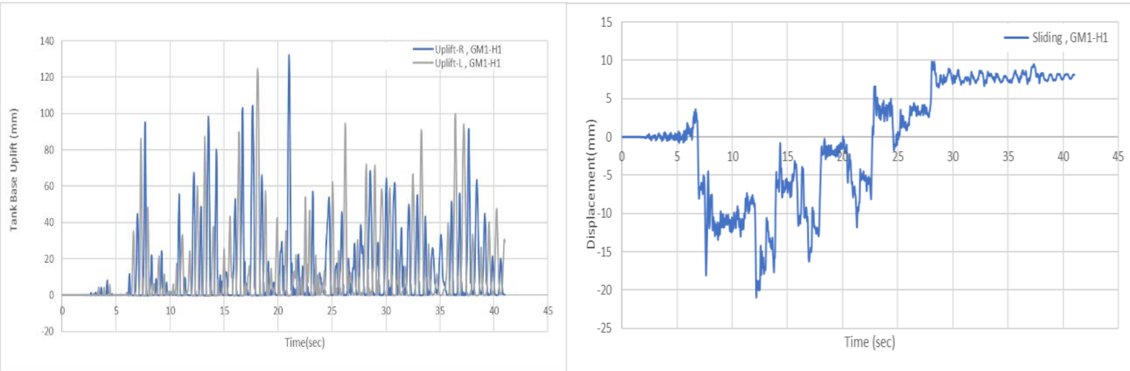

Figure 46: Tank A base uplift history and sliding history under EQ1

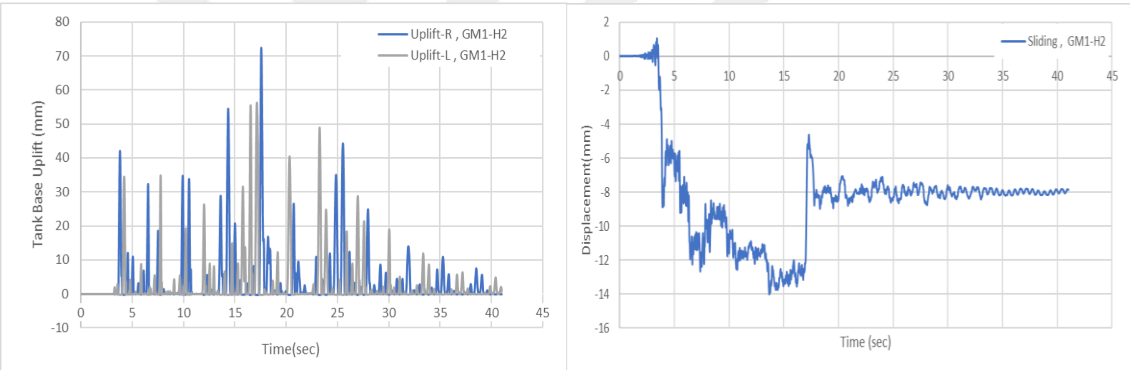

Figure 47: Tank A base uplift history and sliding history under EQ2

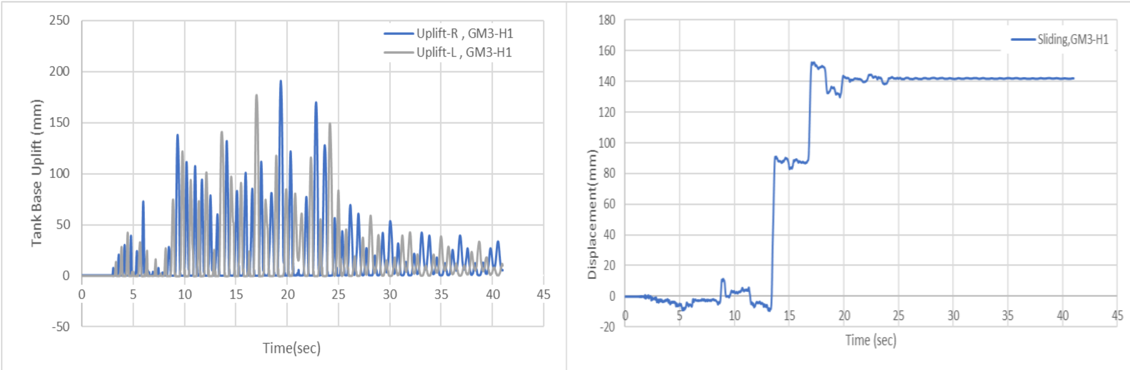

Figure 48: Tank A base uplift history and sliding history under EQ3

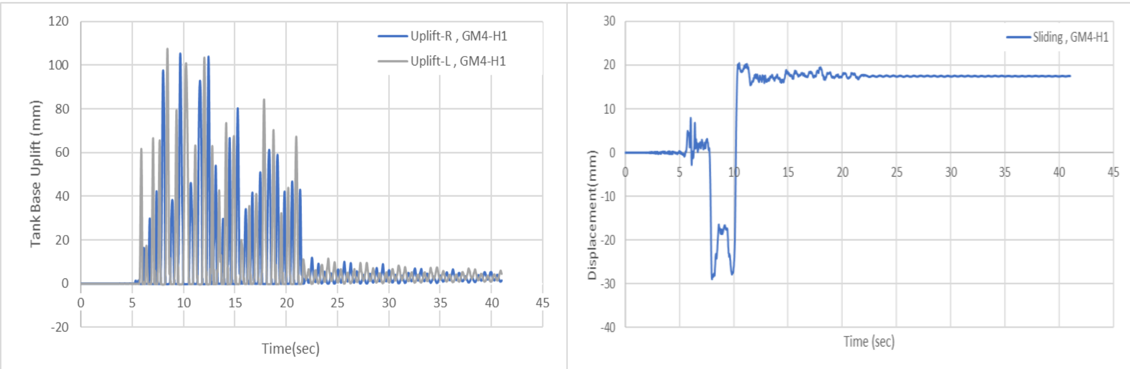

Figure 49: Tank A base uplift history and sliding history under EQ4

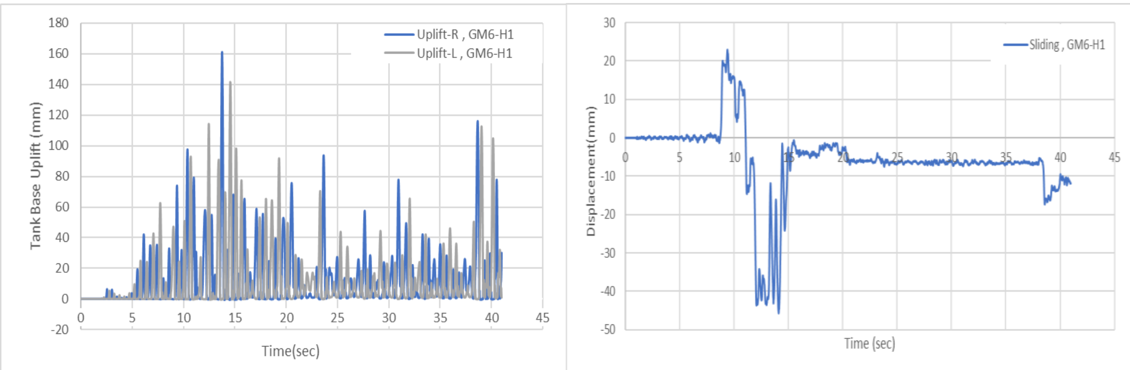

Figure 50: Tank A base uplift history and sliding history under EQ5

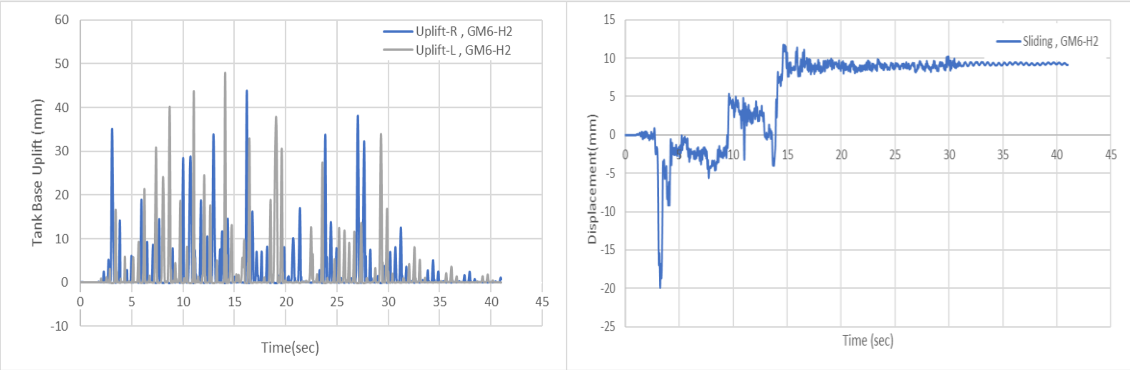

Figure 51: Tank A base uplift history and sliding history under EQ6

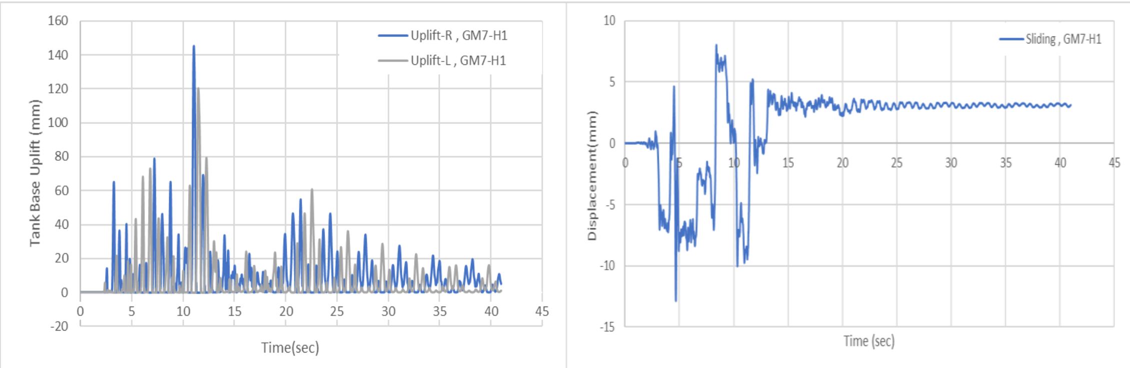

Figure 52: Tank A base uplift history and sliding history under EQ7

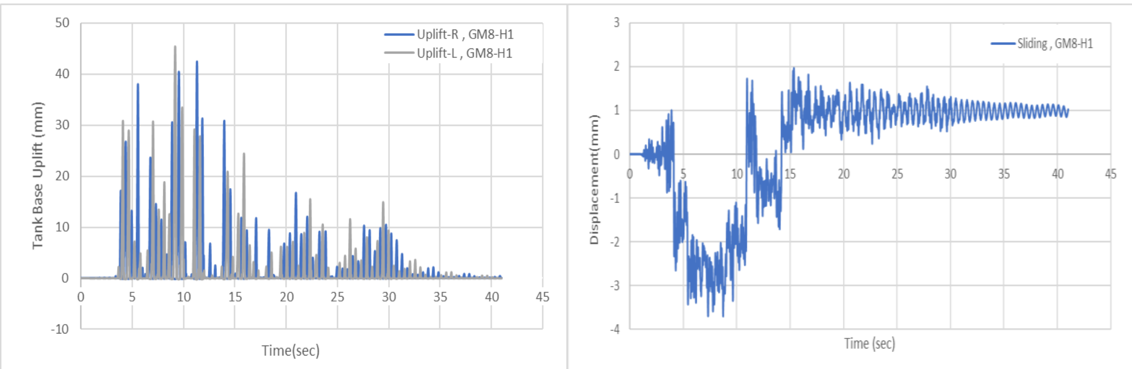

Figure 53: Tank A base uplift history and sliding history under EQ8

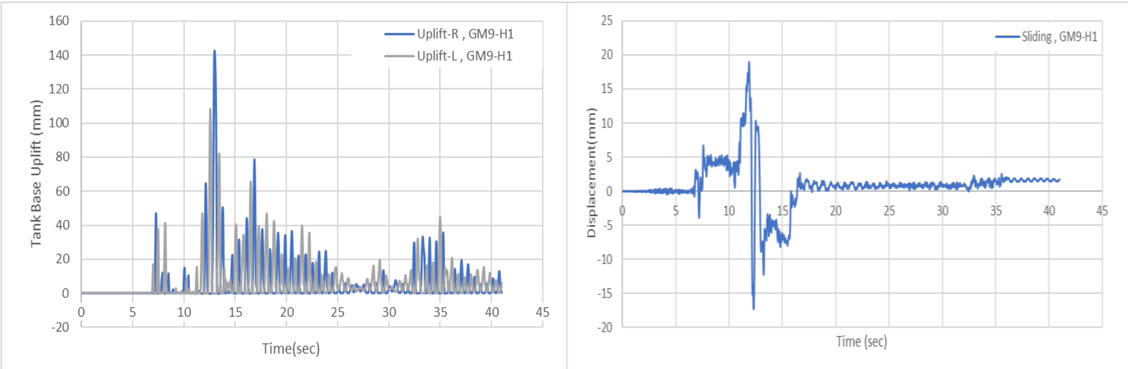

Figure 54: Tank A base uplift history and sliding history under EQ9

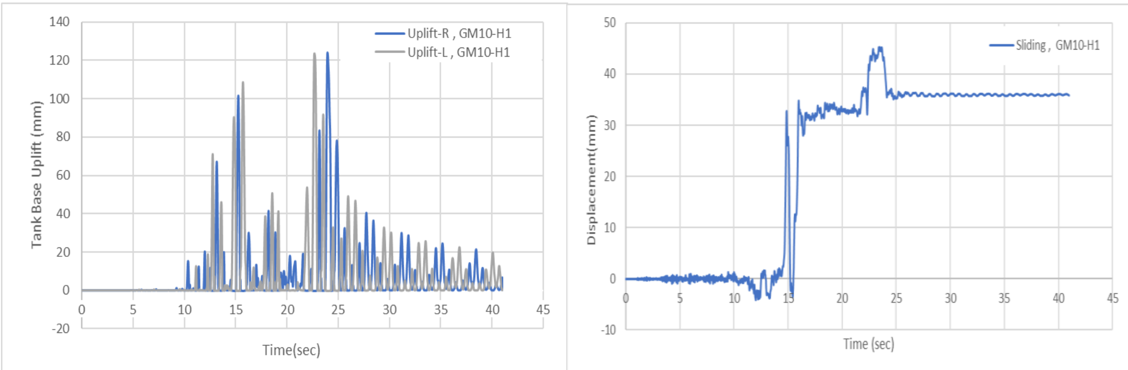

Figure 55: Tank A base uplift history and sliding history under EQ10

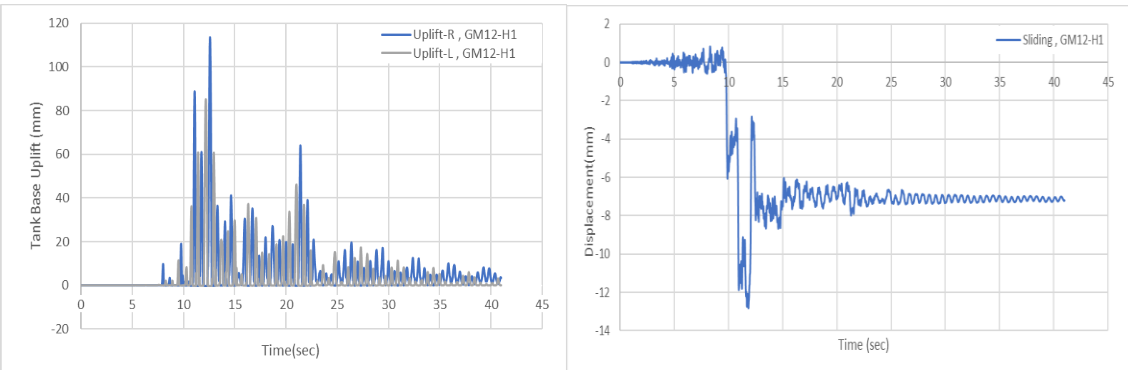

Figure 56: Tank A base uplift history and sliding history under EQ11

6.3.2 Results of Analyses for Tank B

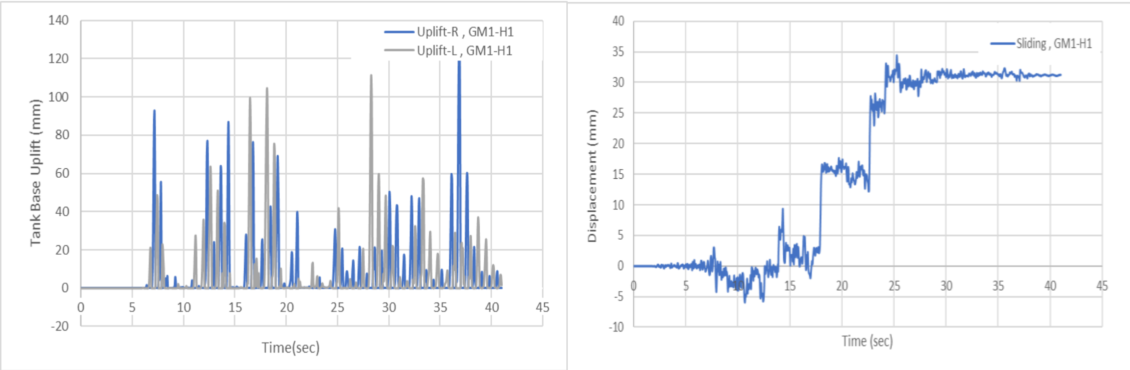

Figure 57: Tank B base uplift history and sliding history under EQ1

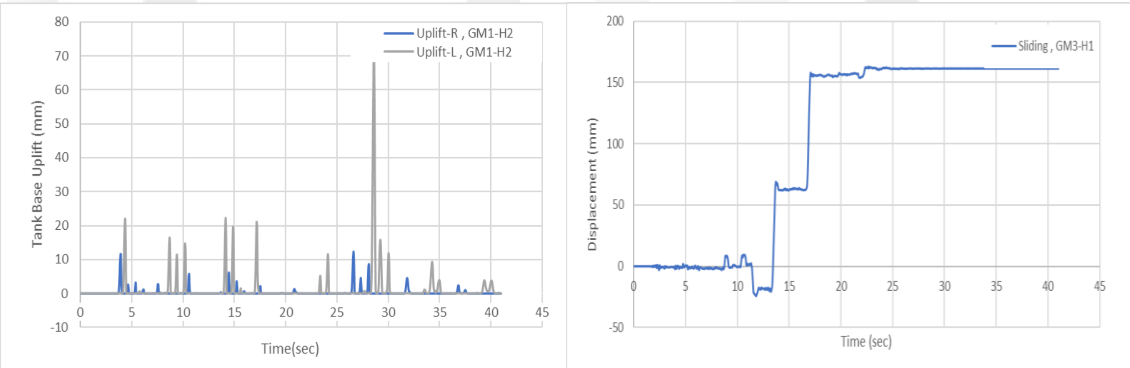

Figure 58: Tank B base uplift history and sliding history under EQ2

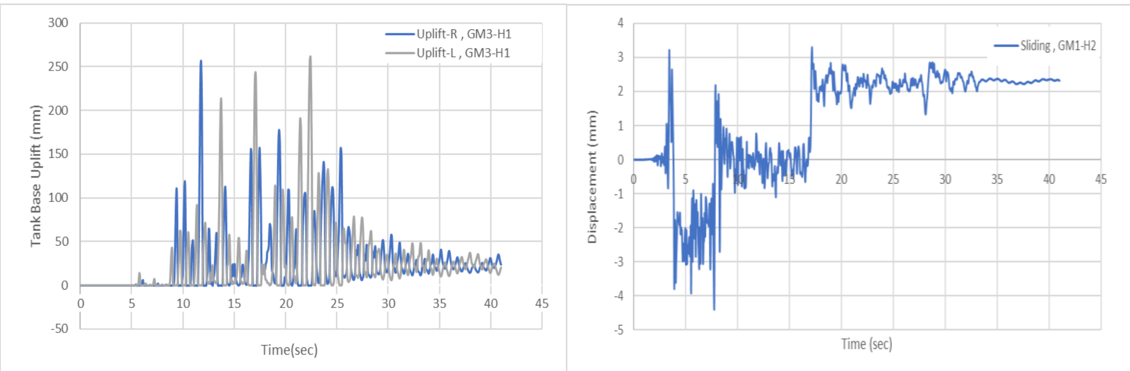

Figure 59: Tank B base uplift history and sliding history under EQ3

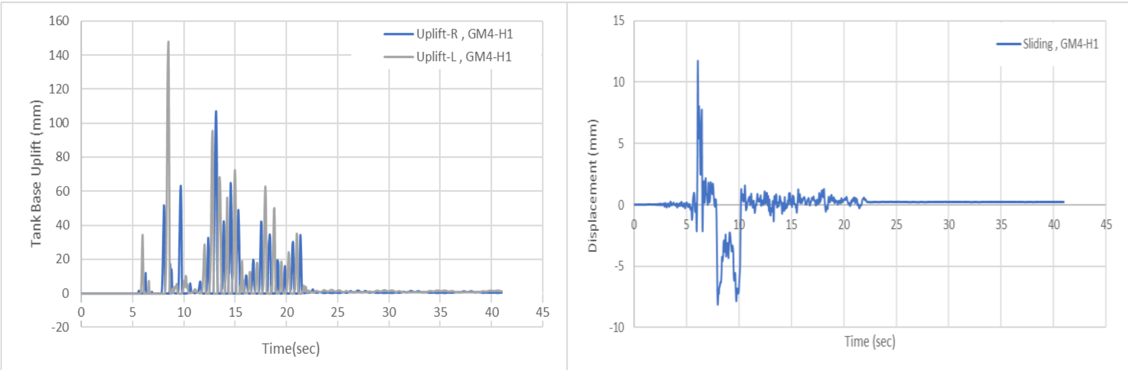

Figure 60: Tank B base uplift history and sliding history under EQ4

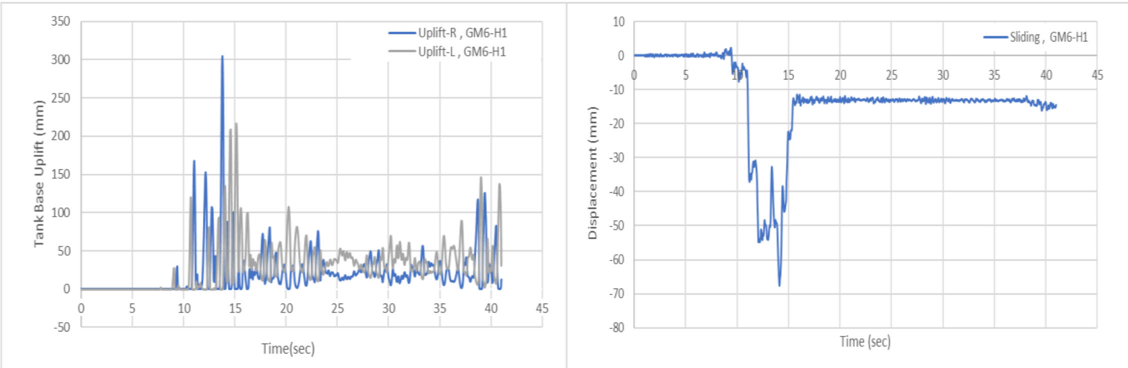

Figure 61: Tank B base uplift history and sliding history under EQ5

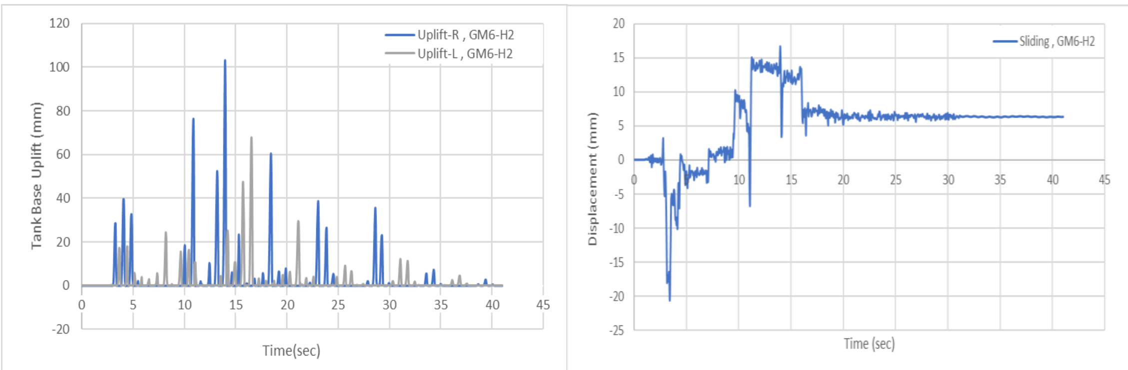

Figure 62: Tank B base uplift history and sliding history under EQ6

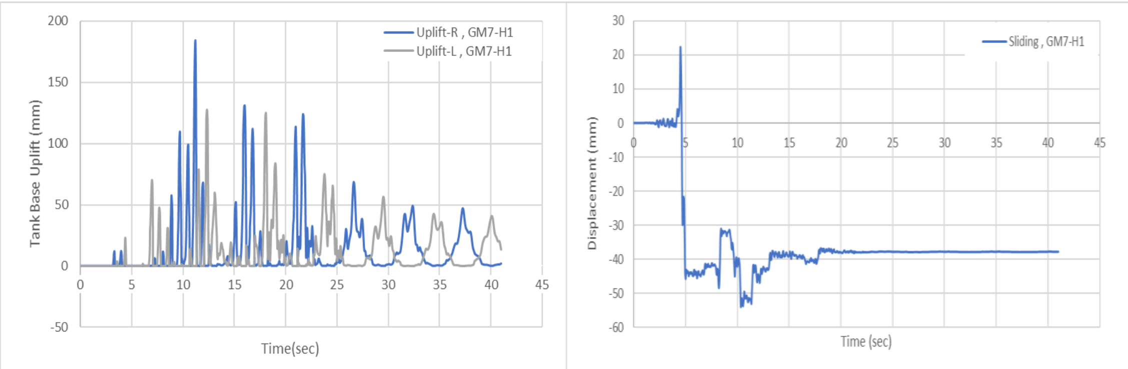

Figure 63: Tank B base uplift history and sliding history under EQ7

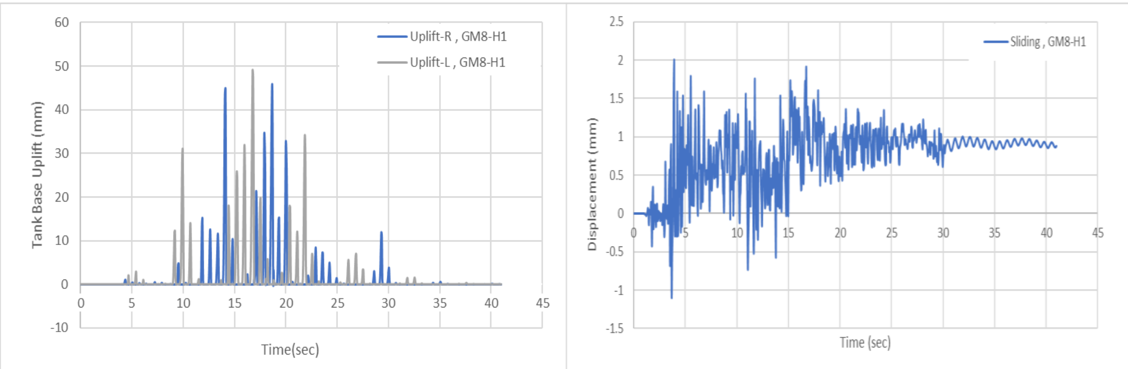

Figure 64: Tank B base uplift history and sliding history under EQ8

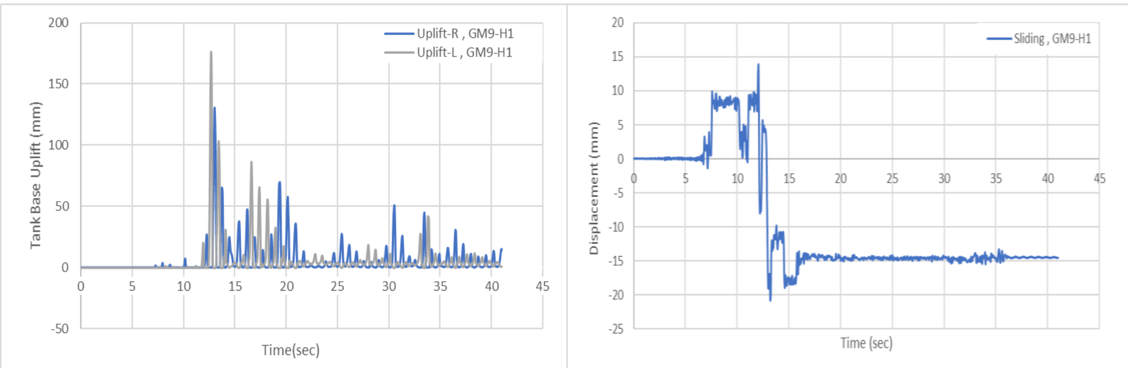

Figure 65: Tank B base uplift history and sliding history under EQ9

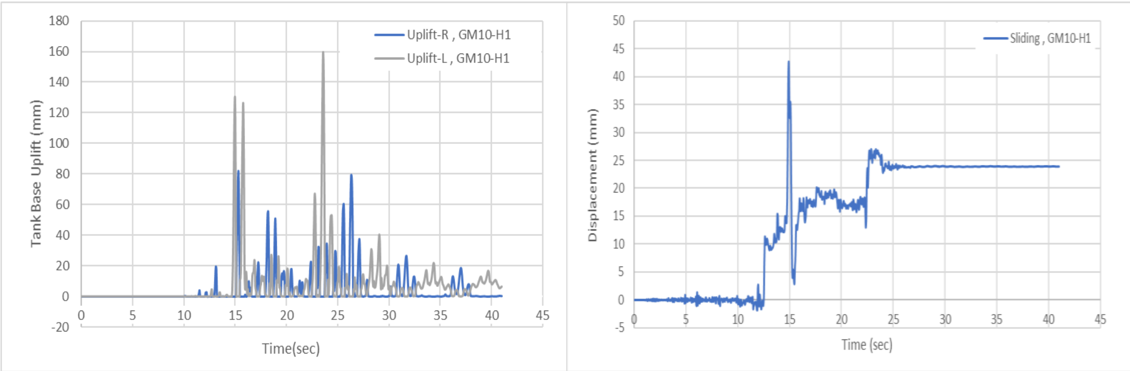

Figure 66: Tank B base uplift history and sliding history under EQ10

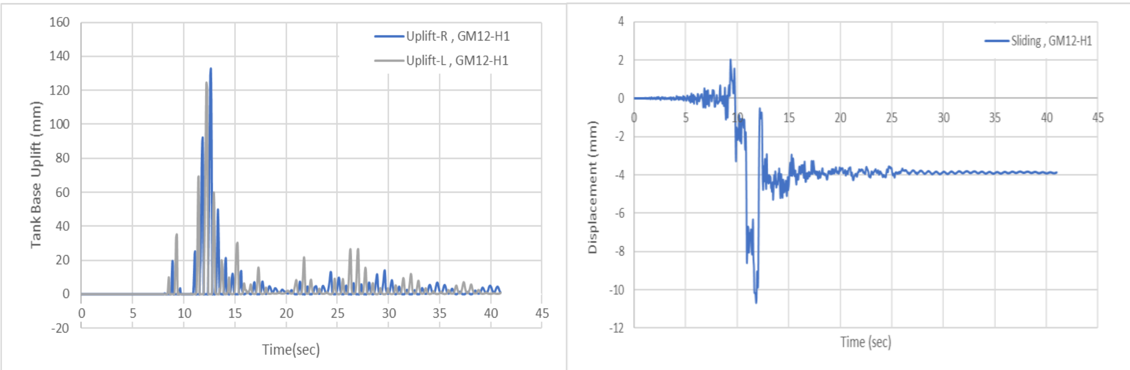

Figure 67: Tank B base uplift history and sliding history under EQ11

6.3.3 Results of Analyses for Tank C

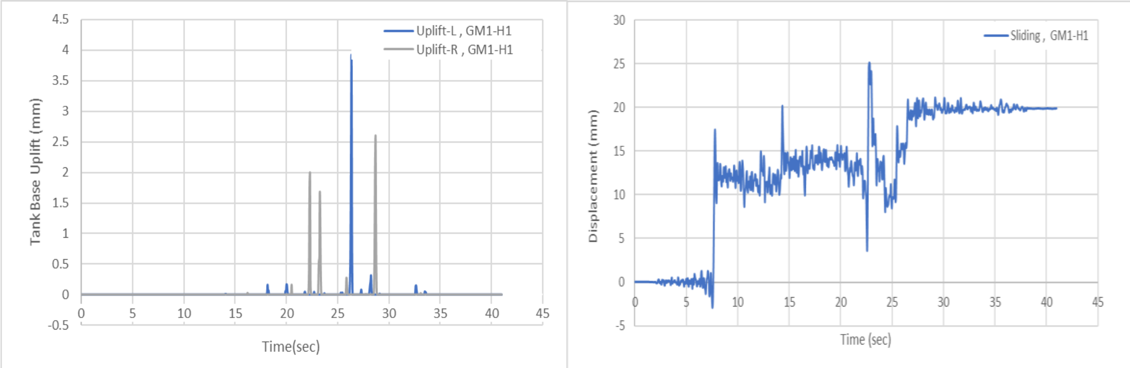

Figure 68: Tank C base uplift history and sliding history under EQ1

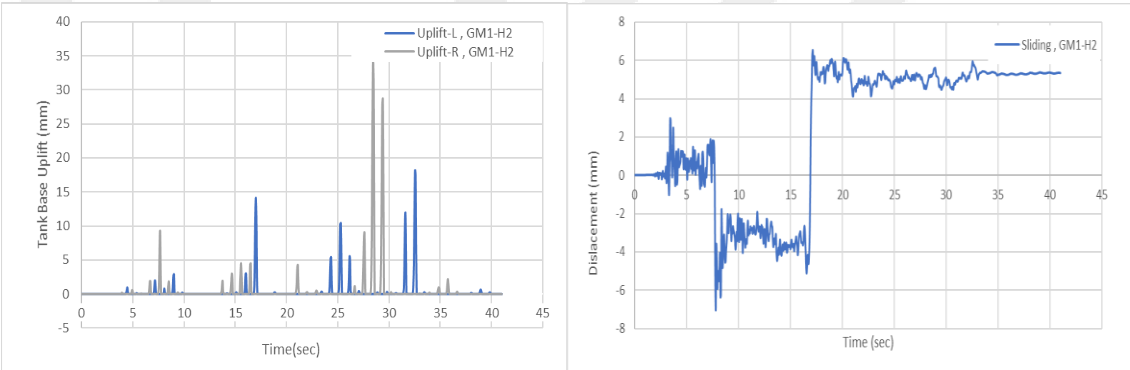

Figure 69: Tank C base uplift history and sliding history under EQ2

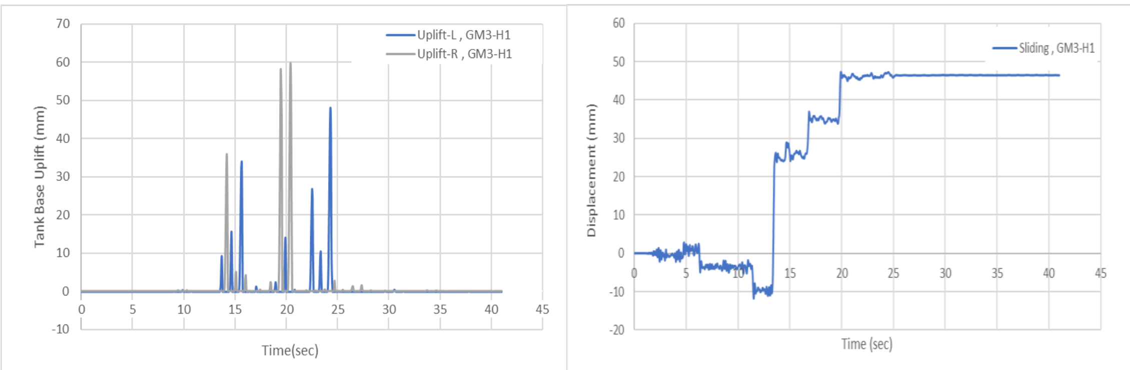

Figure 70: Tank C base uplift history and sliding history under EQ3

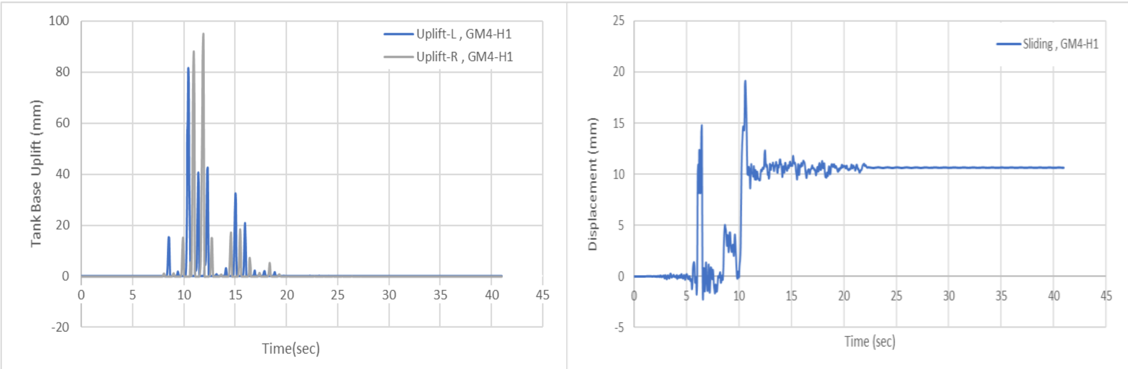

Figure 71: Tank C base uplift history and sliding history under EQ4

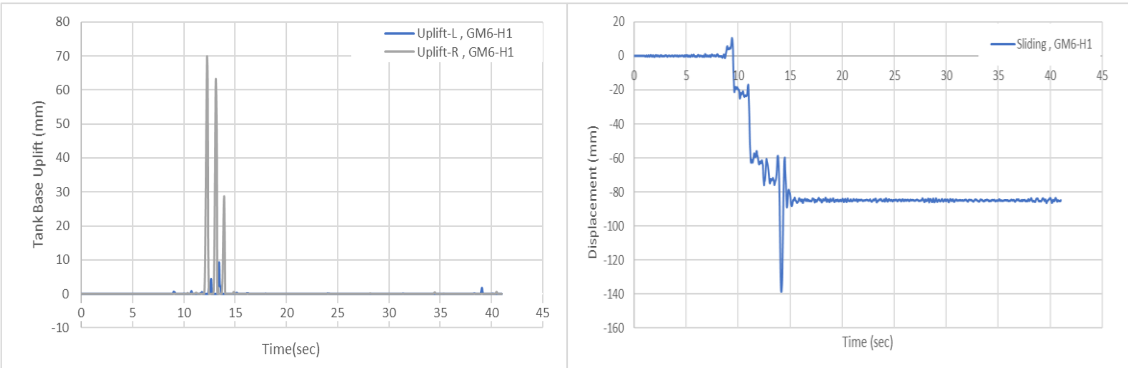

Figure 72: Tank C base uplift history and sliding history under EQ5

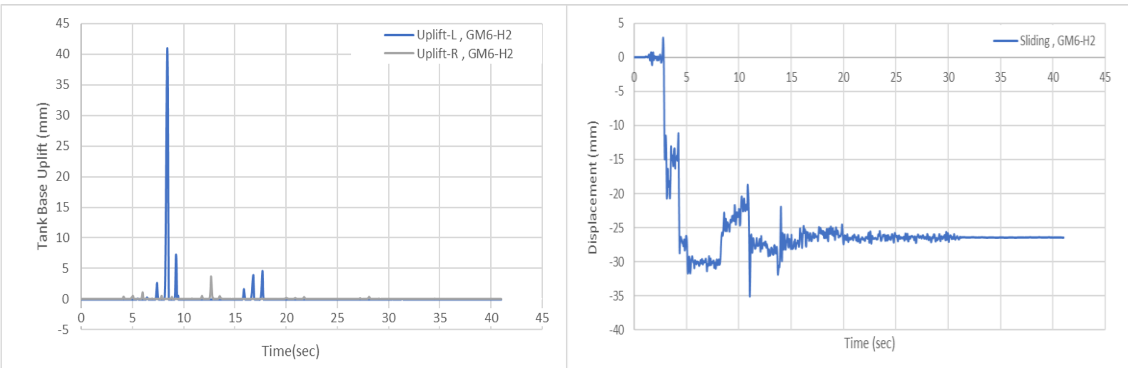

Figure 73: Tank C base uplift history and sliding history under EQ6

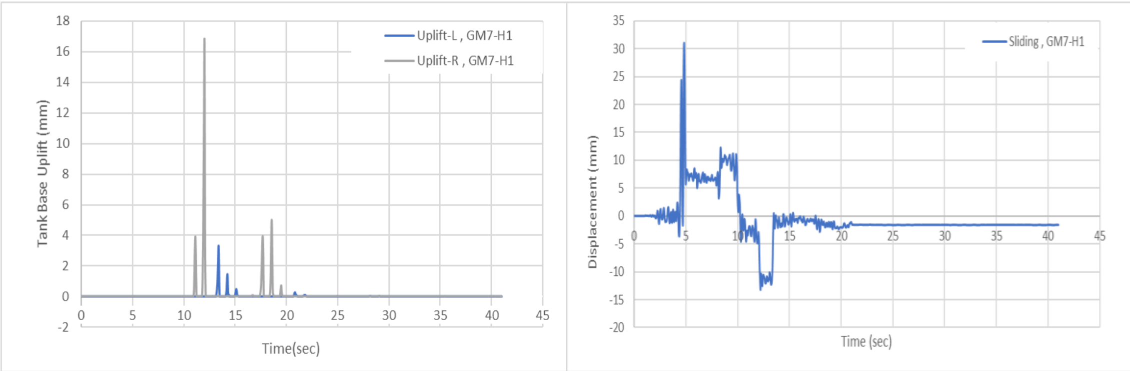

Figure 74: Tank C base uplift history and sliding history under EQ7

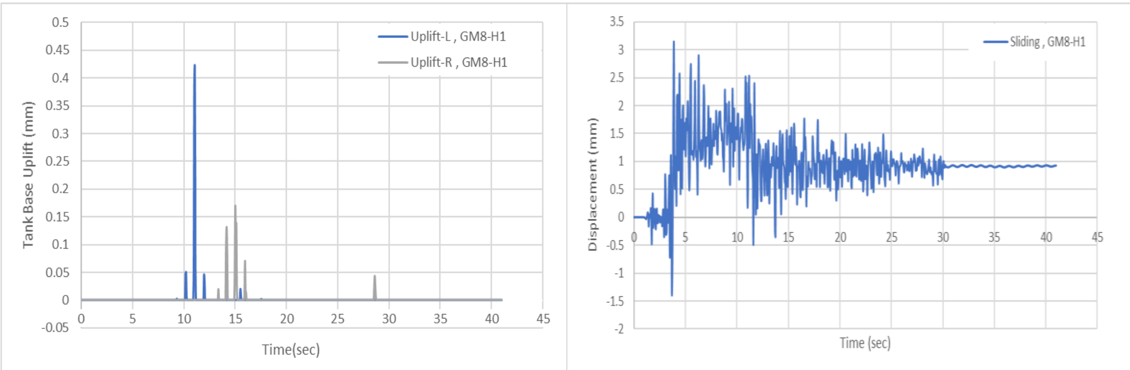

Figure 75: Tank C base uplift history and sliding history under EQ8

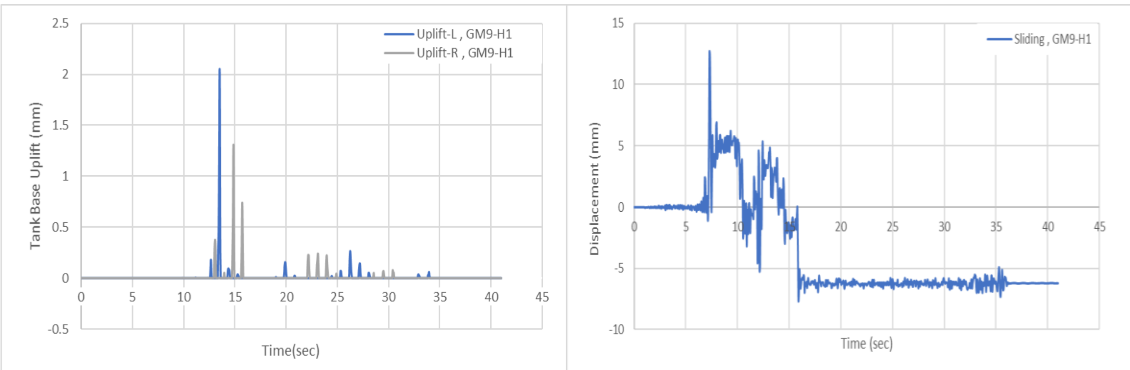

Figure 76: Tank C base uplift history and sliding history under EQ9

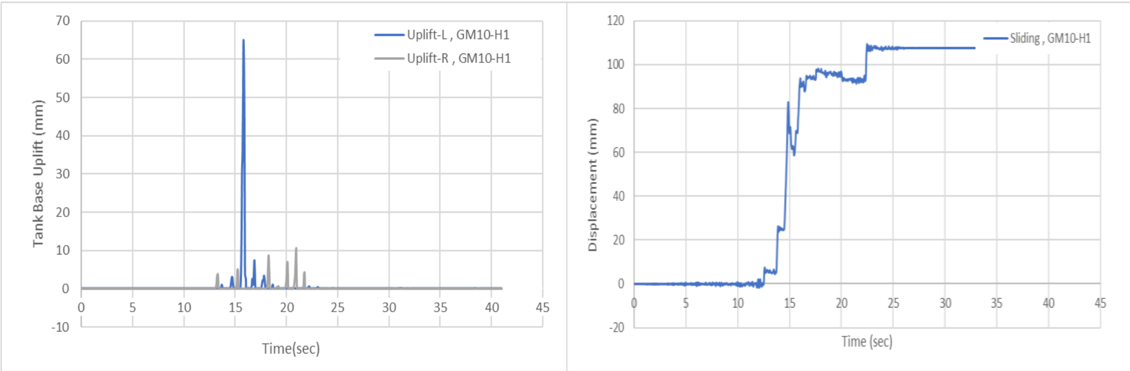

Figure 77: Tank C base uplift history and sliding history under EQ10

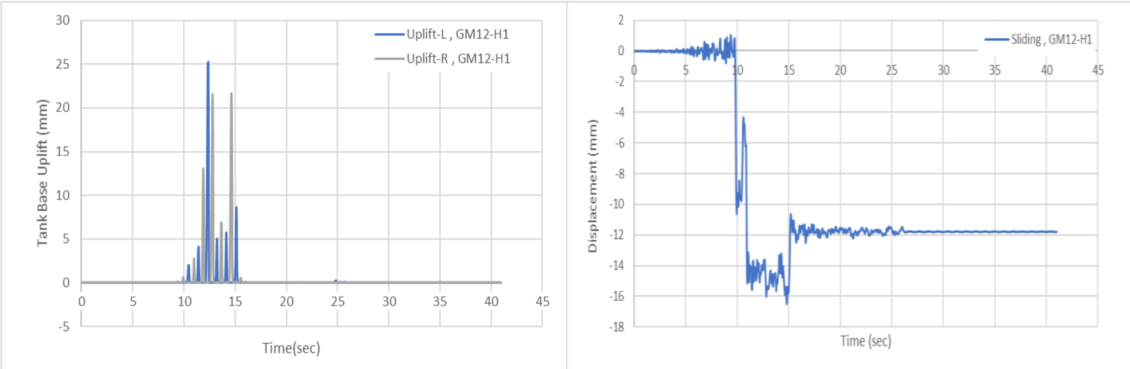

Figure 78: Tank C base uplift history and sliding history under EQ11

6.4 Discussion

6.4.1 Base Uplift and Base Sliding

A Summary of tank seismic response expressed in terms of tank maximum sliding, top drift, and base uplift at the right and left sides is given in Table 6-1 and Table 6-2. Table 6-1 shows the result of the analysis, where the friction coefficient value is assumed to be 0.6. Table 6-2 is prepared for the outputs obtained for the μ=0.42 value.

The results for the analysis group with the greater of the two friction coefficient values used in this study are as follows:

For μ=0.6

- The maximum tank sliding over the foundation is between 1 and 36 mm with an average value of 9 mm. The maximum tank sliding output came from Tank A which has an anchor ratio greater than the other tanks.

The sliding of self-anchored tanks is supposed to be small and that is the reason that they are not anchored. API 650 recommends a 2.5 cm sliding limit for design.

- Tank maximum base uplift varies between 0.4 mm and 397 mm on both sides of the tank, and the average maximum tank uplift is 131 mm.

These levels of tank base uplift can be critical for tank piping; therefore, piping should be designed flexible enough. Tank base uplift histories under EQ3 from Tank A, which at 36 mm also causes the largest displacements, and tank base sliding displacement histories under EQ3 from Tank B, which is 397 mm, are shown in Figure 79 and Figure 80, respectively.

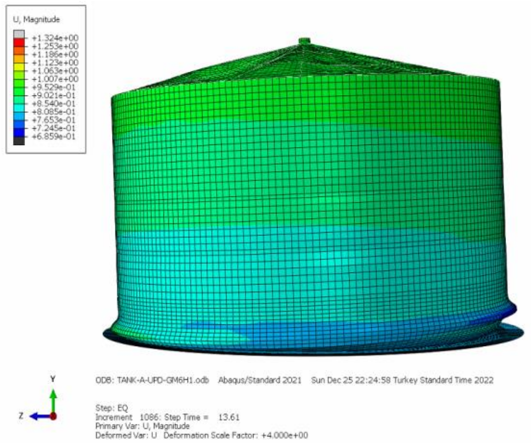

Figure 79: Maximum tank base uplift for μ=0.6

Tank sliding as expected occurs only when base shear is larger than the friction force and occurs over a much smaller time duration. However, tank sliding displacement is in one direction, and it is not a vibration type motion.

For μ=0.42

- The maximum tank sliding over the foundation is between 2 and 163 mm with an average value of 38 mm. The maximum tank sliding output came from Tank B.
- Tank maximum base uplift varies between 0.4 mm and 305 mm on both sides of the tank, and the average maximum tank uplift is 103 mm.

Tank base sliding displacement histories under EQ3 from Tank B, which is 162 mm and tank base uplift histories under EQ5 from Tank B, which is 36 mm, that also cause the largest vertical displacements, are shown in Figure 6.67 and Figure 6.68, respectively.

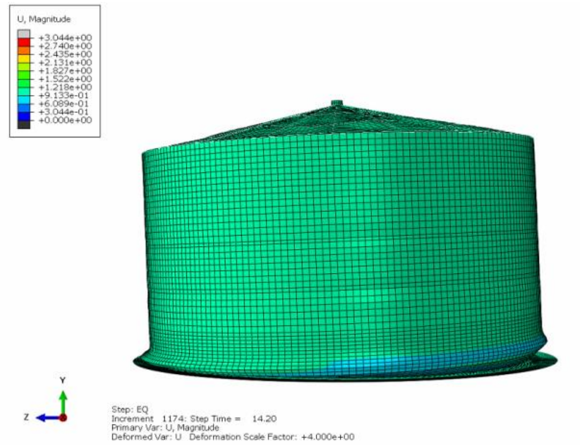

Figure 80: Maximum tank base uplift for μ=0.42

Figure 81 represents the comparison of Tank A's base uplift history and sliding history under different friction coefficients. Additionally, Figure 82 and Figure 83 represent the relevant graphs for Tank B and Tank C, respectively. By analyzing the base uplift and sliding histories, valuable insights can be gained regarding the tank's seismic performance and stability. This comparison helps in understanding the effect of different friction coefficients on the tank's performance and aids in selecting the most suitable coefficient to ensure its safety and reliability.

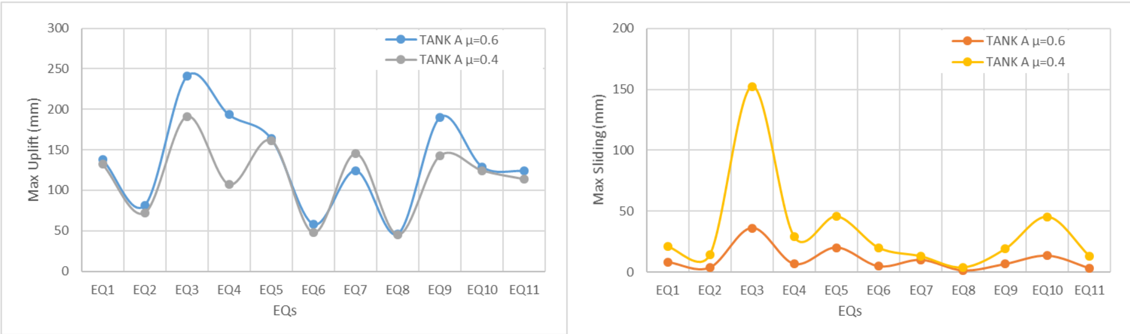

Figure 81: Comparison of sliding history and base uplift history results of Tank A

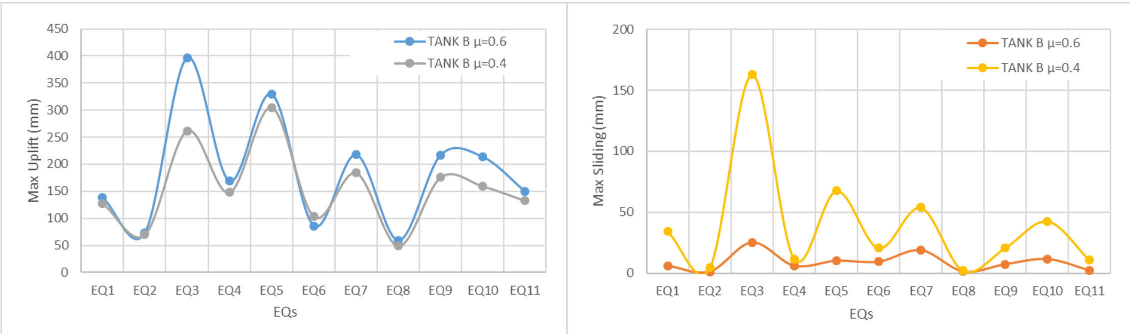

Figure 82: Comparison of sliding history and base uplift history results of Tank B

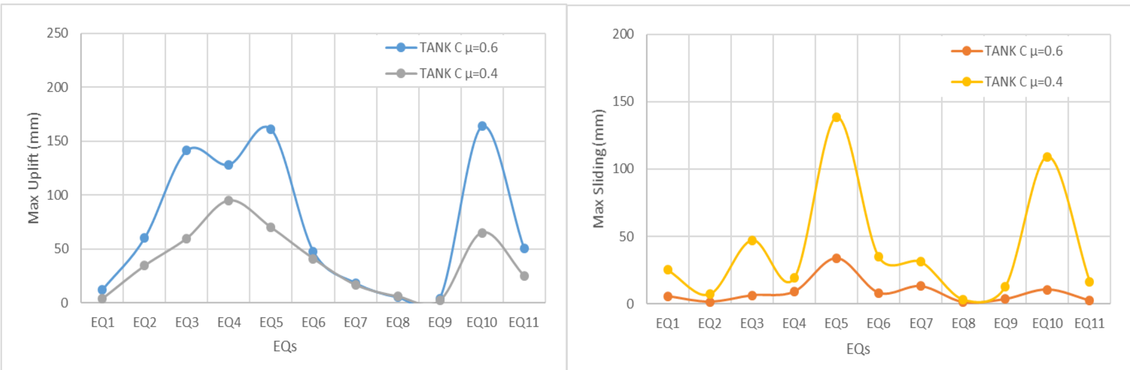

Figure 83: Comparison of sliding history and base uplift history results of Tank C

6.4.2 The Influence of the Anchorage Ratio on Seismic Performance of Tanks

The anchorage ratio plays a significant role in the seismic performance of tanks, particularly in the context of liquid storage tanks subjected to seismic events. It is a crucial parameter in tank design because it affects the tank's ability to resist overturning during earthquake. Sliding and base uplift are key points on how the anchorage ratio influences the seismic performance of tanks. A properly designed anchorage system with an appropriate ratio helps prevent the tank from base uplift during seismic events, thus avoiding potential damage. The seismic behaviors of unanchored tanks with different Anchorage Ratios are illustrated in Figure 84. This graph provides a comparative demonstration of how the anchorage ratio influences the seismic performance of the tanks.

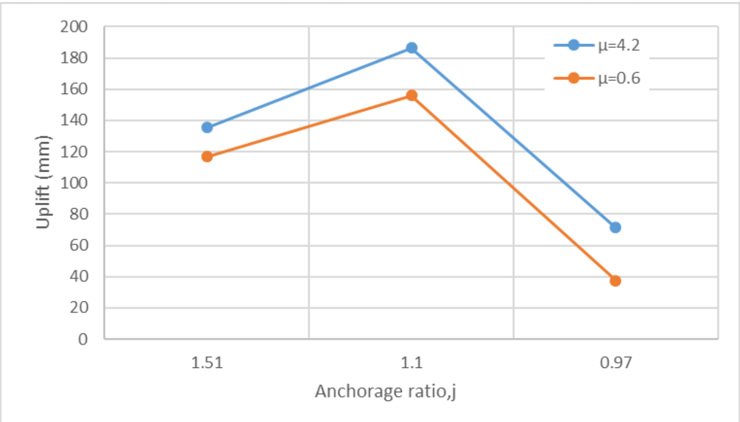

Figure 84: The impact of the Anchorage Ratio of tanks on their seismic behaviour

In these results, contrary to expectations, an increase in the anchorage ratio did not result in an increase in uplift values. This could be attributed to the insufficient number of ground motions used in the analyses. Additionally, conducting more analyses with tanks having different anchorage ratios would provide a more accurate examination. However, as observed, tanks with an anchorage ratio less than 1 have lower uplift values.

6.4.3 %PEEQ (Plastic Equivalent Strain)

PEEQ (Plastic Equivalent Strain) in ABAQUS software refers to a variable that represents the accumulated plastic deformation or strain within a material during a finite element analysis. It is a measure of the plastic strain magnitude that takes into account both the plastic strain components in various directions.

PEEQ is often used to evaluate the onset and progression of plastic deformation in materials undergoing large deformations or undergoing plastic yielding. PEEQ values can help assess the potential for material failure or damage in a structure under load.

%PEEQ is typically reported as scalar quantities and can be displayed as contour plots or used for post-processing purposes, such as calculating safety factors or determining the need for material strengthening.

Plastic strain is a critical factor to consider when analysing unanchored tanks under uplift conditions. Uplift forces can lead to significant deformation and plastic strain accumulation in the tank structure. The magnitude of uplift forces and the flexibility of the tank and its foundation determine the level of plastic strain that occurs.

During an uplift event, the tank experiences both elastic and plastic deformations. Initially, the tank may undergo elastic deformation as it lifts off the ground, but if the uplift forces continue to increase, the material will eventually yield and undergo plastic deformation. Plastic strain represents the irreversible deformation that occurs beyond the elastic limit of the material.

The accumulation of plastic strain can result in various modes of failure in unanchored tanks, such as buckling, excessive bending, or localised damage. Therefore, evaluating the plastic strain distribution within the tank structure is essential for assessing its structural integrity and determining the need for design modifications or reinforcement.

Finite element analysis, like using software such as Abaqus, enables engineers to simulate and evaluate the plastic strain behaviour of unanchored tanks subjected to uplift forces. By understanding the plastic strain response, engineers can design tanks with adequate strength and ductility to withstand uplift events without compromising their structural integrity.

- When each tank model is evaluated within itself, the %PEEQ (plastic strain) value increases as the uplift value increases.
- However, the outputs obtained in the analysis for %PEEQ 1% AND %PEEQ 5% show a decreasing result as expected. It is known that the PEEQ 1% outputs are greater than the PEEQ 5% value for each tank model and coefficient of friction value. (from Figure 85 to Figure 93)
- For the analysis group where the friction coefficient is reduced and assumed as 0.42, it is seen that the uplift values have decreased. For this analysis group where the uplift values decreased, there was a decrease for the %PEEQ values as well. The outputs of the analyses are given in between Table 12- Table 17.

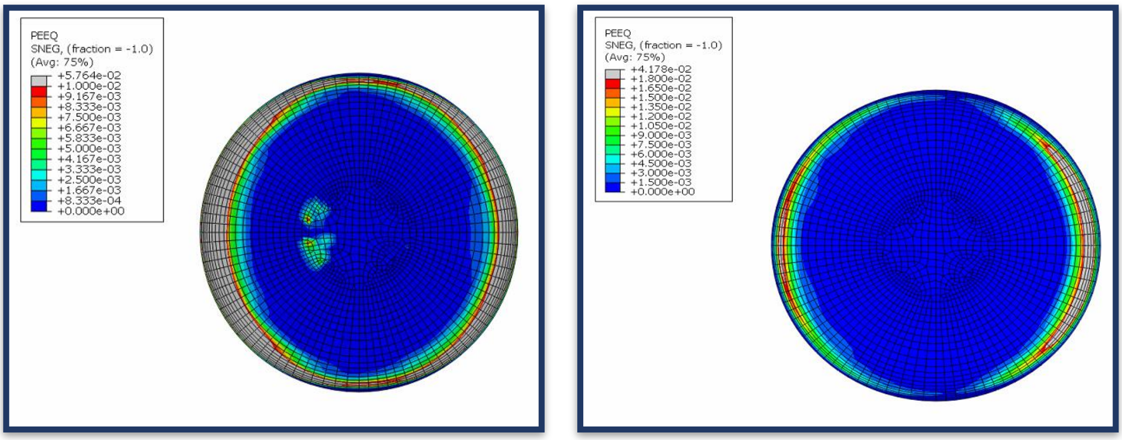

Figure 85: ABAQUS results of the maximum %1 PEEQ and %5 PEEQ for Tank A

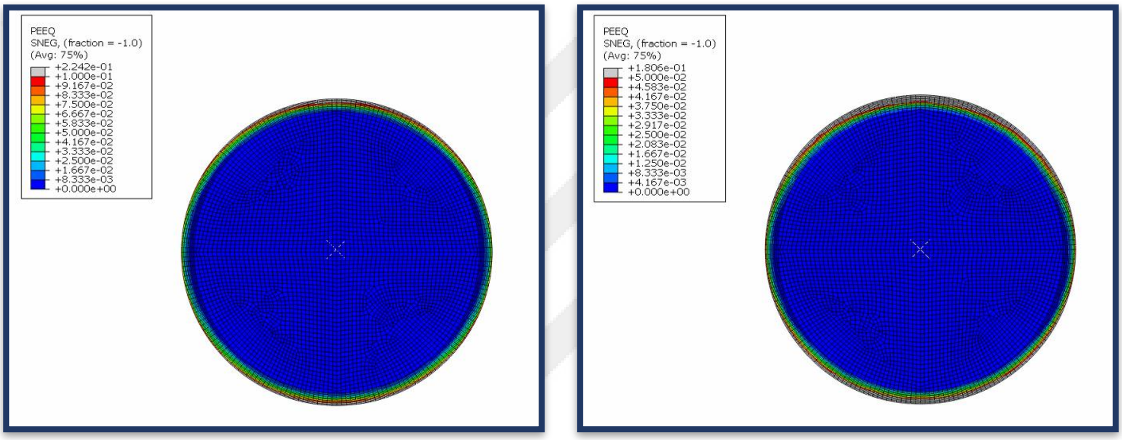

Figure 86: ABAQUS results of the maximum %1 PEEQ and %5 PEEQ for Tank B

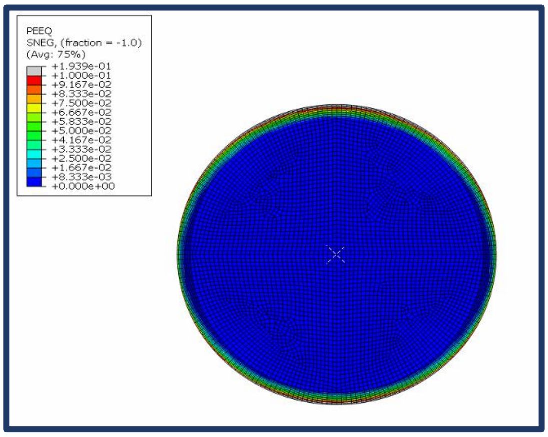

Figure 87: ABAQUS results of the maximum %1 PEEQ for Tank C

Table 12: PEEQ outputs for Tank A- μ=0.6

TANK A (μ=0.6)					
EQ NAME	UPLIFT(mm)	%PEEQ(base %1)	%PEEQ(base %5)	%PEEQ(shell %1)	%PEEQ(shell %5)
GM1-H1	138.41	4.3%	0%	1.5%	0.9%
GM1-H2	81.60	0%	0%	0%	0%
GM3-H1	241.00	7.4%	1.4%	2.3%	1.1%
GM4-H1	193.38	3.3%	0%	1.6%	0.8%
GM6-H1	163.83	8.4%	0%	1.6%	0.8%
GM6-H2	58.27	0%	0%	0%	0%
GM7-H1	124.49	1.5%	0%	1.3%	0.8%
GM8-H1	46.43	0%	0%	0%	0%
GM9-H1	190.48	3.3%	0%	1.6%	0.8%
GM10-H1	129.01	2.6%	0%	1.6%	0.8%
GM12-H1	124.07	0%	0%	1.0%	0%

Table 13: PEEQ outputs for Tank A- μ=0.42

TANK A (μ=0.42)					
EQ NAME	UPLIFT(mm)	%PEEQ(base %1)	%PEEQ(base %5)	%PEEQ(shell %1)	%PEEQ(shell %5)
GM1-H1	132.25	4.3%	0%	1.5%	0.8%
GM1-H2	72.43	0%	0%	0%	0%
GM3-H1	190.81	5.2%	0%	1.6%	1.1%
GM4-H1	107.37	1.4%	0%	1.6%	0.8%
GM6-H1	161.08	6.7%	0%	1.6%	0.8%
GM6-H2	47.94	0%	0%	0%	0%
GM7-H1	145.25	0.9%	0%	1.2%	0%
GM8-H1	45.41	0%	0%	0%	0%
GM9-H1	142.72	0%	0%	0.9%	0%
GM10-H1	124.28	0%	0%	1.2%	0%
GM12-H1	113.80	0%	0%	0.8%	0%

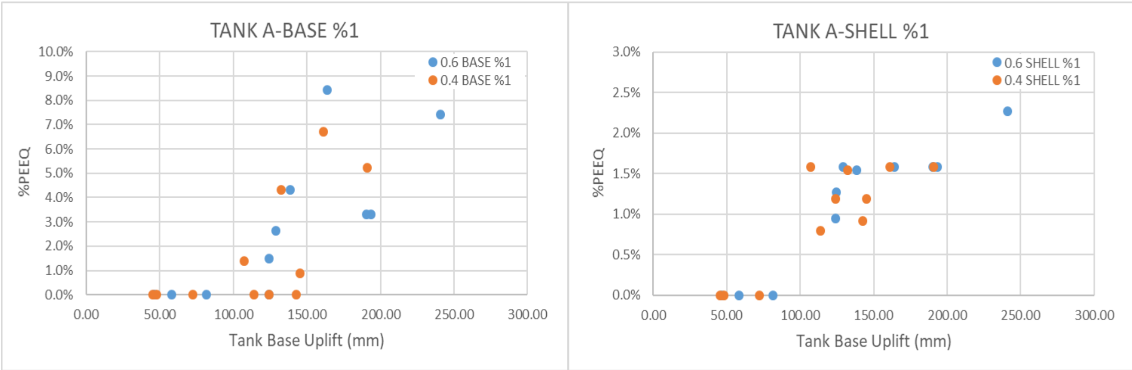

Figure 88: The distribution of %1 PEEQ for Tank A- base and tank shell

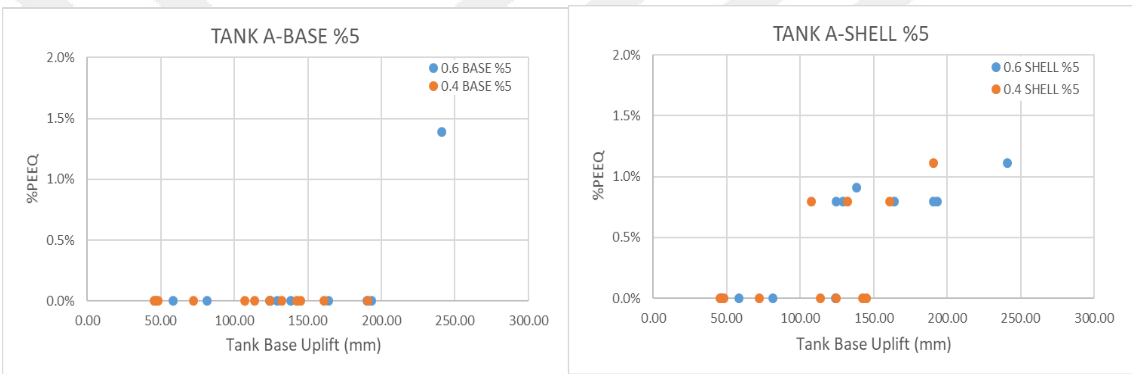

Figure 89: The distribution of %5 PEEQ for Tank A-base and tank shell

Table 14: PEEQ outputs for Tank B- μ=0.6

TANK B (μ=0.6)					
EQ NAME	UPLIFT(mm)	%PEEQ(base %1)	%PEEQ(base %5)	%PEEQ(shell %1)	%PEEQ(shell %5)
GM1-H1	138.21	3.3%	0.4%	0%	0%
GM1-H2	73.62	0%	0%	0%	0%
GM3-H1	396.94	4.7%	3.3%	6.2%	0.8%
GM4-H1	169.26	2.7%	0.4%	0%	0%
GM6-H1	330.09	4.5%	3.1%	6.2%	0%
GM6-H2	86.21	0.8%	0%	0%	0%
GM7-H1	217.75	3.7%	0.8%	0.8%	0%
GM8-H1	59.43	0%	0%	0%	0%
GM9-H1	217.32	3.7%	0.6%	2.0%	0%
GM10-H1	213.63	3.3%	0.7%	1.5%	0%
GM12-H1	149.70	2.0%	0%	0%	0%

Table 15: PEEQ outputs for Tank B- μ=0.42

TANK B (μ=0.42)					
EQ NAME	UPLIFT(mm)	%PEEQ(base %1)	%PEEQ(base %5)	%PEEQ(shell %1)	%PEEQ(shell %5)
GM1-H1	127.84	2.5%	0.4%	0%	0%
GM1-H2	69.95	0%	0%	0%	0%
GM3-H1	261.76	4.1%	2.5%	5.4%	0%
GM4-H1	147.76	2.5%	0.0%	0%	0%
GM6-H1	305.01	3.8%	1.6%	5.4%	0%
GM6-H2	103.26	0.4%	0%	0%	0%
GM7-H1	184.08	3.1%	0.6%	0%	0%
GM8-H1	49.20	0%	0%	0%	0%
GM9-H1	175.92	2.7%	0.4%	0%	0%
GM10-H1	159.30	2.5%	0.4%	0%	0%
GM12-H1	132.63	1.4%	0%	0%	0%

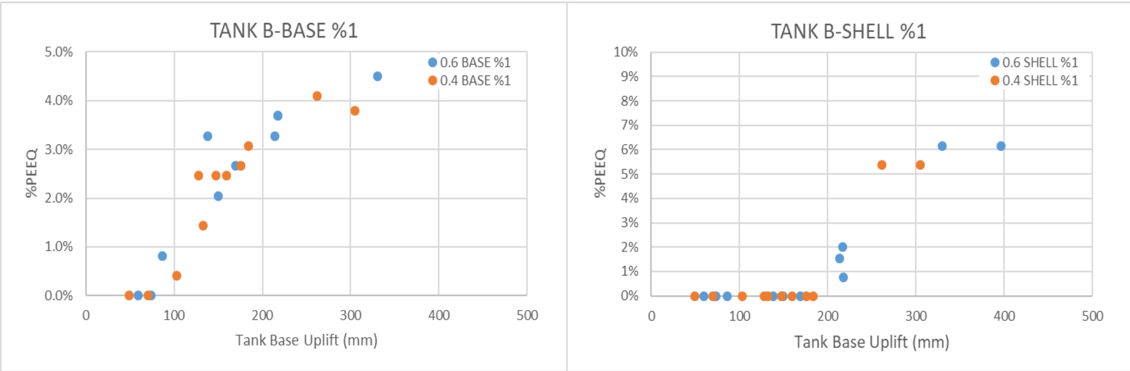

Figure 90: The distribution of %1 PEEQ for Tank B-base and tank shell

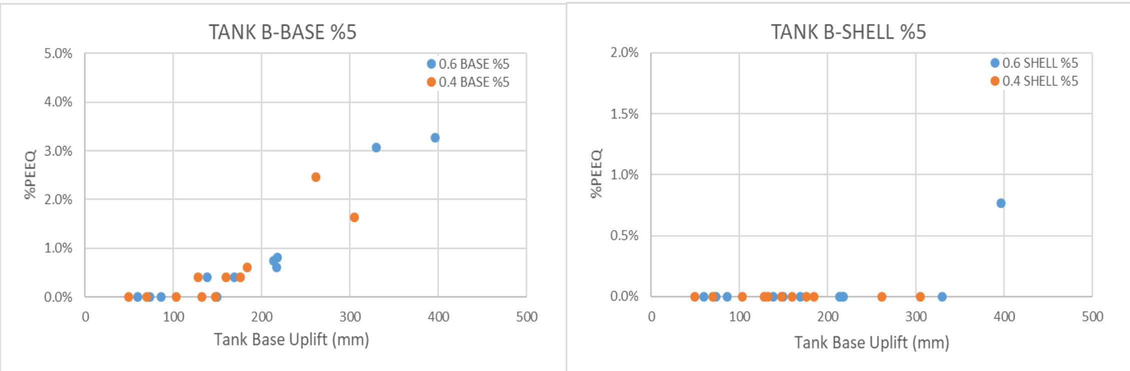

Figure 91: The distribution of %5 PEEQ for Tank B-base and tank shell

Table 16: PEEQ outputs for Tank C- μ=0.6

TANK C (μ=0.6)					
EQ NAME	UPLIFT(mm)	%PEEQ(base %1)	%PEEQ(base %5)	%PEEQ(shell %1)	%PEEQ(shell %5)
GM1-H1	11.95	0%	0%	0%	0%
GM1-H2	60.03	0%	0%	0%	0%
GM3-H1	141.39	0%	0%	0%	0%
GM4-H1	128.22	0.5%	0%	0%	0%
GM6-H1	161.03	1.0%	0%	0%	0%
GM6-H2	47.72	0%	0%	0%	0%
GM7-H1	18.16	0%	0%	0%	0%
GM8-H1	0.44	0%	0%	0%	0%
GM9-H1	3.71	0%	0%	0%	0%
GM10-H1	163.74	0.1%	0%	0%	0%
GM12-H1	50.48	0%	0%	0%	0%

Table 17: PEEQ outputs for Tank C- μ=0.42

TANKC (μ=0.42)					
EQ NAME	UPLIFT(mm)	%PEEQ(base %1)	%PEEQ(base %5)	%PEEQ(shell %1)	%PEEQ(shell %5)
GM1-H1	3.87	0%	0%	0%	0%
GM1-H2	34.44	0%	0%	0%	0%
GM3-H1	59.82	0%	0%	0%	0%
GM4-H1	94.83	0%	0%	0%	0%
GM6-H1	69.85	0%	0%	0%	0%
GM6-H2	40.97	0%	0%	0%	0%
GM7-H1	16.81	0%	0%	0%	0%
GM8-H1	0.42	0%	0%	0%	0%
GM9-H1	2.04	0%	0%	0%	0%
GM10-H1	65.08	0%	0%	0%	0%
GM12-H1	25.26	0%	0%	0%	0%

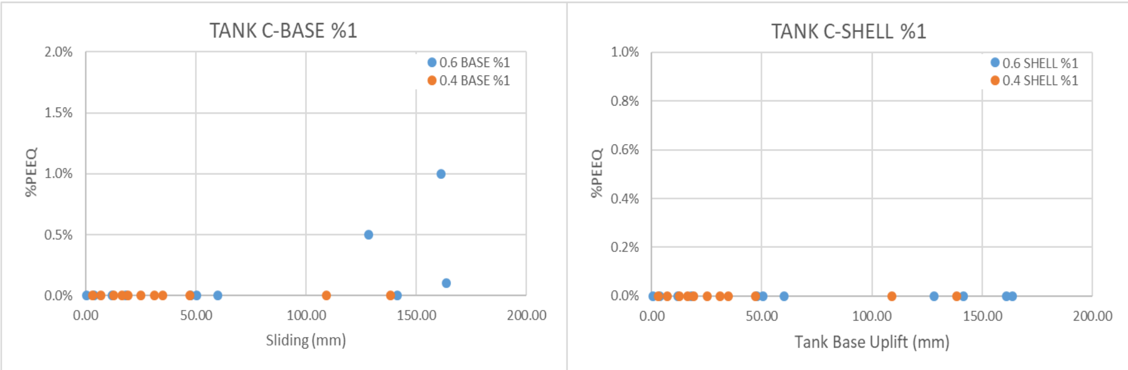

Figure 92: The distribution of %1 PEEQ for Tank C-base and tank shell

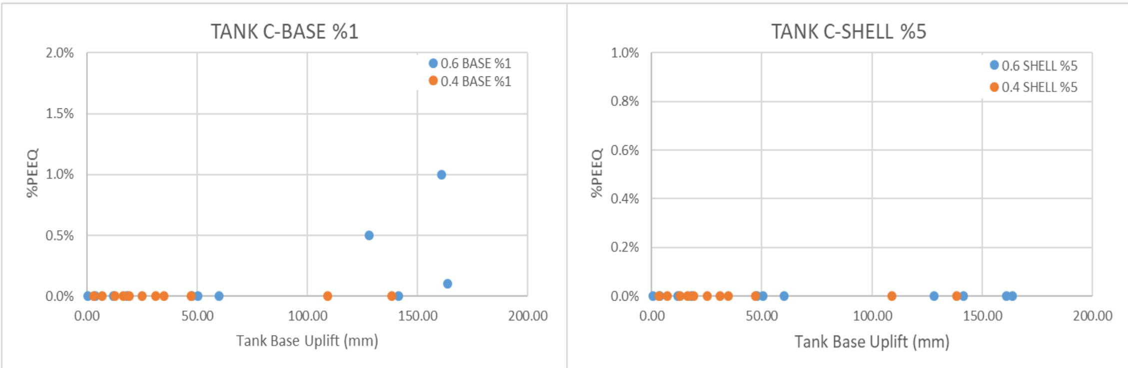

Figure 93: The distribution of %5 PEEQ for Tank C-base and tank shell

CHAPTER VII

CONCLUSIONS

This chapter comprises a summary of the study including scope and purpose, the findings of the time history analyses, and a discussion of the results regarding the effect of the H/D ratio and selected friction coefficient on the seismic behaviour of the unanchored steel storage tank.

7.1 Summary

There is a lack of comprehensive studies in the existing literature that specifically address the seismic performance of unanchored cylindrical steel storage tanks. There is a limited number of studies available on the effects of H/D ratio, friction coefficient, and their influence on the seismic performance of storage tanks (such as base uplift and base sliding). To address this gap, in this study, the seismic performance of tanks with different H/D ratios was examined, the impact of the anchorage ratio (j) value in design through analysis results was evaluated, and the effect of the friction coefficient on uplift and sliding behaviour was observed. In total, three tanks were designed with different H/D ratios, corresponding to different anchorage ratios, in accordance with API 650 and TBDY 2018 regulations. The study examined the earthquake performance of three tanks with different anchorage ratios and investigated the effects of different friction coefficients on tank behaviour under earthquake load. The seismic performance of three unanchored liquid-storage tanks with tank diameter ranging from 24.4 m to 55.0 m and liquid height between 12.2 m to 21 m were investigated using mechanical spring-mass analogy in 3D. The seismic performance of the three tanks was computed using 11 strong ground motion records. The computed tank base uplift versus time histories was monitored and compared. The results indicate that the traditional mechanical spring analogy model, which is the basis for the current seismic design provisions API 650 and Eurocode 8. The H/D ratios of these three tanks are X, Y, and Z, respectively. This study examined the seismic performance of three unanchored industrial liquid-storage tanks in a high earthquake-risk area. Finite element models were created using ABAQUS to determine the tanks' structural behaviour through time history analysis.

Hence, to observe the effect of the H/D ratio of the tanks and the friction coefficient value used in the modelling, and to evaluate potential tank damage, the tank base sliding, base uplift, and material damage were reported based on the results of time history analysis.

7.2 Overall Outcomes

The seismic performance of three existing typical self-anchored industrial liquid-storage tanks located in the Kocaeli industrial region was studied using API 650 spring-mass model approach for liquid content. A 3D finite element model was created to perform tank seismic performance under 11 selected recorded near-field strong ground motions. Tank sliding and base uplift over its foundations were considered in the developed finite element model. In addition, analyses were repeated with a different friction coefficient to understand the relationship between friction and earthquake performance of unanchored tanks. Based on the obtained response, the following inferences could be made regarding the effects of these two main objectives on the seismic behaviour of unanchored tanks.

Based on computed tank seismic performance, the following conclusions were made:

- Liquid modelling with the spring-mass approach is easy and computationally reasonable.
- The results obtained from the analytical-finite element models, particularly using the ABAQUS finite element software, were found to be in good agreement. The seismic response analysis of the tank conducted using the ABAQUS finite element method has provided a comprehensive understanding of the base uplift and base sliding movements exhibited by the unanchored liquid storage tank.
- Unanchored tank reduces tank wall stresses and material yielding along the tank wall. However, tank sliding, and effects of base uplift are disadvantages of self-anchored tanks.
- For the three-dimensional dynamic analysis of liquid storage tanks, a simplified model capable of taking into account the nonlinear moment-rotation relationship and the soil-foundation stiffness was developed.
- When the friction coefficient was reduced from 0.6 to 0.42, the uplift results for each tank increased as the resistance to movement of the tank decreased.

For μ=0.6,

- The maximum sliding of the tank over the foundation ranged from 1 to 36 mm, with an average value of 9 mm. Tank A, which had a higher anchor ratio compared to the other tanks, exhibited the maximum sliding output.
- Tank maximum base uplift varied between 0.4 mm and 397 mm on both sides of the tank, and the average maximum tank uplift was 131 mm.
- Tank base sliding displacement histories under EQ3 from Tank B which is 397 mm, whereas tank base uplift histories under EQ3 from Tank A which is 36 mm cause the largest displacements.

For μ=0.42

- The maximum tank sliding over the foundation was between 2mm and 163 mm with an average value of 38 mm. Maximum tank sliding output was for Tank B.
- Tank maximum base uplift varied between 0.4 mm and 305 mm on both sides of the tank, and the average maximum tank uplift was 103 mm.
- Tank base sliding displacement histories under EQ3 from Tank B were is 162 mm, whereas tank base uplift histories under EQ5 from Tank B which is 36 mm, caused the largest vertical displacements.
- Significant tank shell and base plate yielding was observed at tank shell and base plate connection regions, where tank base uplift occurred. These regions are critical for plastic strain.
- When each tank model was evaluated within itself, the %PEEQ (plastic strain) value increased as the uplift value increased.

- The outputs obtained in the analysis for %PEEQ 1% AND %PEEQ 5% showed a decreasing result as expected.
- The PEEQ 1% outputs were greater than the PEEQ 5% value for each tank model and coefficient of friction value. (from Figure 84 to Figure 92)
- The uplift values decreased where the friction coefficient was reduced and assumed as 0.42. Also, the %PEEQ values as well.

7.3 Future Work

In this study, the simplified spring-mass model used in the modelling of unanchored tanks is a quick and cost-effective method. However, it does not capture the full seismic behaviour of unanchored tanks-liquid structures with tank base uplift and sliding. In this method, the sloshing movement of the liquid stored in the tank is ignored. In order to account for sloshing phenomena in liquid storage tanks, various modelling techniques can be employed to obtain the structural response. It is important to evaluate the behaviour of the model at the upper part of the tank to assess the impact of sloshing phenomena on failure criteria associated with sloshing. Therefore, conducting a comprehensive analysis that considers all relevant failure criteria would enable a more reliable assessment of the tank's structural performance class for an overall evaluation of the liquid storage tank. Analysing the tanks while considering the modelling of the liquid will lead to more accurate results.

REFERENCES

[1] B. ERKMEN, “Seismic Performance Evaluation and Retrofit of Liquid Storage Tanks- Case Study,” *Sak. Univ. J. Sci.*, vol. 26, no. 69580, pp. 347–356, 2022, doi: 10.16984/saufenbilder.997699.

[2] H. N. Phan, F. Paolacci, and S. Alessandri, “Enhanced Seismic Fragility Analysis of Unanchored Steel Storage Tanks Accounting for Uncertain Modeling Parameters,” *J. Press. Vessel Technol.*, vol. 141, no. 1, 2018, doi: 10.1115/1.4039635.

[3] H. Sezen and A. Whittaker, “Performance of industrial facilities during the 1999 Kocaeli, Turkey, earthquake,” *In 13th world conference on earthquake engineering*, pp. 1-6, 2004

[4] G. C. Manos, “Evaluation of the earthquake performance of anchored wine tanks during the San Juan, Argentina, 1977 earthquakes,” *Earthq. Eng. \& Struct. Dyn.*, vol. 20, pp. 1099–1114, 1991.

[5] A. Çelik and M. Köse, “Dynamic buckling analysis of cylindrical steel water storage tanks subjected to Kobe earthquake loading,” *Steel Constr.*, vol. 13, 2020, doi: 10.1002/stco.201900003.

[6] B. Erkmen, “Evaluation of Code Provisions for Seismic Performance of Unanchored Liquid Storage Tanks,” in *Proceedings of the 6th ECCOMAS Thematic Conference on Computational Methods in Structural Dynamics and Earthquake Engineering (COMPDYN 2017)*, Rhodes Island, vol. 1, pp. 1700-1710 , 2017.

[7] American Petroleum Institute, “Welded Tanks for Oil Storage.” Washington, D.C., USA, 13th Edition,2021.

[8] European Committee for Standardization, “Eurocode 8: Design of Structures for Earthquake Resistance - Part 1: General Rules, Seismic Actions and Rules for Buildings.”, Brussels: European Committee for Standardization, 2005.

[9] J. C. Virella, L. A. Godoy, and L. E. Suárez, “Dynamic buckling of anchored steel tanks subjected to horizontal earthquake excitation,” *J. Constr. Steel Res.*, vol. 2, no. 6, pp. 521–531, 2006.

[10] D. C. Barton and J. V Parker, “Finite element analysis of the seismic response of anchored and unanchored liquid storage tanks,” *Earthq. Eng. \& Struct. Dyn.*, vol. 15, no. 3, pp. 299–322, 1987, doi: https://doi.org/10.1002/eqe.4290150303.

[11] Z. Ozdemir, M. Souli, and Y. M. Fahjan, “Application of nonlinear fluid-structure interaction methods to seismic analysis of anchored and unanchored tanks,” *Eng. Struct.*, vol. 32, no. 2, pp. 409–423, 2010.

[12] G.W. Housner, “Dynamic pressures on accelerated fluid containers,” *Bull. Seismol. Soc. Am.*, vol. 47, pp. 15–35, 1957.

[13] R. Peek, “Analysis of Unanchored Liquid Storage Tanks Under Seismic Loads,”, Ph.D dissertation, Earthquake Engineering Research Laboratory, California Institute of Technology Pasadena, California, Pasadena, CA, 1986. Available: https://thesis.library.caltech.edu/11848/2/Peek_R_1986.pdf

[14] P.K. Malhotra, “Seismic Response of Soil-Supported Unanchored Liquid-Storage Tanks,” 1997, doi: 10.1061/(ASCE)0733-9445(1997)123:4(440).

[15] A. Niwa and R. W. Clough, “Buckling of cylindrical liquid-storage tanks under

earthquake loading," *Earthq. Eng. \& Struct. Dyn.*, vol. 10, pp. 107–122, 1982.

[16] G.W. Housner, "The Dynamic Behavior of Water Tanks,", *Bulletin of the seismological society of America*, vol. 53, no. 2, pp. 381-387. 1963.

[17] A.S. Veletsos, "Seismic response and design of liquid storage tanks," in *Guidelines for the seismic design of oil and gas pipeline systems*, ASCE, 1984, pp. 255–370.

[18] A.S. Veletsos, and J.Y. Yang, "Earthquake response of liquid storage tanks," in *Proceedings of second annual ASCE Engineering Mechanics Specialty Conference*, Raleigh, North Carolina, 1977, pp. 1-24.

[19] R. Peek, "Analysis of Unanchored Liquid Storage Tanks Under Seismic Loads,", Ph.D dissertation, Earthquake Engineering Research Laboratory, California Institute of Technology Pasadena, California, Pasadena, CA, 1986. Available: https://thesis.library.caltech.edu/4425/5/natsiavas_s_1988.pdf

[20] M.A. Haroun, "Vibration Studies and Tests of Liquid Storage Tanks,", *Earthquake Engineering & Structural Dynamics 11*, vol. 2, pp. 179-206. 1983.

[21] M.A. Haroun, and S.H.B adawi, "Seismic Behaviour of unanchored ground-based cylindrical tanks," in *Proceedings of ninth World Conference on earthquake Engineering*, Tokyo, Japan, 1988, vol. 6, pp. 643-648 .

[22] A. S. Veletsos, "Seismic effects in flexible liquid storage tanks," in *Proceedings of 5th World Conference on Earthquake Engineering*, 1974, pp. 630–639.

[23] G. W. Housner, "The dynamic behaviour of water tanks," *Bull. Seismol. Soc. Am.*, vol. 53, no. 2, pp. 381–387, 1963.

[24] M. A. Haroun, "Dynamic Analyses of Liquid Storage Tanks,", Ph.D dissertation,

Earthquake Engineering Research Laboratory, California Institute of Technology Pasadena, Pasadena, California, 1980.

[25] M. A. Haroun, “Vibration studies and tests of liquid storage tanks,” *Earthq. Eng. Struct. Dyn.*, vol. 11, pp. 179–206, 1983.

[26] P. K. Malhotra, T. Wenk, and M. Wieland, “Simple Procedure for Seismic Analysis of Liquid-Storage Tanks,” *Struct. Eng. Int.*, vol. 10, pp. 197–201, 2000, doi: 10.2749/101686600780481509.

[27] D.T. Lau, and X. Zeng, “Dynamic uplift analysis of unanchored cylindrical tanks,” in *Earthquake Engineering, tenth world conference*, Balkerna, Rotterdam, 1992, vol. 9, pp. 5011-5016

[28] J. Colombo and J. Almazán, “Simplified 3D model for the uplift analysis of liquid storage tanks,” *Eng. Struct.*, vol. 196, 2019, doi: 10.1016/j.engstruct.2019.109278.

[29] K. V Steinbrugge and A. R. Flores, “The Chilean earthquakes of May, 1960: a structural engineering viewpoint,” *Bull. Seismol. Soc. Am.*, vol. 53, pp. 225–307, 1963.

[30] American Lifelines Alliance (ALA), “Seismic Fragility Formulations for Water Systems, Part 1: Guideline” American Society of Civil Engineers (*ASCE)*, 2001.

[31] G. W. Housner, “The dynamic behavior of water tanks,” *Bull. Seismol. Soc. Am.*, vol. 53, pp. 381–387, 1963.

[32] I. Christovasilis, “Seismic Analysis of Liquefied Natural Gas Tanks,” 2006. doi: 10.13140/RG.2.2.16992.07688.

[33] M. Erdik, “Report on 1999 Kocaeli and Duzce Earthquakes,” *Structural Control for Civil and Infrastructure Engineering: World Scientific 2001*, Istanbul, pp. 149–

186, 2001.

[34] G. Fabbrocino, I. Iervolino, and G. Manfredi, “Seismic Risk Formulation of Atmospheric Steel Tanks in Oil Storage Systems,” *In proc. PMAPS*, Naples - Italy, 2008.

[35] A. Bakhshi and A. Hassanikhah, “Comparison between seismic responses of anchored and unanchored cylindrical steel tanks,” in *14th World Conference on Earthquake Engineering*, Beijing, China, October 12–17,2008. Available: https://www.iitk.ac.in/nicee/wcee/article/14_06-0101.PDF

[36] K. Bakalis and S. A. Karamanos, “Uplift mechanics of unanchored liquid storage tanks subjected to lateral earthquake loading,” *Thin-Walled Struct.*, vol. 158, pp. 107-145, 2021, doi: https://doi.org/10.1016/j.tws.2020.107145.

[37] L.S. Jacobsen, “Impulsive Hydrodynamics of Fluid Inside a Cylindrical Container, and of Fluid Surrounding a Cylindrical Pier,” *Bull. Seismol. Soc. Am.*, vol. 39, no. 3, pp. 189–204, 1949.

[38] A. Veletsos and J. Yang, “Earthquake Response of Liquid Storage Tanks, Advances in Civil Engineering through Engineering Mechanics, ASCE, Raleigh, pp. 1-24, 23-25 May 1977.

[39] M.A. Haroun, and G.W. Housner, “Earthquake Response of Deformable Liquid Storage Tanks,”, *ASME. J. Appl. Mech.*, vol. 48, pp. 411-418, 1981, doi: 10.1115/1.3157631.

[40] P.K. Malhotra, and A.S. Veletsos, “Beam Model for Base-Uplifting Analysis of Cylindrical Tanks,” 1994, doi: 10.1061/(ASCE)0733-9445(1994)120:12(3471).

[41] P.K. Malhotra, and A.S. Veletsos, S. Anestis, “Uplifting Analysis of Base Plates

in Cylindrical Tanks," *J. Struct. Eng.*, vol. 120, no. 12, pp. 3489–3505, 1994

[42] W. Auli, and D.F. Fischer, and F.G. Rammerstorfer, "Uplifting of Earthquake-Loaded Liquid-Filled Tanks," in *1985 PVP Conf.*,vol 98-7, pp. 71-85, New Orleans, Louisiana, 1985.

[43] P. K. Malhotra and A. S. Veletsos, "Uplifting response of unanchored liquid-storage tanks," *J. Struct. Eng.*, vol. 120, no. 12, pp. 3524–3546, 1994.

[44] R. Peek and P. Jennings, "Simplified analysis of unanchored tanks," *Earthq. Eng. \& Struct. Dyn.*, vol. 16, pp. 1073–1085, 1988.

[45] M. Ormeno, and T. Larkin, and N. Chouw, "Influence of uplift on liquid storage tanks during earthquakes," *Coupled Syst. Mech.*, vol. 1, no. 4, pp. 311–324, 2012.

[46] New Zealand Society for Earthquake Engineering, *Seismic Design of Storage Tanks*. New Zealand Society for Earthquake Engineering, 2009.

[47] A. S. Veletsos and C. E. Ventura, "Efficient analysis of dynamic response of linear systems," *Earthq. Eng. \& Struct. Dyn.*, vol. 12, no. 4, pp. 521–536, 1984.

[48] *Turkish Seismic Earthquake Code (TBDY)*, [Online], Available: https://www.resmigazete.gov.tr/eskiler/2018/03/20180318M1-2-1.pdf.

[49] ABAQUS, Inc., "ABAQUS/Standard, User's Manual." The Abaqus Software is a product of Dassault Systèmes Simulia Corp. Providence, RI, USA: Dassault Systèmes, Version 13.1, USA, 2014.

[50] The Disaster and Emergency Management Presidency (AFAD), "Turkey Earthquake Risk Maps." 2022, [Online], Available: https://tdth.afad.gov.tr

[51] P. PEER, "NGA-West2 Database. Pacific Earthquake Engineering Research Center," *Univ. California, Berkeley, CA*, 2013.

VITA

İrsen Nihan Kocras graduated from Civil Engineering Department of Özyeğin University in 2020. She started her master's degree in Özyeğin University in 2020 and worked as a teaching assistant in the meantime. Her research interests are the design and seismic performance of industrial structures, earthquake engineering. In the thesis study, she focused on the impact of their anchorage ratio on the seismic behavior of unanchored steel storage tanks.